REMOVAL EFFICIENCY, CLEANUP MECHANISM, AND DAMAGE ANALYSIS OF A NOVEL TREATMENT FOR OIL-BASED DRILLING FLUID FILTER CAKE REMOVAL

A Dissertation

by

JING ZHOU

Submitted to the Office of Graduate and Professional Studies of
Texas A&M University
in partial fulfillment of the requirements for the degree of

DOCTOR OF PHILOSOPHY

Chair of Committee,	Hisham A. Nasr-El-Din
Committee Members,	Stephen A. Holditch
	Jerome Schubert
	Mahmoud El-Halwagi
Head of Department,	Jeff Spath

May 2019

Major Subject: Petroleum Engineering

ABSTRACT

Removing oil-based drilling fluid (OBDF) filter cake is a difficult task. Low removal efficiency of filter cake may result in pay zone damage, including drilling fluid filtrate incompatibilities with reservoir fluids, fines migration, and undesirable change of permeability and porosity. The cost-effective and single-stage application of new surfactant/oxidant system to enhance the removal efficiency of OBDF filter cake and minimize the formation damage and corrosion damage.

Rotational viscometer optimized the formulation of OBDF by regulating the rheological properties. Filter press simulated various high-pressure/high-temperature (HP/HT) well conditions in laboratory to form the OBDF filter cakes and remove them from sandstone disks. Drop shape analysis was performed to illustrate non-ionic surfactant treatment on OBDF emulsion. Inductively Coupled Plasma (ICP) equipment disclosed the cleanup mechanism of filter cake components by breakers. Formation damage was disclosed by experimental results of X-ray Computed Tomography (CT) scan and Coreflood implements. Corrosion rate was tested with L-80 metal to determine the most efficient corrosion inhibitor concentration.

Surfactant used in the new removal system breaks OBDF emulsion and thus expands the contact area between dense filter cake and effective breaker. Coated breaker can be circulated out of wellbore after the removal work, based on its low density and tightly coated property. HP/HT filter cake removal tests indicate the optimized new system can disperse and remove the OBDF filter cake by up to 98 wt% removal

efficiency. After 12 hours filter cake removal test, the optimized surfactant/oxidant system results in 4.38 % loss of initial porosity mostly and carried out the retained permeability up to 72.66 %. 1.5 and 2 wt % of 0% coated persulfate with 5 vol % of Rodine 31-a gave an industry accepted corrosion rate of 0.033 lb/ft^2 and 0.045 lb/ft^2, respectively, although pitting was still present on the faces of coupon.

With optimized formulation and soaking time, the cleaning solutions will benefit the oilfield industry significantly by removing OBDF filter cake under challenging well conditions. The new surfactant/oxidant system minimizes the effects of drilling fluids on formation properties, based on its quick removal steps, high removal efficiency, and acceptable formation damage and corrosion damage.

DEDICATION

This dissertation is dedicated to

My Beloved Parents, for their love and effort to make me who I am;

My beloved husband for his support and love during this journey;

My dear son for his accompany and love during my life;

My dear brother and lovely sister, for their support and help.

ACKNOWLEDGEMENTS

I would like to thank my committee chair academic advisor, Dr. Nasr-El-Din. I am grateful for his continuous encouragement, guidance, and support during the last four year. I appreciate his help on devoting his invaluable time to review my research work and evaluate its results. I hope to extend my appreciation to my committee members, Dr. Holditch, Dr. Schubert, and Dr. El-Halwagi, for their guidance and support throughout the course of my research.

Thanks also go to student members, lab technicians, and administrative officers of Dr. Nasr-El-Din group. Many thanks also to my friends and colleagues and the department faculty and staff for making my time at Texas A&M University a great experience.

Finally, thanks to my parents, my husband, my son, my brother, and my sister for their encouragement, patience, and love to me.

CONTRIBUTORS AND FUNDING SOURCES

Contributors

This work was supervised by a dissertation committee consisting of Professor Hisham A. Nasr-El-Din [advisor] and Stephen A. Holditch and Jerome J. Schubert of the Department of [Home Department] and Professor Mahmoud M. El-Halwagi of the Department of [Outside Department].

All work conducted for the dissertation was completed by the student independently.

Funding Sources

Graduate study was supported by a fellowship from Texas A&M University.

NOMENCLATURE

API	American Petroleum Institute
A	Cross-Sectional Area of the Filter-Core Outcrop, $in.^2$
BP	Bingham Plastic
CT_{wet}	CT Number of Wet Disk
CT_{dry}	CT Number of Dry Disk
CT_{brine}	CT Number of Brine Disk
CT_{air}	CT Number of Air Disk
E^0	Standard Electrode Potential
GLDA	N, N-Dicarboxymethyl Glutamic Acid Tetrasodium Salt
HEDTA	N-(2-Hydroxyethyl) Ethylenediaminetriacetic Acid
HP/HT	High-Pressure/High-Temperature
HSO_5^-	Persulfuric Acid Ion
HSO_4^-	Hydrogen Sulfate
$K_{initial}$	Permeability of Initial Filter Cake
K_{final}	Permeability of Final Filter Cake
$K_{final\ /}\ K_{initial}$	Average Permeability Ratio
L	Flow Routine Length as Constant, cm
$(NH_4)_2S_2O_8$	Ammonium Persulfate
$Na_2S_2O_8$	Sodium Persulfate

OBDF	Oil-Based Drilling Fluid
Q	Average Brine Flow Rate, cm^3/s
$S_2O_8^{2-}$	Persulfate Ion
PV	Plastic Viscosity
V_s	Mixing / Separation Volume of OBDF Emulsion
WBDF	Water-Based Drilling Fluid
W_{disk}	Weight of Disk before the Filter Cake Formed
$W_{disk + initial\ filter\ cake}$	Weight of Disk plus the Weight of Initial Filter Cake
$W_{disk + remaining\ filter\ cake}$	Weight of Disk plus the Weight of Remaining Filter Cake
YP	Yield Point
ΔP	Pressure Difference across the Filter Cake, psi
μ	Viscosity, cp

TABLE OF CONTENTS

Page

LIST OF FIGURES

Page

LIST OF TABLES

Page

1. [1]INTRODUCTION

1.1. Problem with OBDF Filter Cake

1.1.1. OBDF Filter Cake

Various functions of drilling fluids during drilling operations are including: (1) exert hydrostatic pressure over the permeable formation, suppress the formation pressure, and prevent well blowouts; (2) remove and carry drill cuttings from the downhole to well surface; (3) cool and lubricate drill bit in downhole condition. Drilling fluids are commonly categorized into three general types, namely water-based drilling fluids (WBDF), oil-based drilling fluids (OBDF) and synthetic based drilling fluids (SBDF). OBDF systems were developed and introduced in the 1960s.

The application rate of OBDF currently has reached over 80% in North America and Mexico. They can provide relatively excellent capacities for clay swelling inhibition, good lubrication performance, pollution reduction, thin filter cake characters, borehole walls collapse prevention, and high temperature stabilization. OBDF are significant sources of chemical exposure during drilling operation, and they might cause subsequently environmental effects on oil and gas formations after drilling operation.

Based on positive differential pressure between OBDF and pore-throat pressure, OBDF will form filter cake during the introduction of filtrate into the target zone. Filter

[1] *Reprinted with permission from "A Cost-Effective Application of New Surfactant/Oxidant System to Enhance the Removal Efficiency of Oil-Based Filter Cake" by J. Zhou et al., 2018. SPE-190115-MS, Copyright 2018 by Society of Petroleum Engineers.

cake have very thin thickness (no more than the space between formation surface and rig), and very low permeability (range from 0.01 mD to 0.0001 mD). Filter cake controls filtrate through the porous formations, reduces the filtrate invaded into formation, and minimizes the invasion of drilling fluids additive which have particles with small size.

OBDF is one type of drilling fluids that can enhance wellbore stability in water-sensitive reservoirs. OBDF includes oil as the continuous phase and water as the dispersed phase, in conjunction with viscosifiers, emulsifiers, filtration control agents, and weighting materials. OBDF can provide relatively excellent capacities for clay swelling inhibition, good lubrication performance, pollution reduction, thin filter cake characters, borehole walls collapse prevention, and high temperature stabilization. Based on positive differential pressure between OBDF and pore-throat pressure, OBDF will form filter cake during the introduction of filtrate into the target zone (**Figure 1**). OBDF filter cake is composed of colloid particles and water-in-oil emulsion (water droplets dispersed in an oil phase, as shown in **Figure 2**).

Most of filter cake compositions can be attributed to the drilling fluid weighting material, and the rest are functional additives, such like viscosifiers, emulsifiers, alkalinity control agents, and filtration control agents. OBDF filter cake solids are mainly hydrophobic, and the filter cake permeability is much lower than the rock permeability. Filter cake is used as a barrier between the wellbore and the formation. It minimizes unwanted propagation of solids and fluids.

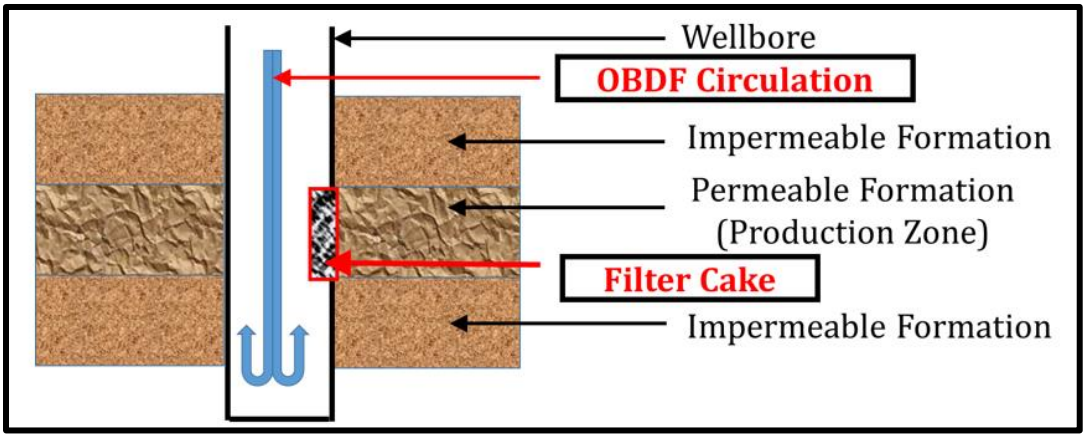

Figure 1 Filter cake formation.

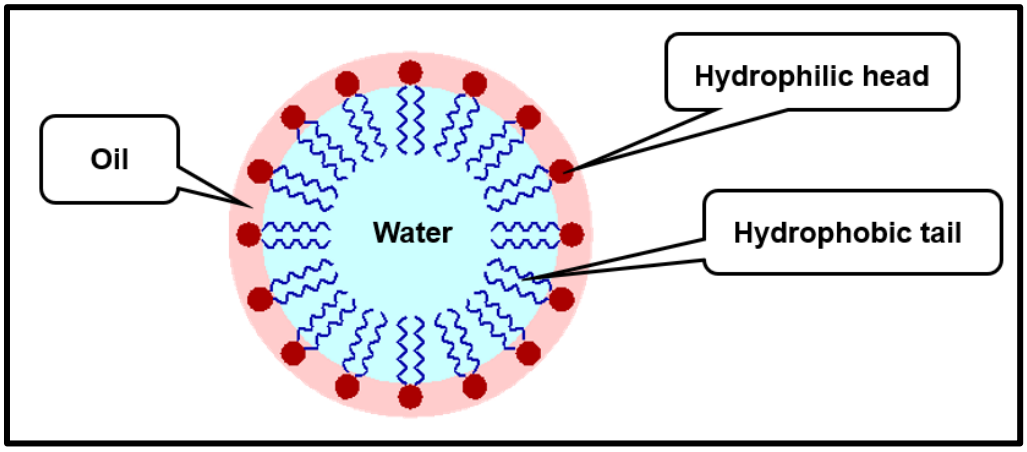

Figure 2 Water–in–oil emulsion. Reprinted with permission from SPE-190115-MS.

In open-hole completions, OBDF filter cakes can cause formation damage like plugging of pore throats, sticking of drill pipes, and shrinkage of borehole. In the oil and gas industry, before a well is put into production, a cleaning solution is applied to disperse, break down, and remove the filter cake (Allogo et al. 2016). Although the surface tension of oil is lower than of water, OBDF filter cake could be adsorbed and retained on the formation surface tightly after the drilling. Inadequate removal of filter

cake in HP/HT conditions creates the potential of pore-throat plugging and drawdown wellbore pressure (Alimuddin et al. 2016).

1.1.2. Formation Damage from OBDF Filter Cake

Development of drilling and completing horizontal wells can drive the enlarged production flow area, which boosts production of oil or gas. However, these horizontal wells have long open-hole sections that contact with the drilling fluid and filter cake for long periods of time which might cause formation damage (Bennion et al. 1996; Christian et al. 2009; Vickers et al. 2011; Menezes et al. 2012). Siddique et al. (2017) explained that in oil and gas industry, the drilling process produces three main types of wastes: drill cuttings, drilling fluid filtrate and filter cake.

Main factors of OBDF formation damage refer to the solids phase invasion, multi-phase flow effect, wettability reversal, emulsion or filter cake plugging. In view of mechanically drilling equipment, filter cake might also cause the stuck pipe incidents together with the near well-bore formation damage. Operator companies employ several methods to mitigate the stuck pipe incidents (**Figure 3**). These methods consist of decreasing the drilling fluids density to minimize the overbalance, minimizing stationary time, increasing drill collar or drill string stabilization, but all will highly raise the drilling costs and drilling periods.

Yonebayashi et al. (2017) designed a series of laboratory works to identify the reasons that formation damage caused by OBDF filter cake, such as near well-bore formation damage (including wettability change, emulsion or filter cake blockage), or

plugging in certain sections of the case hole that including the perforation tunnel. They found that a certain level of formation damage was concerned from the near-wellbore area in the oil-bearing zone of the reservoir, other than from the certain sections of the case hole.

It is imperative to design filter cake cleaning solutions which can help in mitigating the issues and costs arising due to the oil-based filter cake. To design a sustainable and viable filter cake management and removal plan, the first step is to identify the basic composition and the sources of pollutants inside the oil-based filter cake. OBDF filter cake is composed of colloid particles and water droplets dispersed in an oil phase (water-in-oil emulsion).

About 70 % to 80 % of the mineral composition of filter cake can be attributed to the drilling fluid weighting material, and the rest are functional additives, such like viscosifiers, emulsifiers, alkalinity control agents, and filtration control agents. OBDF filter cake solids are mainly hydrophobic, and the filter cake permeability is much lower than the rock permeability. Filter cake consist of diesel or mineral oil containing different types of polycyclic aromatic hydrocarbons (PAHS) and are also considered as a flammable hazard source.

Although the surface tension of oil is lower than of water, filter cake could be also adsorbed and retained on the formation surface after the drilling. The change in wettability of the formation surface from water-wet to oil-wet by the emulsifiers of OBDF, would heighten the flow resistance of oil and gas in the percolation channel, adversely affecting well production (Siddique et al. 2017, **Figure 4**). Emulsifiers inside

OBDF created water-in-oil emulsions, altered the formation surface to be more oil-wet, and made oil-wetting components of OBDF invaded into the formation pore throats.

The contact surface between formation water and oil-wetting components of OBDF filter cake, can easily form stable water-in-oil emulsion under the effect of emulsifiers that may damage reservoirs by plugging pore throats and fractures.

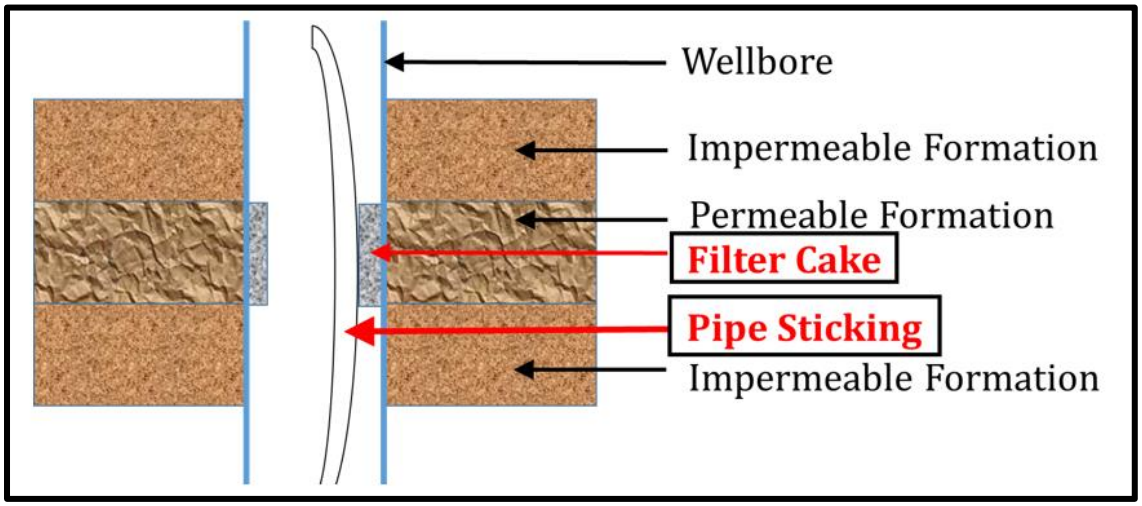

Figure 3 Pipe sticking incidents in drilling.

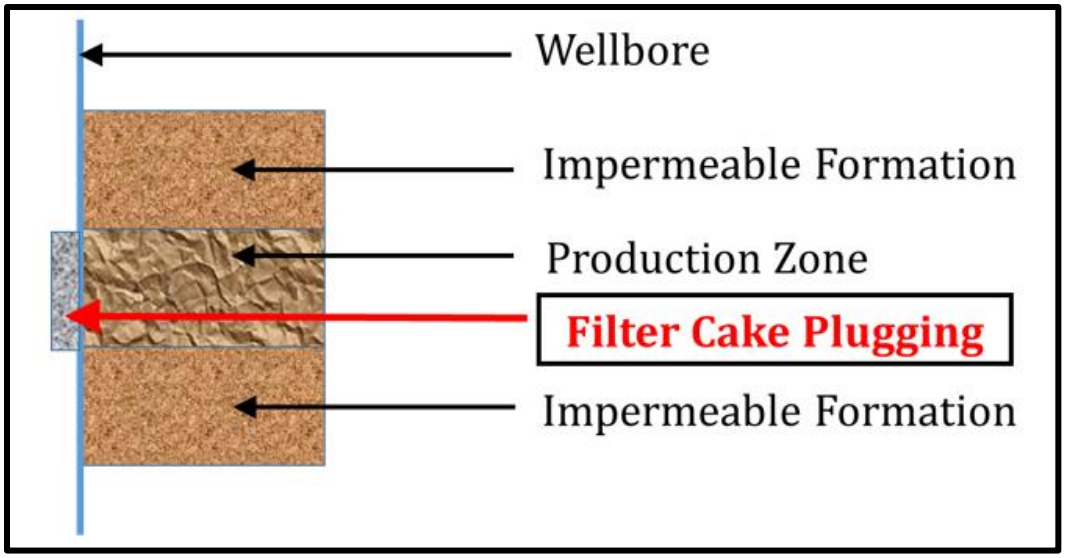

Figure 4 Filter cake plugging in production.

1.1.3. Remove OBDF Filter Cake

Different mechanisms have been developed and improved, which aimed at treating filter cake. They are including non-biological treatment processes, disposal options and bioremediation technologies. After completion of drilling, a cleanup treatment to remove the OBDF filter cake is needed to minimize skin damage and formation damage, extend production flow, and restore the productive zone to a near-natural state.

The most important function of cleanup treatment for OBDF filter cake is to break down the external water-in-oil emulsion, wash the damaged zone of formation surface, and store the formation's fluid transfer properties. The cleaning steps of OBDF filter cakes fall primarily into three major parts: (1) break OBDF emulsion with the degradation of emulsifiers inside OBDF filter cake; (2) lower the surface tension and reduce the contact angle between formation surface and oil-wetting additives inside

OBDF filter cake; (3) breakdown the long chains of organic additives to lower the viscosity and the resistance of flow, and upgrade the rate of circulating out; (4) dissolve weighting materials if possible.

1.2. Application of Surfactant and "Breaker" to Clean OBDF Filter Cake

Formate brines, live mineral acids, HCl, organic acids, chelating agents, or a combination of these additives, are conventional chemicals to remove water-based drilling fluid (WBDF) filter cake. Multiple stages and large volumes of solvents are always applied in OBDF filter cake removal using conventional chemicals. Single-stage cleaning solutions have been proposed, tested, and applied into drilling work because of their simple operation and economic application. The new surfactant/oxidant system developed in this work will be single-stage, and the optimized formula will also be examined in the laboratory.

1.2.1. Surfactant Treatment for OBDF Emulsion

Basic surfactant consists of a hydrophilic (strongly attracted to water) part and a hydrophobic (very little attraction for water) part. When added to form an aqueous cleaning solution, the hydrophilic part arranges itself toward the water phase while the hydrophobic part tries to remove itself from the water by attaching to any surface beside water.

The major surfactant classes are anionic, cationic, amphoteric, and nonionic surfactants. Surfactants are classified by the ionic charge of the hydrophilic group in water solution. Anionic surfactant has a negative charge. They tend to be affected by

water hardness ions and generate higher foam levels, than other surfactant classes (Anton et al. 1990 and 2007). Cationic surfactants might attach on sandstone surface (have negative charges) and induce chemical pollutes to sandstone reservoirs.

Amphoteric surfactants develop a negative or positive charge depending on whether the pH of solution is alkaline or acidic. Amphoteric surfactants provide mildness, intensify wetting properties, low foaming characteristics, stability, and good hydrotropic or coupling ability. Nonionic surfactants do not have an ionic charge. They are lower foaming and are less affected by water hardness ions (Ca and Mg). Nonionic surfactant does not dissociate when dissolved in water and have the broadest range of properties depending upon the ratio of hydrophilic-lipophilic balance (HLB). This balance is affected by temperature. The hydrophobic ability is strengthened, and solubility is cut down as temperature is elevating (Yaghmur et al. 2002).

Surfactants adsorb onto a variety of surfaces in the process to lower the surface tension between the different media (Bourrel et al. 1982; Parekh and Sharma 2004). When treat OBDF filter cake, the surfactant was optimized to reduce capillary force, destroy the emulsion on: (1) filtrate-cake surface; (2) the mixture of oil-based filtrate and formation water; (3) the solid-phase cementing structure (Menezes et al. 1989; Zanten et al. 2010).

The surfactant must flocculate the water droplets in OBDF emulsion firstly. During flocculation, the droplets clump together forming aggregates or flocs. Coalescence follows the flocculation and is the second step in the breaker process. During coalescence, water droplets fuse to form larger drops. Coalescence leads to

complete phase separation (oil and water) and emulsion breaking. This displacement changes properties like interfacial viscosity or elasticity of the protecting film, thus enhancing destabilizations.

The surfactant makes the reservoir water wet, break the water-in-oil emulsion, hence resulting to faster cleanup and recovery of hydrocarbon (Yan et al. 1993). It will lower the surface tension of the liquid, helping the hydrocarbon to overcome the resistance of a liquid/gas interface (El Sherbeny et al. 2013; Sabatini et al. 2003).

Davison et al. (2000) firstly used the combination of surfactant and inorganic/organic solvent to remove oil-based filter cakes. Al-Otaibi et al. (2010) stated that in Saudi Arabia many sandstone reservoirs are drilled with invert emulsion drill-in fluid to avoid the risk of clays swelling, but production impairment due to drilling fluids damage effect was observed in some horizontal wells drilled with inverted emulsion drill-in fluid and completed with stand-alone screens because of improper mud management. They proposed a single-stage microemulsion based treatment to remove OBDF filter cake screen blockage.

The microemulsion composes of sodium brine, surfactant, corrosion inhibitor, and organic acid breaker. Microemulsion system can also be a single-phase that oil and water are co-solubilized by the surfactants and it can be designed as a treatment for OBDF displacement/cleanup and removal of formation damage in open-hole and cased hole (Ezrahi et al. 1999; Garti et al. 2004; Quintero et al. 2009; Darugar et al. 2012; Brege et al. 2012). Mesophase systems (surfactant and acid blend) are customized blends based on microemulsion technology.

They have been used to destroy invert emulsion filter cakes that weighted by calcium carbonate in open-hole production and water injection applications (Christian 2009; Quintero et al. 2010; Pietrangeli et al. 2014; Addagalla et al. 2015 and 2016). The mesophase systems have high oil solubilization, high diffusion coefficients through porous media, and the reduction of interfacial tension between organic and aqueous phases to near zero, making them excellent candidates for removing formation damage in sandstone.

1.2.2. Oxidant and Formic Acid Treatment for Filter Cake Components

The degradation and cleanup of organic components of filter cake is achieved by reducing the fluid viscosity using chemical additives called ‘breakers”. There are many different types of breakers used in the industry, but they can be divided into two categories: enzymes and oxidizers.

Numerous laboratory studies have been conducted by using these enzymes and oxidizers to understand and migrate the damage caused by use of crosslinked polymer fluids (Imqam et al. 2014). Enzymes only attack specific biopolymer chains, and always lose their effectiveness when quickly denatured in high temperatures.

Oxidizers work by reacting with active sites on the polymer chains, and, under ideal conditions, will break the polymer chain at key linkages, thus degrading the polymer strand to its base units of simple sugars (O’Driscoll et al. 1998).

Ammonium persulfate and sodium persulfate are the most common oxidants used in the industry (Sarwar et al. 2011). Al-Muntasheri et al. (2017) stated that in

polymer-based aqueous fluids, persulfate breakers can be used to reduce fluid viscosity by degrading polymer chains and reducing the molecular weight of polymers. Ammonium persulfate and sodium persulfate salts dissociate in water to form the persulfate anion ($S_2O_8^{2-}$), which has a strong oxidation potential (E^0 = 2.01V) and generates sulfate-free radicals that react with polymers.

These sulfate-free radicals will extract any hydrogen atoms on the polymer backbones. Ammonium persulfate has a higher solubility in water than sodium persulfate and potassium persulfate (Persulfate Technical Information 2011). **Equations 1**, **2,** and **3** lay out the electromotive force data and indicate that $S_2O_8^{2-}$ has the strongest oxidation potential.

$$S_2O_8^{2-} + 2H^+ + 2e^- \rightarrow 2HSO_4^-,\ E^0 = 2.12V \quad \textbf{Equation 1}$$

$$H_2O_2 + 2H^+ + 2e^- \rightarrow 2H_2O,\ E^0 = 1.77V \quad \textbf{Equation 2}$$

$$HSO_5^- + 2H^+ + 2e^- \rightarrow HSO_4^- + H_2O,\ E^0 = 1.44V \quad \textbf{Equation 3}$$

Different products will be created by the reaction of persulfate ions with water. The reactive products of persulfate ions with water might be H_2O_2, HSO_4^-, and HSO_5^-. Higher solubility of ammonium persulfate promotes it to produce higher concentration of H_2O_2, HSO_4^-, and HSO_5^- in dilute acidic condition. These three breakers, H_2O_2, HSO_4^-, and HSO_5^-, can strongly break down OBDF filter cake layers and components. Coated chemicals always have resistance to release in the exposure conditions such as higher temperature and hydrogen sulfide.

A surfactant is an amphiphilic molecule, composed of a hydrophobic tail group with a carbon chain length, and a hydrophilic head group (Okoro et al. 2015). The viscosities of surfactants used in the oil and gas industry may vary from less than 1 cp, to slightly more than 1,000 cp. These surfactants act as emulsifiers and oil-wetting agents. They are composed of organic, fatty-acid soaps (Salazar et al. 2007).

Many factors can affect the surfactants' behavior, including salinity and temperature, and these factors will be discussed in this report. Surfactant-enhanced in-situ chemical oxidation (Hoag 2010), creates the solubilized oil-in-water micro-emulsion and destroys the non-aqueous phase. The oxidants (sodium persulfate and hydrogen peroxide) generate powerful free-radical oxidant systems and destroy solubilized contaminants.

Dense non-aqueous phase liquid (DNAPL) is denser than water, but does not dissolve in water, and this term is used primarily to denote groundwater, surface water, and sediment contaminants. At the molecular level, surfactant grubs and solubilizes the

DNAPL, then free radicals are made by activating oxidants. OBDF filter cake can be dispersed and removed by a surfactant/oxidant system with the same mechanism. This research proposes a brine-based OBDF filter cake removal system, which penetrates, disperses, and removes the OBDF filter cake, depending on the powerful oxidant (persulfate salts) and non-ionic surfactant.

Ammonium persulfate and sodium persulfate are the most common breakers used in the industry (Sarwar et al. 2011). Ammonium persulfate has a higher solubility (**Figure 5**) in water than sodium persulfate and potassium persulfate. **Figure 6** gives the molecular structures of sodium persulfate ($Na_2S_2O_8$) and ammonium persulfate [$(NH_4)_2S_2O_8$].

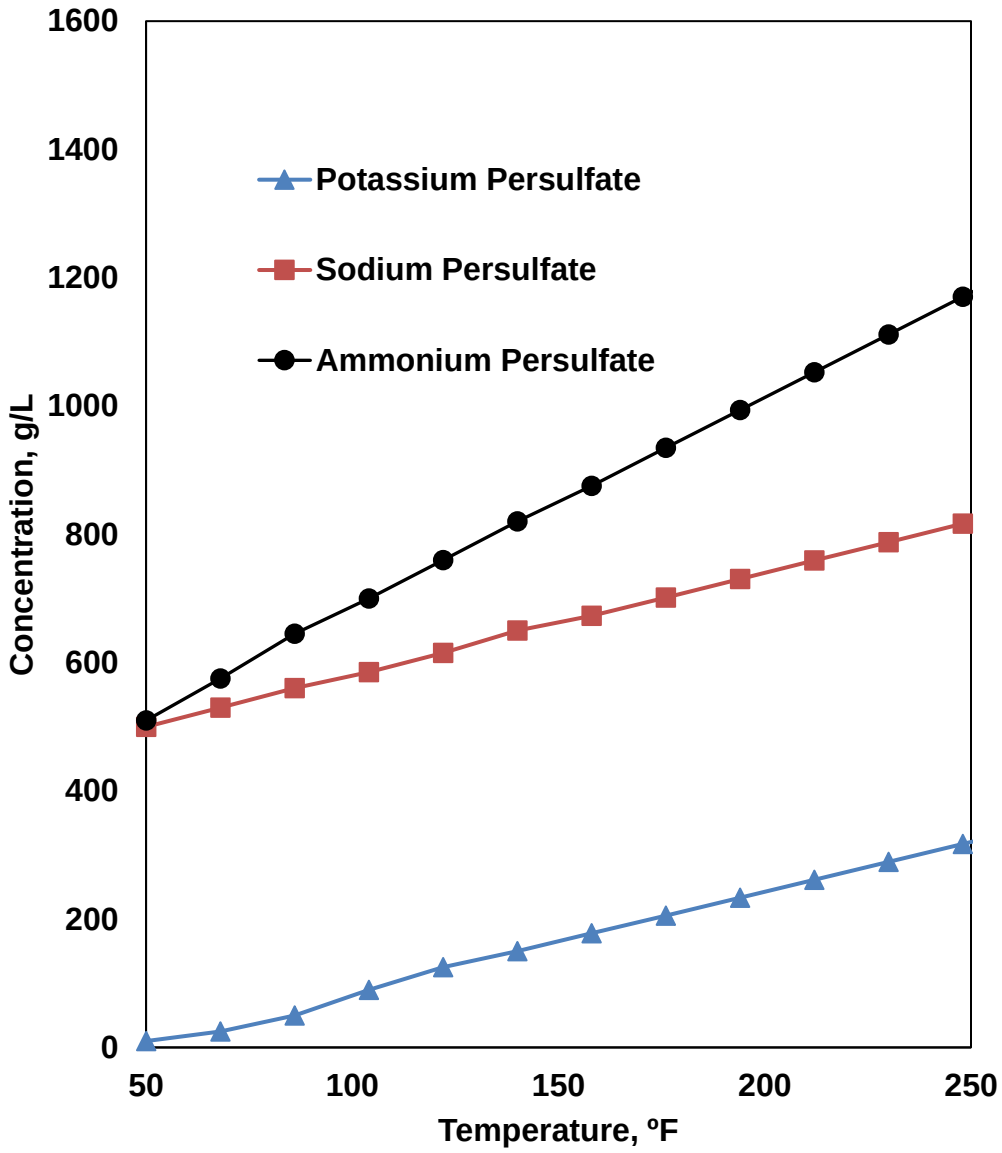

Figure 5 Solubility of common persulfate salts in water. "Reprinted from [Persulfate Technical Information 2011].

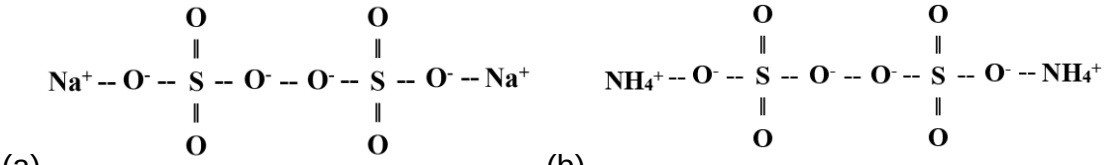

Figure 6 Molecular structures of (a) sodium persulfate and (b) ammonium persulfate. Reprinted with permission from SPE-190115-MS.

Different products will be created by the reaction of persulfate ions with water (**Equations 4**, **5**, **6**, and **7**). The removal efficiency of a persulfate breaker is highly dependent on pH and temperature. The pH values of the new surfactant/oxidant system will be measured after soaking the OBDF filter cake 4, 8, and 12 hours under differential pressure and temperature conditions.

Neutral (pH 3 to 7): $S_2O_8^{2-} + H_2O \longrightarrow 2HSO_4^- + \frac{1}{2} O_2$, …….…. **Equation 4**

Dilute acid (pH > 0.3; [H⁺] < 0.5M): $S_2O_8^{2-} + 2H_2O \xrightarrow{H^+} 2HSO_4^- + H_2O_2$,

……..…….…. **Equation 5**

Strong acid ([H⁺] > 0.5M): $S_2O_8^{2-} + H_2O \longrightarrow HSO_4^- + HSO_5^-$,

…….…. **Equation 6**

Alkaline (pH > 13): $S_2O_8^{2-} + OH^- \longrightarrow HSO_4^- + SO_4^{2-} + \frac{1}{2} O_2$,

…… **Equation 7**

When treat OBDF filter cake, the surfactant was optimized to reduce capillary force, destroy the OBDF emulsion (water-in-oil emulsion). Surfactant adsorption will always increase the production based on lower capillary pressure when removing filter cakes from reservoirs with small pore throats. The surfactant must flocculate the water droplets in OBDF emulsion firstly.

During flocculation, the droplets clump together forming aggregates or flocs. Coalescence follows the flocculation and is the second step in the breaker process. During coalescence, water droplets fuse to form larger drops. Coalescence leads to complete phase separation (oil and water) and emulsion breaking. This displacement changes properties like interfacial viscosity or elasticity of the protecting film, thus enhancing destabilizations (Yan et al. 1993; Sabatini et al. 2003; El-Sherbeny et al. 2013).

After the breakdown of OBDF emulsion, filter cake cleanup is achieved by reducing the fluid viscosity using chemical additives called ‘breakers”. Oxidizers work by reacting with active sites on the polymer chains, and, under ideal conditions, will break the polymer chain at key linkages, thus degrading the polymer strand to its base units of simple sugars (O’Driscoll et al. 1998). Al-Muntasheri et al. (2017) stated that in polymer-based aqueous fluids, persulfate breakers can be used to reduce fluid viscosity by degrading polymer chains and reducing the molecular weight of polymers.

1.2.3. Formic Acid

Formic acid (HCOOH) is the simplest carboxylic acid. It is commercially available in various concentrations and relatively cheaper than the other organic acids, like oxalic acid, lactic acid and citric acid et al. Formic acid is much less corrosive to metals than the strong acids like HCl and HF. Formic has density of 1.192 g/cm^3 and pH is $\leq$1.

Completion fluids with low surface tension are required to reduce the capillary forces. Formic acid has the lowest surface tension than acetic, and lactic acid systems (Al Moajil et al. 2015). Al-Otaibi et al. (2010) used the combination of acetic acid and surfactant to remove $CaCO_3$ weighted invert emulsion drilling fluids filter cake. Binmoqbil et al. (2009) proposed an in-situ acid-precursor which can generate formic acid, to facilitate the reactivity of the produced acid with calcium carbonate weighting materials, after incorporated a special surfactant blend to alter the wettability of the oily filter cake. Formic acid can dissolve $CaCO_3$ and form calcium formate $Ca(HCO_2)_2$.

Formic acid can also react with Mn_3O_4 to product two chemical, which depends on charge of Mn ion: $Mn(OCOH)_2 \bullet 2H_2O$ (it is for Mn^{2+}) and $Mn_3(OCOH)_6[OCOH]_3 \bullet 2H_2O$ (it is for Mn^{3+}). The red monoclinic crystals of Mn(II) formate dehydrate [$Mn(OCOH)_2 \bullet 2H_2O$] are obtained by the reaction of formic acid with Mn_3O_4 (Kemmitt and Peacock 1973). Al Moajil et al. (2008; 2010; 2012) published a series of papers to manifest that at temperature above 212°F, formic acid will have the highest Mn_3O_4 dissolve ability than sulfonic acid, malic acid, citric acid, lactic acid, and acetic acid.

2. PREVIOUS STUDIES

With well-established surfactant additives, the OBDF emulsion can be broke down to expand the contact area between dense filter cake and effective breaker. Davison et al. (2000) firstly used the combination of surfactant and inorganic/organic solvent to remove oil-based filter cakes. Al-Otaibi et al. (2010) stated that in Saudi Arabia many sandstone reservoirs are drilled with invert emulsion drill-in fluid to avoid the risk of clays swelling, but production impairment due to drilling fluids damage effect was observed in some horizontal wells drilled with inverted emulsion drill-in fluid and completed with stand-alone screens because of improper mud management. They proposed a single-stage microemulsion (composes of sodium brine, surfactant, corrosion inhibitor, and organic acid breaker) based treatment to remove OBDF filter cake screen blockage.

Microemulsion system can also be a single-phase that oil and water are co-solubilized by the surfactants and it can be designed as a treatment for OBDF displacement/cleanup and removal of formation damage in open-hole and cased hole (Ezrahi et al. 1999; Garti et al. 2004; Quintero et al. 2009; Darugar et al. 2012; Brege et al. 2012).

3. OBJECTIVES

The cleanup mechanism and the removal efficiency will be investigated when applying the new surfactant/oxidant system to clean OBDF (with clay and without clay) filter cake in this research. This paper proposes the application of the new removal system (5 or 18 wt% KCl-based) to optimize OBDF filter cake removal efficiency and minimized the damage with the new surfactant/oxidant system (**Figures 7**, **8**, and **9**).

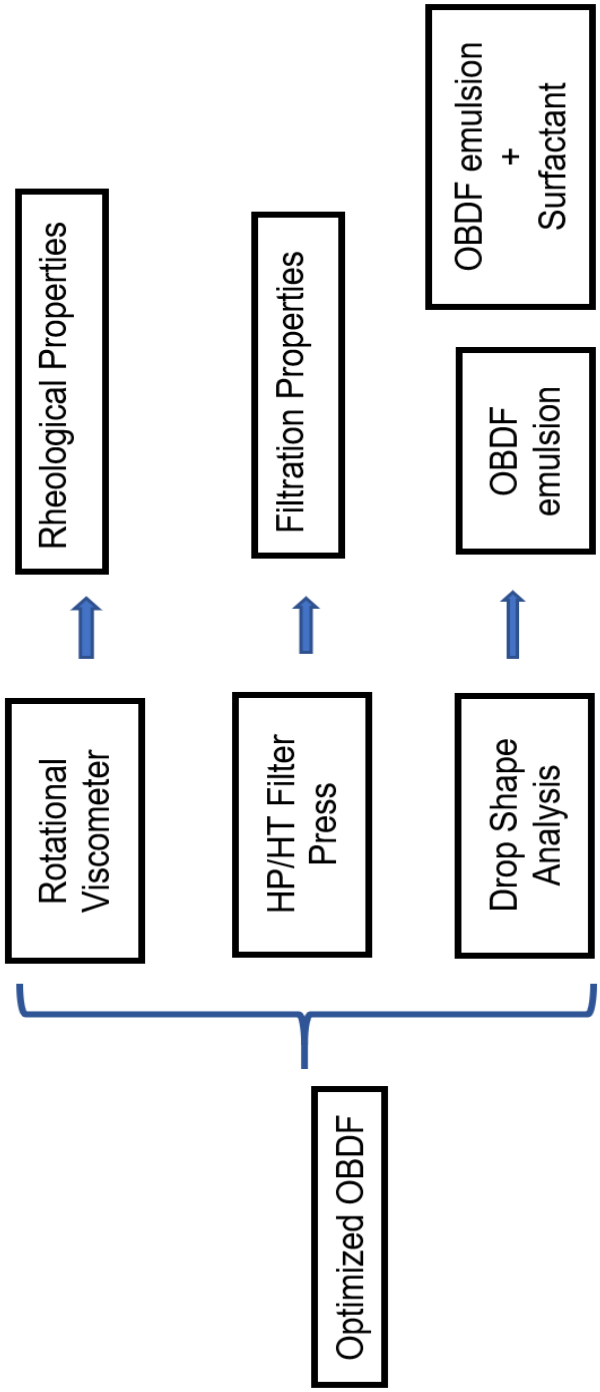

Figure 7 Performance evaluation of OBDF.

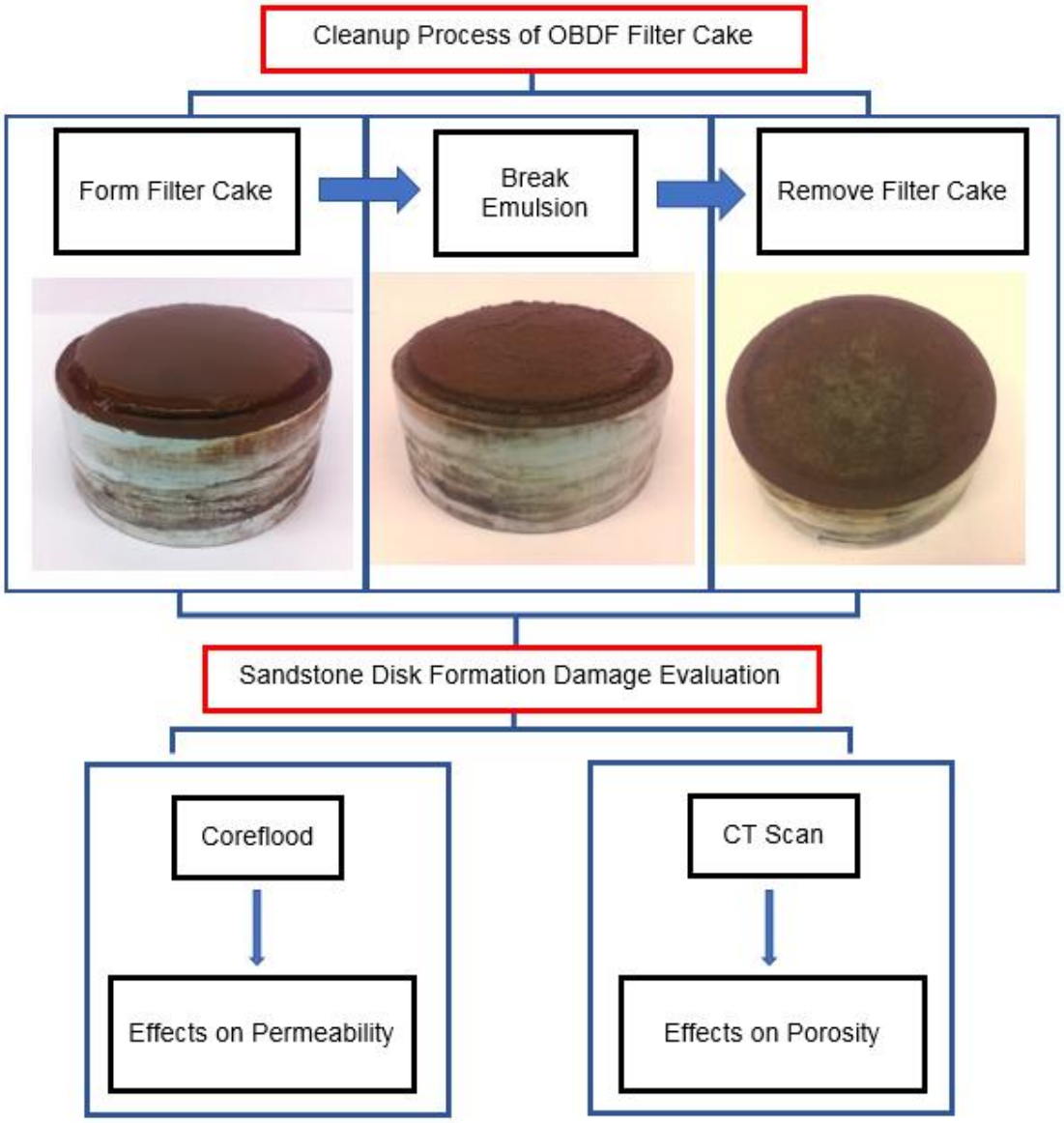

Figure 8 Chart description of OBDF filter cake cleanup process and relative formation damage evaluation based on disk level.

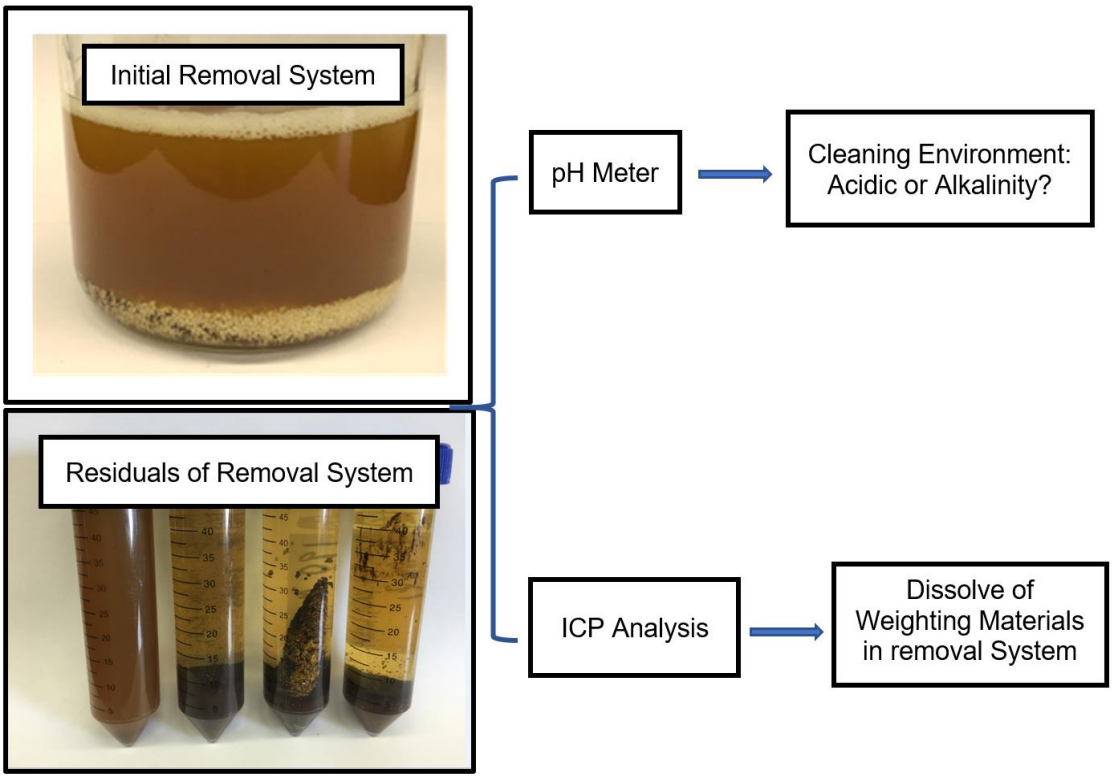

Figure 9 Experimental methods of removal system formation damage evaluation.

4. [2]EXPERIMENTAL STUDIES

4.1. Experimental Set-Ups

4.1.1. Equipment

Equipment operated in laboratory consist of: Hydraulic Core-cutting Machine, Nitrogen Pressure Cylinder, Rolling Oven, Drilling Fluid Multi-Mixer, Rotational Viscometer, X-ray Computed Tomography (CT) Scan, High Pressure and High Temperature (HP/HT) Filter Press, Inductively Coupled Plasma (ICP), X-ray Diffraction (XRD), Coreflood, Drop Shape Analysis, Parr Benchtop Corrosion Reactor.

4.1.2. Materials

4.1.2.1. Novel Surfactant/Oxidant Formulations.

Four cleaning solutions were prepared and tested to optimize the cleanup of filter cakes. The variable parameters to prepare the new surfactant/oxidant system were the type and quantity of coated persulfates. The KCl concentration of each cleaning solution was 5 or 18 wt%. A corrosion inhibitor at 0.3 wt% was added to each cleaning solution. **Figure 10** and **Table 1** show the components of the cleaning solutions tested in the present study.

---

*Reprinted with permission from "A Cost-Effective Application of New Surfactant/Oxidant System to Enhance the Removal Efficiency of Oil-Based Filter Cake" by J. Zhou, 2018. SPE-190115-MS, Copyright 2018 by Society of Petroleum Engineers.

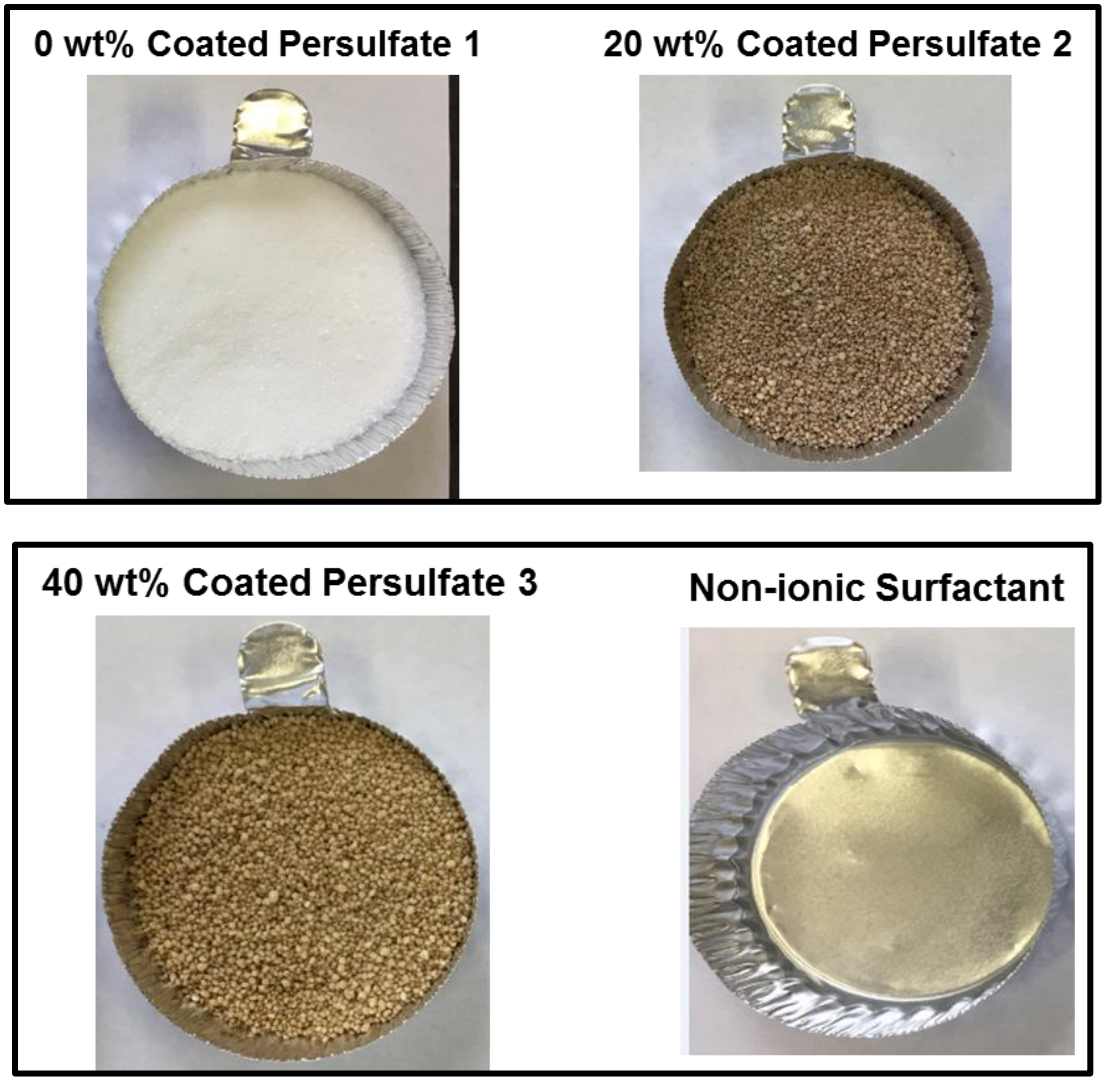

Figure 10 Components of the new surfactant/oxidant system. Reprinted with permission from SPE-190115-MS.

Table 1 Formulations of the new surfactant/oxidant system. Reprinted with permission from SPE-190115-MS.

Cleaning Solution	5 or 18 wt% KCl, cm^3	0 wt% Coated Sodium Persulfate 1, g	20 wt% Coated Ammonium Persulfate 2, g	40 wt% Coated Ammonium Persulfate 3, g	Non-ionic Surfactant, g	Corrosion Inhibitor, wt%
B1	250	12.5	-	-	6.25	0.3
B2	250	-	15.625	-	6.25	0.3
B3	250	-	-	20.825	6.25	0.3
B4	250	4.175	5.2	6.95	6.25	0.3

4.1.2.2. OBDF Formula

The prepared OBDF in this paper can also be called Invert-Emulsion Drilling Fluids (IEDF). IEDF is one type of OBDF that has the stable ability to form water-in-oil emulsion and control sand production, with the adding of emulsifiers into conventional OBDF formulation. 1.7 S.G. OBDF was mixed using a multi-mixer in a stainless-steel mixing cup.

The functional descriptions of each component are as follows:

(1) The prepared OBDF had mineral oil as the continuous phase, and water as the dispersed phase. Mineral oil is less toxic than diesel oil, and the oil retention properties of OBDF with mineral oil are less than OBDF with diesel (Jha et al. 2014).

Mineral oil was added to the OBDF in the amount of 161.7 g. The specific gravity of used mineral oil was 0.79-0.81 (at 15.6°C) and the viscosity of mineral oil was 1.9-2.2 cp (at 40°C) (Rehman et al. 2012).

(2) 18.7 g lime was added to control the alkalinity of OBDF. Lime can reinforce the pH value of OBDF to 10. Lime is an inorganic compound with the chemical formula as $Ca(OH)_2$. It is a colorless crystal or white powder.

(3) Two types of viscosifiers, named modified hectorite and modified smectite, were added into targeted OBDF, for improving the viscosity of OBDF in HP/HT conditions. Modified hectorite and modified smectite are both lipophilic minerals, which are modified by oil-wetting agent.

The oil-wetting agent is quaternary fatty acid amine in this research. These lipophilic minerals present as finely dispersed particles in oil phase, which can easily invade into pore throats and seepage channel of oil-bearing zone. Earth materials containing oil are called oil-bearing zone (oil-bearing sediments), which also include oil sands (tar sands).

(4) The emulsifiers added to OBDF were blend of polyamide and mineral oil, and blend of glycol ether with fatty acid. Emulsifiers in OBDF provided high viscoelasticity and shear properties of non-Newtonian fluids.

Water-in-oil emulsion was formed among mineral oil, water and emulsifiers in prepared OBDF. The emulsion can cause wetting reversal, such as transform wettability on rock surface from hydrophilicity to lipophilicity. Accordingly, the oil phase and lipophilic colloid are more easily attached to the rock surface.

(5) 97 wt% $CaCl_2$ with amount of 10 g was added to achieve osmotic wellbore stability when drilling water-sensitive reservoirs. Osmosis is the spontaneous movement of molecules through a semi-permeable membrane into a region of higher molecules concentration, to equalize the ions concentrations on both sides of membrane.

$CaCl_2$ balanced the Ca concentration between formation water and OBDF, thus prevent Ca invading into OBDF from formation water.

(6) 16.7 g organophilic lignite was lipophilic mineral modified by quaternary fatty acid amine, to provide filtration control and rheological stability. Lignite, also called brown coal, is the lowest rank of coal due to its relatively low heat content. Organophilic lignite as bridging materials helped to form low permeable filter cake.

(7) 40 g Calcium carbonate ($CaCO_3$) with a density of 2.78 g/cm^3 and a mean pore size (D50) of 50 μm, 205 g manganese tetroxide (Mn_3O_4) with a density of 4.8 g/cm^3 and a D50 of 1 μm were used as the weighting materials in OBDF (Zhou and Nasr-El-Din 2017).

With the adding of Mn_3O_4, OBDF achieved very low plastic viscosity (PV) at the fluid density requirement and the ability to suspend Mn_3O_4 at lower fluid viscosity (Franks and Marshall 2004). The size distributions of weighting materials were measured by sieve analysis tester because size distributions significantly affect the shut-off process and the ability of OBDF to flow back to the wellbore.

Same size range of weighting materials in this study was sieved with specific micron mish before using. The chemical compositions of used weighting materials in

this study were evaluated by X-ray Fluorescence (XRF) equipment (Al Moajil and Nasr-El-Din 2013).

Mn_3O_4 is a strong oxidant because it has tetragonal symmetry and nonstoichiometric behavior when compared with a tetrahedral MnO and octahedral Mn_2O_3 (Gillot et al. 2001; Berbenni and Marini 2003). Mn_3O_4 has 74.3 wt% Mn ion and $CaCO_3$ has 38.9 wt% Ca ion. These two concentrations were recorded as important values, to evaluate the ability of cleaning solutions to dissolve weighting materials in ICP elements evaluation. OBDF (**Tables 3** and **4**) were mixed using a multi-mixer in a stainless-steel mixing cup.

Table 2 XRF analysis of OBDF weighting materials. Reprinted with permission from SPE-190115-MS.

	Mn_3O_4	$CaCO_3$
Element	**wt%**	**wt%**
Mn	74.3	-
Ca	-	38.9
Fe	2.5	-
Zn	0.3	-
Pb	0.2	-
K	0.1	-
Si	0.1	0.2
Al	-	0.1
Mg	-	0.3
Ba	-	0.1
Sr	-	0.1
Total	100	100

Table 3 OBDF (with clay) formulation. Reprinted with permission from SPE-190115-MS.

Component	Function	Laboratory (per 320 cm^3)		Field (per bbl)		Mixing Time (minutes)
		Quantity	Unit	Quantity	Unit	
Mineral Oil	Continuous Phase	161.7	g	161.7	bbl	-
Organophilic Clay	Viscosifier	4	g	4	lbm	10
$Ca(OH)_2$	Alkalinity Control	18.7	g	18.7	lbm	10
Polyamide/Mineral Oil Blend	HT Primary Emulsifier	10	g	10	lbm	10
Glycol Ether/Fatty Acid Blend	HT Secondary Emulsifier	10	g	10	lbm	10
Deionized Water	Dispersed Phase	16.3	g	0.045	lbm	10
$CaCl_2$ (97 wt%)	Osmotic Wellbore Stabilizer	10	g	10	lbm	10
Organophilic Lignite	HT Filtration Control	16.7	g	16.7	g	10
$CaCO_3$ (2.71 g/cm^3, D_{50} = 50 µm)	HT Filtration Control	40	g	40	lbm	10
Mn_3O_4 (4.8 g/cm^3, D_{50} = 1 µm)	Weighting Material	205	g	205	lbm	15

Table 4 OBDF (without clay) formulation. Reprinted with permission from SPE-190115-MS.

Components	Function	Laboratory (per 320 m^3)		Field (per bbl)		Mixing Time (minutes)
		Quantity	Unit	Quantity	Unit	
Mineral Oil	Continuous Phase	161.7	g	161.7	bbl	-
Polymer	Viscosifier	4	g	4	lbm	10
$Ca(OH)_2$	Alkalinity Control	18.7	g	18.7	lbm	10
Polyamide/Mineral Oil Blend	HT Primary Emulsifier	10	g	10	lbm	10
Glycol Ether/Fatty Acid Blend	HT Secondary Emulsifier	10	g	10	lbm	10
Deionized Water	Dispersed Phase	16.3	g	0.045	lbm	10
$CaCl_2$ (97 wt%)	Osmotic Wellbore Stabilizer	10	g	10	lbm	10
Organophilic Lignite	HT Filtration Control	16.7	g	16.7	g	10
$CaCO_3$ (2.71 g/cm^3, D_{50} = 50 µm)	HT Filtration Control	40	g	40	lbm	10

Mn_3O_4 (4.8 g/cm^3, D_{50} = 1 µm)	Weighting Material	205	g	205	lbm	15

4.1.2.3. Berea Sandstone Disks

The mineralogy of Berea sandstone disk was measured by an X-ray diffraction (XRD) test (**Figure 11**). According to **Table 5** and **Figure 12**, Berea sandstone disks used to complete this research mainly consist of 81.79 wt% quartz, 9.07 wt% muscovite and other minimal minerals.

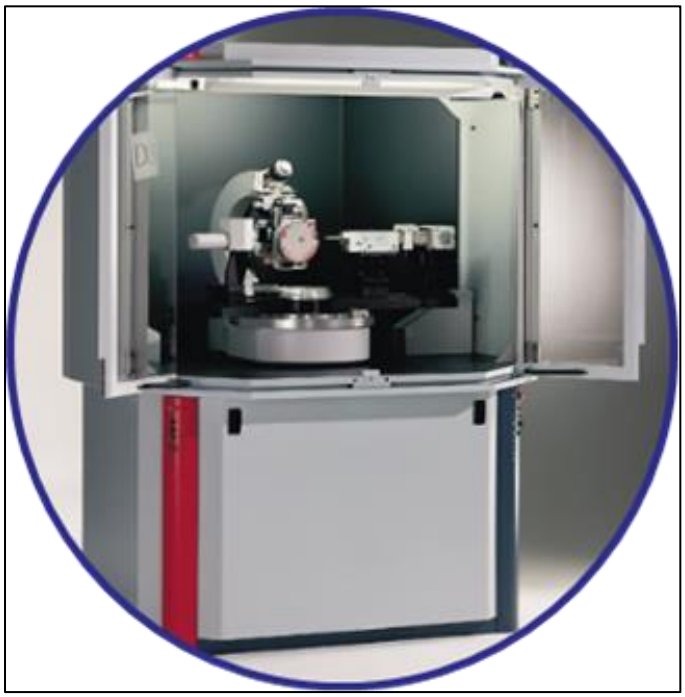

Figure 11 Display of X-Ray diffraction spectrum (XRD) equipment. Reprinted with permission from SPE-190115-MS.

Table 5 X-Ray diffraction (XRD) of Berea sandstone disk. Reprinted with permission from SPE-190115-MS.

Mineral	Formula	Concentration, wt%
Quartz	SiO_2	81.79
Muscovite	$KAl_2(AlSi_3O_{10})(F,OH)_2$	9
Kaolinite	$Al_2Si_2O_5(OH)_4$	6
Feldspar	$KAlSi_3O_8$ – $NaAlSi_3O_8$ – $CaAl_2Si_2O_8$	3
Others	----	0.21

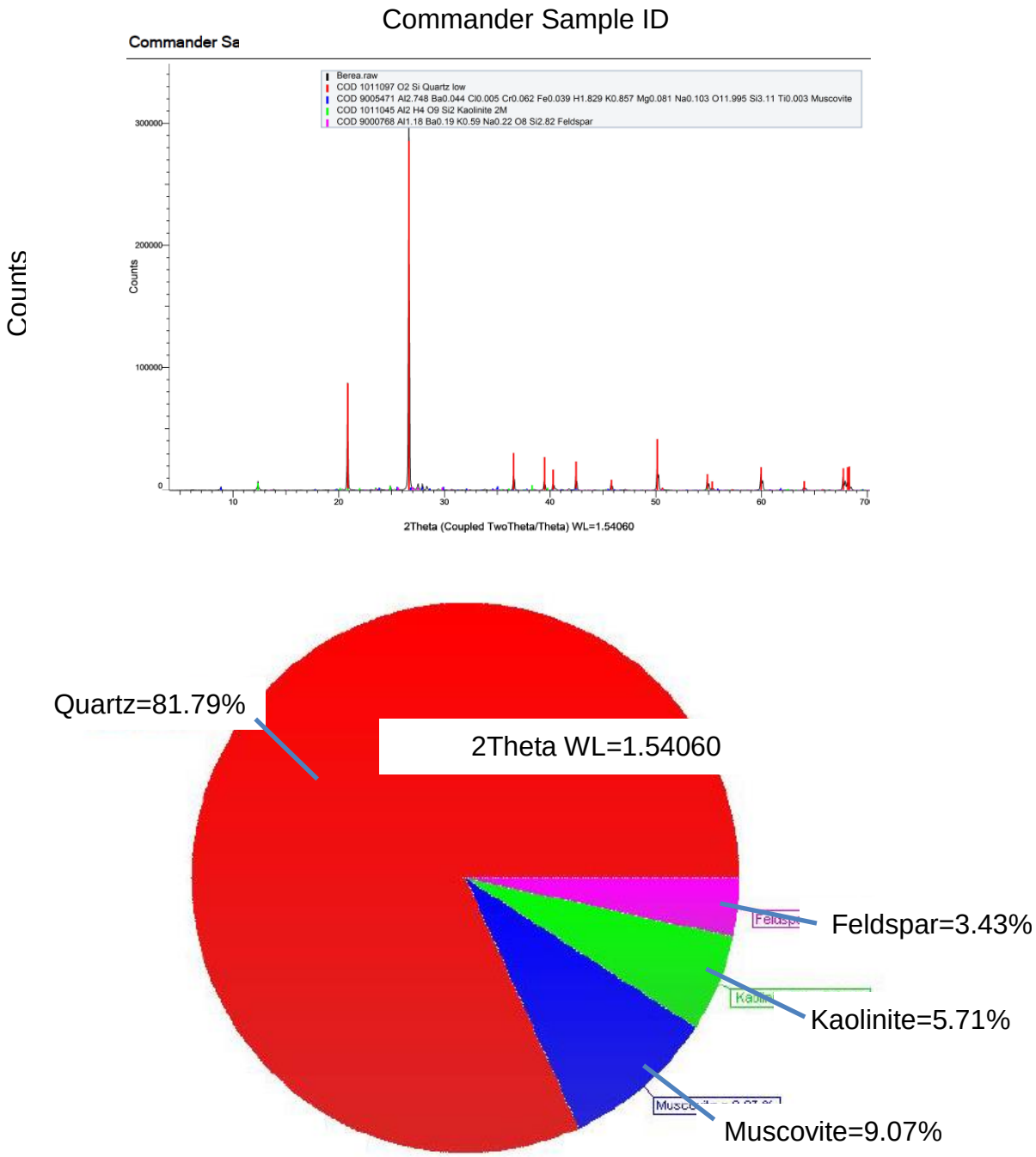

Figure 12 X-Ray diffraction (XRD) of Berea sandstone disk. Reprinted with permission from SPE-190115-MS.

Three types of sandstone disks were prepared by slicing and smashing same sandstone blocks. Type 1 disks were 2.5 in. in diameter and 1 in. in thickness, which were used for the HP/HT filter press test, to form and remove OBDF filter cake. Type 2 disks were 1.5 in. in diameter and 1 in. in thickness, which were used for the coreflood test and CT scan test, to evaluate the formation damage by cleaning solutions. Type 3 disks were with size of 0.62 in. * 0.72 in. * 0.25 in., and they were used for the contact angle test, to evaluate the effects of surfactant.

The permeability of Berea Sandstone Disk was indicated from the Coreflood test. The selected Berea Sandstone Disks had an initial permeability of 50 mD. CT scan provided the porosity number of sandstone disks. Three types of net disks ($W_{net\ disk}$) were dried in oven for 8 hours, and then saturated in 5 wt% KCl solution 24 hours, to simulate the formation condition. After that, weight of net disk ($W_{net\ disk}$) was measured as a parameter of calculate the removal efficiency.

4.1.2.4. Corrosion Inhibitor

Significant scientific and technological efforts have been made to control corrosion problems. The most effective and efficient corrosion inhibitors are organic compounds that have π bonds, heteroatoms (P, S, N, and O) and inorganic compounds (Liu et al. 2015). The corrosion rates have been found to depend on the concentrations of the pollutants mainly chloride and sulfate ions, where the largest deterioration if found for the largest chloride concentrations (Garcia et al. 2003). High corrosion rates for low carbon steel at marine test sites while for weathering steels the corrosion rate is

substantially smaller under the same conditions but even smaller in rural and industrial sites (Oh et al. 1996).

As shown in **Figure 13-a**, Rodine 31a was used as the corrosion inhibitor of novel surfactant/oxidant system. The main composition of Rodine 31a are including 1,3-diethyl-2-thiourea, sulfuric acid, and alkylphenol ethoxylate.

4.1.2.5. L-80 Coupon

L-80 is always used in sour wells. Several metal coupon obtained from Imotron Instruments BV have the compositions shows in **Figure 13-b**. L-80 is a type of low-carbon steel and was used to perform the corrosion test in this research (de Wolf et al. 2012).

Revision Number: 003.3 **Issue date:** 10/26/2018

1. PRODUCT AND COMPANY IDENTIFICATION

Product name: **BONDERITE S-AD 31A ACID INHIBITOR ADDITIVE known as RODINE 31A**

IDH number: 592763

Product type: Corrosion inhibitor

Restriction of Use: None identified

Region: United States

Company address:
Henkel Corporation
One Henkel Way
Rocky Hill, Connecticut 06067

Contact information:
Telephone: +1 (860) 571-5100
MEDICAL EMERGENCY Phone: Poison Control Center
1-877-671-4608 (toll free) or 1-303-592-1711
TRANSPORT EMERGENCY Phone: CHEMTREC
1-800-424-9300 (toll free) or 1-703-527-3887
Internet: www.henkelna.com

3. COMPOSITION / INFORMATION ON INGREDIENTS

Hazardous Component(s)	CAS Number	Percentage*
1,3-Diethyl-2-thiourea	105-55-5	10 - 30
Sulfuric acid	7664-93-9	10 - 30
Alkylphenol ethoxylate	9036-19-5	1 - 5

Figure 13-a Data sheet of corrosion inhibitor. Reprinted with permission from SPE-190115-MS.

Element	Cr-13 (S41000)	Super Cr-13 (S41427)	Duplex 2205 (S31803)	SA2832 (N08028)	L-80 Low-carbon steel
C	0.13	0.02	0.017	0.008	0.24
Mn	0.39	0.42	1.43	1.5	1.25
Si	0.4	0.22	0.36	0.3	0.2
Cu	0.1	0.03	0.31	1.21	0.1
Ni	0.3	5.6	3.71	30.65	0.05
Cr	12.2	12.2	22.42	26.75	0.35
Mo	0.03	2.02	3.18	3.46	0.1
Fe	balance	balance	balance	balance	balance

Figure 13-b Data sheet of L-80 coupon. Reprinted with permission from SPE-190115-MS.

4.1.2.6. Crude Oil

The definition of crude oil could be explained as the mixture of naturally existing hydrocarbons that has been refined to be diesel, gasoline, heating oil et al. and the classification of it are mainly according to the origins and contents inside. Heavy crude

oil will have lower API gravity but with more heat when burning, when compared with light oil.

The main constituents of the crude oils, saturates, aromatics, resins, and asphaltenes (SARA) were determined to establish the relationship between the stability and composition of crude oil. The saturate fraction consists of nonpolar material including linear, branched, and cyclic saturated hydrocarbons. Aromatics are more polarizable because they contain one or more aromatic rings. The distinction between resins and asphaltenes is that resins are miscible with heptane or pentane and asphaltenes are insoluble in that (Fan et al. 2002).

4.2. Drop Shape Analysis

Wettability (**Figure 14**) is an important parameter when determine the flow and distribution of reservoirs fluids in porous formations (Quintero et al. 2017). Wettability affects oil-water relative permeability, fluid movement, cleaning effectiveness, and solids mobilization.

Water-in-oil emulsion inside of filter cake was reported to alter core wettability by Menezes et al. (1989). Significant transformation of wettability can change the gas or liquid phase flow resistance and may induce the adsorption of solid particles and emulsion on the rock surface.

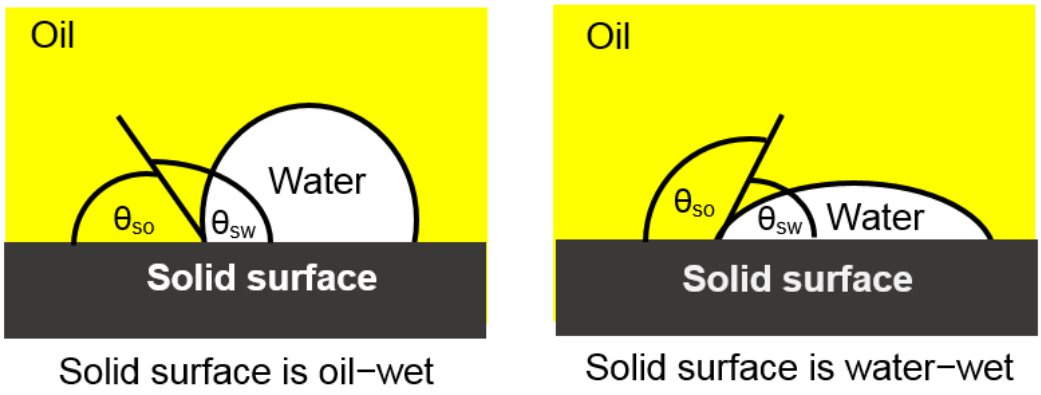

Figure 14 Wettability definition. Reprinted with permission from SPE-190115-MS.

Drop Shape Analysis (**Figure 15**) was used to measure the contact angle among Berea Sandstone Disk, water and crude oil drop. The contact angles of a crude oil droplet on the disk surface were measured to study the wettability change of sandstone rocks treated by different solutions.

Net sandstone disks were dried in rolling oven for 8 hours firstly. After drying, these disks were pre-treated by four different solutions: (1) Saturated in 5 wt% KCl solution for 24 hours, to measure the initial wettability of sandstone disk. (2) Saturated in OBDF (with clay or without clay) emulsion for 24 hours, to measure the wettability of sandstone disk after polluted by OBDF emulsion. (3) Saturated in blend of OBDF emulsion and 2.5 wt% surfactant (1:1 ratio) for 24 hours, to measure the wettability recovery of sandstone disk with the treatment of surfactant for OBDF emulsion.

Figure 15 Drop shape analysis.

When measuring the contact angle, the sandstone disk was held in a cell that fulling with water. As the surrounding temperature of disk was heated up to 250°F, the contact angle was measured using the captive drop method, with injection of a crude oil drop to the disk surface. Crude oil drop was maintained on the disk surface for at least 2 minutes before using Drop Shape Analysis software to capture the drop image and the contact angle value. The higher contact angle represented the higher contact area between crude oil and disk surface, lower hydrophobicity of the surface, and lower interfacial tension. **Equation 8** was used to calculate the emulsion breakdown efficiency.

$$\textit{Emulsion Breakdown Efficiency} = \frac{\theta_{disk\ saturated\ by\ emulsion} - \theta_{disk\ saturated\ by\ surfactant+emulsion}}{\theta_{disk\ saturated\ by\ emulsion}} \quad \text{..... Equation 8}$$

Where

$\theta_{initial}$ =the contact angle among initial disk, water, and crude oil;

$\theta_{treated\ by\ emulsion}$=the contact angle among disk saturated by OBDF emulsion, water, and crude oil;

$\theta_{saturated\ by\ surfactant+emulsion}$=the contact angle among disk saturated by OBDF emulsion and surfactant, water, and crude oil.

4.3. Rheological Properties Test

The rheological properties of OBDF were measured by a rotational viscometer (**Figure 16**) under 250°F. This equipment calculated values for the plastic viscosity (PV), yield point (YP), and 10 seconds/10 minutes gel strengths. All rheological properties were measured based on API 13B-1 recommendations.

Figure 16 Rotational viscometer. Reprinted with permission from SPE-190115-MS.

The PV and YP are parameters from the Bingham plastic (BP) rheology model. BP rheology model is a two-parameter rheological model widely used in the drilling fluid to indicate the flow properties. Bingham plastic fluids guide as a linear shear-stress with shear-rate behavior.

PV is the slope of the linear line and YP is the threshold stress. PV value represents the viscosity of a drilling fluid when extrapolated to infinite shear rate, expressed in units of cp. YP represents the stress required to move the fluid. Sufficiently low PV values are achieved with appropriate YP numbers that aid in the minimization of particles sag and enhanced overall wellbore cleaning.

In the present study, the rolling speeds of rotational viscometer were fixed at 3rpm (reading viscosity=θ_3), 6rpm (reading viscosity=θ_6), 300rpm (reading viscosity=θ_{300}), and 600rpm (reading viscosity=θ_{600}) rev/min, accordingly, the shear rates of cylinder were 5.11, 10.21, 510.67, and 1,021.38 seconds^{-1}. The PV and YP values of OBDF could be calculates from **Equations 9** and **10**:

$$\mathbf{PV = \theta_{600} - \theta_{300}} \quad \textbf{Equation 9}$$

$$\mathbf{YP = \theta_{300} - 0.5*\theta_{600}} \quad \textbf{Equation 10}$$

The gel strength represents the dial reading on the viscometer after keeping the fluid static for an interval of 10 seconds/10 minutes and indicates the suspension ability of the fluid for drilling cuttings (Wagle et al. 2016). The gel strength of drilling fluid is a very important property that determines if the drilling fluid can carry out its basic functions of adequately suspending the cuttings and transporting them to the surface while supporting the stability of the formation (Olatunde et al. 2012).

4.4. Filtration Properties Measurement

Filtrate of OBDF might result in introduction of an immiscible liquid in sandstone reservoirs, causing entrapment of an additional third phase in the porous media that would exacerbate formation damage effects.

Spurt loss and total volume of filtrate are two important factors to be investigated. Spurt loss means instantaneous liquid that passes through a filter medium prior to deposition of filter cake. Total filtrate volume represents total volume of liquid passes through filter cakes driven by differential pressure in 30 minutes.

In general, minimize the values of spurt loss and total filtration volume is one of the useful method to prevent severe formation damage. HP/HT filter press (**Figure 17**) measured the filtration properties under simulated formation conditions (140°F/300 psi, 190°F/300 psi, and 250°F/500 psi). Filter loss was measured at static conditions, the filtration fluids were collected for a total of 30 minutes. The filtrate volume was recorded as a function of time. Spurt loss and total filtrate volume were obtained from the 30 minutes filtration test.

Figure 17 HP/HT filter press. Reprinted with permission from SPE-190115-MS.

4.5. Filter Cake Removal Test

4.5.1. Filter Cake Formation

HP/HT filter press equipment was handled to form filter cake at 250°F heating temperature and 500 psi differential pressure using the Mn_3O_4 weighted OBDF. Formulated OBDF was aged in an HP/HT filter press cell. Type 1 (2.5 in. in diameter and 1 in. in thickness) disks were used to form and remove OBDF filter cake in HP/HT filter press.

The Berea Sandstone Disks were used as the filter media and the filter cake was formed on the top of Berea Sandstone Disk. After 30 minutes heat-aging period, the OBDF

filter cake was generated successfully with 500 psi nitrogen differential pressure to atmosphere. The filter cake was photographed, and the thickness and weight ($W_{core + initial\ filter\ cake}$) were determined before the treatment from cleaning solutions.

4.5.2. Properties of Filter Cake

The thickness of filter cake was measured using vernier caliper. The permeability of OBDF filter cake can be calculated from **Equation 11**. It was a statement of Bourgoyne et al. (1991) model. The calculated permeability was a function of total filtrate volume and square root of time. The pressure drop across the filter cake was determined as the difference between the total applied differential pressure and the pressure drop across the disk (calculated using Darcy's equation for linear flow). The filtrate viscosity was assumed to be constant as 0.32 cp at 250° F (Mahmoud et al. 2017).

$$V_f = 8.4 * 10^{-5} * \sqrt{K_c} * \Delta p * \left(\frac{f_{sc}}{f_{sm}} - 1\right) * A * \frac{\sqrt{t}}{\sqrt{\mu}} \quad \text{..... Equation 11}$$

Where

A=the cross-sectional area of the core, in.^{2}

K_c= the permeability of the filter cake, D

V_f=the total filtrate volume, ft^3

Δp=the pressure drop across the filter cake, psi

μ=filtrate viscosity, cp

f_{sc}=the volume fraction of the solids in the filter cake

f_{sm}=the volume fraction of the solids in the drilling fluid

t=the time of filtration, seconds

4.5.3. Filter Press Test

Formulated OBDF were aged in an HP/HT filter press cell. OBDF filter cakes were built on Berea sandstone disks under simulated formation conditions (140°F/300 psi, 190°F/300 psi, and 250°F/500 psi). After the creation of the filter cakes (**Figure 18**), the new surfactant/oxidant system filled the cell above the filter cakes, and then the cell was put back into the filter press to conduct the filter cake removal process. The cleaning solution samples were collected during 4, 8, and 12 soaking hours to test the pH values and the filter cakes (**Figure 19**) were also taken out from cell after soaking 12 hours to test the removal efficiencies.

Static fluid loss tests were performed based on API 13B-1 recommendations. **Equation 12** was used to calculate the removal efficiency.

$$Removal\ Efficiency = \frac{W_{disk + initial\ filter\ cake} - W_{disk + remaining\ filter\ cake}}{W_{disk + initial\ filter\ cake} - W_{net\ disk}}$$

…….. **Equation 12**

Where

$W_{disk + initial\ filter\ cake}$ = the weight of disk plus the weight of filter cake before being cleaned by the cleaning solution

$W_{disk + remaining\ filter\ cake}$ = the weight of disk plus the weight of filter cake after being treated by the cleaning solution

$W_{net\ disk}$ = the weight of net disk before the filter cake formed solution; and W_{disk} is the weight of net disk before the filter cake formed.

Figure 18 Berea sandstone disks with filter cake formation. Reprinted with permission from SPE-190115-MS.

Figure 19 Berea sandstone disks after filter cake removal. Reprinted with permission from SPE-190115-MS.

4.6. Average Permeability Ratio (Kfinal/Kinitial) Calculation

Tjon-Joe-Pin et al. (1993) stated that disk flow testing can be used to measure the effectiveness of a cleaning solution treatment. The cross-sectional area (A) and the thickness (L) of the Berea sandstone disks were carefully measured and recorded. The disks were placed in a disk holder, and then loaded into a filter press.

This filter press allowed differential pressure (ΔP) to be applied in radial and vertical directions. Before the formation of OBDF filter cake on disk, 5 wt% KCl flowed through the blank disk in the initial direction, which was defined as the treatment

direction. The flow rate (Q) was recorded in cm^3/second. After the cleaning of OBDF filter cake using the new surfactant/oxidant system, disk flow testing was repeated in the production direction, which was the reverse of the treatment direction.

5 wt% KCl solution (with viscosity as μ) was assumed to be Newtonian fluids, and the permeability of the disk ($K_{initial}$ or K_{final}) was calculated using Darcy's equation (**Equation 13**). The average permeability ratio ($K_{final} / K_{initial}$) was used to indicate the permeability percent change of Berea sandstone disks after OBDF filter cakes removed by cleaning solutions.

$$K_{final} / K_{initial} = \frac{\mu * Q_{final} * A}{\Delta P * L} / \frac{\mu * Q_{initial} * A}{\Delta P * L} = Q_{final} / Q_{initial} \quad \text{Equation 13}$$

Where

Q =flow rate, cm^3/min

L = disk thickness, in.

K=effective permeability, mD

μ=fluid viscosity, cp

Δp=differential pressure, psi

A=cross-sectional area, in.

4.7. Inductively Coupled Plasma (ICP) Analysis and pH Test

The cleaning solution samples were collected from the HP/HT filter press cell after 4, 8, and 12 soaking hours. The pH meter (**Figure 20**) was used to measure the pH

change of cleaning solutions before and after the reaction with filter cake components. Inductively Coupled Plasma (ICP) (**Figure 21**) test was used to analysis the elements of cleaning solution residuals, thus evaluate the ability of cleaning solutions to dissolve weighting materials.

There were two weighting materials of OBDF filter cake: $CaCO_3$ and Mn_3O_4. Calcium ion was the key parameter to evaluate the concentration of dissolved $CaCO_3$ and manganese ion was the key parameter to evaluate the concentration of dissolved Mn_3O_4 in cleaning solutions. Cleaning solutions samples collected after 12 hours filter cake removal test were filtered by filter papers firstly, to remove the effects of solids on the ICP results. Then cleaning solutions were diluted to 500 ppm, to satisfy the concentration requirement of ICP test. Elements concentrations were obtained from the digital software of ICP equipment.

Figure 20 pH meter. Reprinted with permission from SPE-190115-MS.

Figure 21 Inductively coupled plasma (ICP). Reprinted with permission from SPE-190115-MS.

4.8. Permeability Loss Calculation from Coreflood Equipment

Coreflood test (**Figure 22**) was used to measure the permeability of Berea Sandstone Disks before and after the treatment of cleaning solutions at optimized wellbore conditions (250^{o}F and 500 psi). Standard coreflood apparatus consists of a core holder, a sample cylinder for injection of fluids, an injection pump, and two pressure transducers. The selected net Berea Sandstone Disks were from the same sandstone block that had an average permeability of 50 mD in this study.

After the removal of filter cake, Type 1 (2.5 in. in diameter and 1 in. in thickness) disks cut into Type 2 (1.5 in. in diameter and 1 in. in thickness) disks, to satisfy the size requirement of coreflood test. Types 2 disks were dried 8 hours in oven, and then saturated in 5 wt% KCl solution for 24 hours. After the pre-treatment, Type 2 disks were brought to measure the retained permeability by coreflood equipment.

Firstly, 5 wt% KCl solution was injected into production side of the disks (reverse to the side that formed filter cake, which was treatment side). Three different flow rates (2, 4, and 6 cm^3/min) were fulfilled by injection pump of coreflood equipment, and inlet/outlet pressures were measured using digital software. The retained permeability of disk, which represented a ratio between the initial and final permeability, was calculated by **Equations 14** and **15** (Elkatatny and Nasr-El-Din 2012).

$$K = \frac{122.812 * q * \mu * h}{\Delta p * d^2}, \ldots \quad \textbf{Equation 14}$$

Where

d=diameter through which water flow, in.

h= disk thickness, in.

K=permeability of the disk, mD

q=flow rate, cm^3/min

μ=fluid viscosity, cp

Δp=differential pressure, psi

$$K_r = \frac{K_f}{K_i} * 100, \ldots \quad \textbf{Equation 15}$$

Where

K_f=final permeability, mD

K_i= initial permeability, mD

K_r= retained permeability

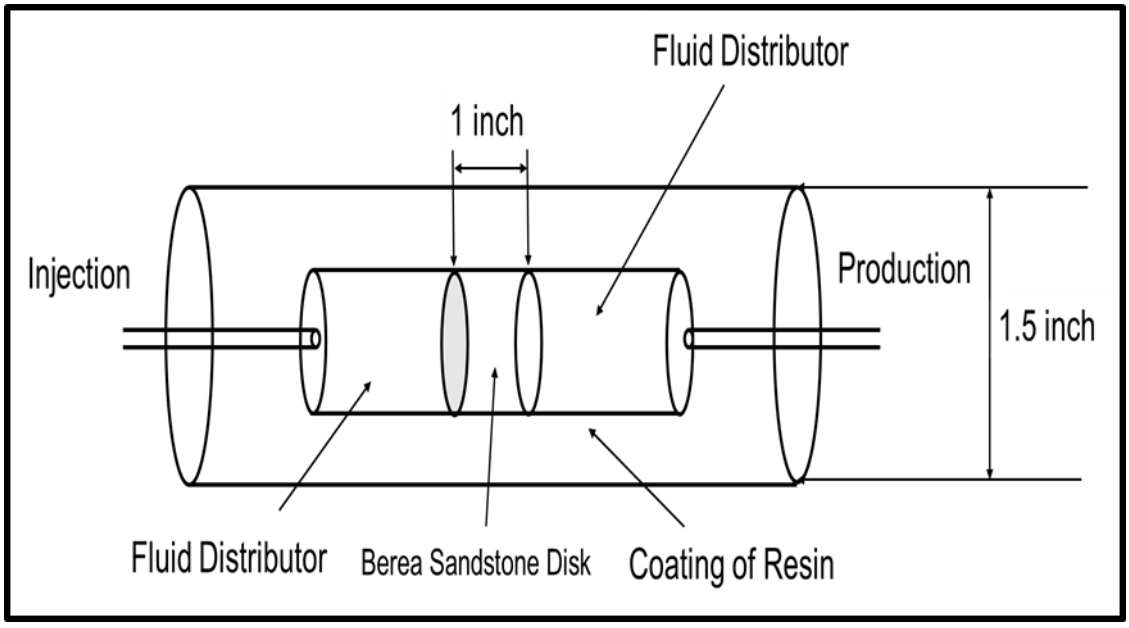

Figure 22 Coreflood test. Reprinted with permission from SPE-190115-MS.

The pre-treatment steps of disks are summarized as follows:

1. Form clay-free OBDF filter cake on sandstone disk (~ 50 mD) at 250°F / 500 psi;
2. Use 5wt% brine–based cleaning solutions to remove filter cake by soaking 12 hours at 250°F / 500 psi;
3. Saturated sandstone disk by 5 wt% brine;
4. Perform Core flood tests @ 74˚F / 1,000 psi differential pressure.

4.9. X-Ray Computed Tomography (CT) Scanning

CT scanning combines a series of X-ray views taken from various angles and computer processes to create cross-sectional images of the samples. CT scanning (**Figure 23**) is a radiological imaging technique that measures density distribution (Zhou

and Nasr-El-Din 2017). CT numbers are normalized values of the calculated X-ray absorption coefficient of a pixel (picture element) in a computed tomogram that provide radio density which is expressed in Hounsfield units (HU).

Because X-ray attenuations are related to density, the CT image gives the density distribution within every point of the object scanned. For reference, the CT number of water is 0 HU and air is -1,000 HU. CT scan provided the porosity number of sandstone disks before and after the treatment of OBDF filter cake by cleaning solutions. After measurement of retained permeability, Type 2 Berea sandstone disks were dried in oven for 8 hours and scanned by CT, to measure the value of CT_{dry}, treated disk. Then they were saturated in 5 wt% KCl solution for 24 hours, to carry out the value of CT_{wet}, treated disk.

The porosity of disks after the treatment of cleaning solutions could be obtained from **Equation 16**. Assume the CT numbers of 5 wt% KCl (CT_{brine}) were both 54.47.

$$\boldsymbol{Porosity, vol\%} = \frac{\boldsymbol{CT_{wet} - CT_{dry}}}{\boldsymbol{CT_{brine} - CT_{air}}} \quad \textbf{Equation 16}$$

Where

CT_{wet} = the CT number of wet disk

CT_{dry} = the CT number of dry disk

CT_{brine} = the CT number of brine

CT_{air} = the CT number of air

Figure 23 X-Ray computed tomography. Reprinted with permission from SPE-190115-MS.

The pre-treatment steps of disks are summarized as follows:

1. Form clay-free OBDF filter cake on sandstone disk (~ 50 mD) at 250°F / 500 psi;
2. Use 5wt% brine–based cleaning solutions to remove filter cake by soaking 12 hours at 250°F / 500 psi;
3. Saturated sandstone disk by 5 wt% brine;
4. Perform CT Scan test.

4.10. Compatibility Test

4.10.1. Primary Causes for Formation Damage

The primary causes for formation damage are criteria into seven types as shown in the following list:

(1) Type of drilling fluid used

(2) Emulsifiers over loading

(3) Fines migration

(4) Emulsion blockage

(5) Bridging package design

(6) Losses while drilling

(7) Completion fluid incompatibility with reservoir fluids

4.10.2. OBDF Emulsion

An emulsion is a temporarily stable mixture of immiscible fluids, such as oil and water. Common emulsions can be oil suspended in water or water suspended in oil. OBDF emulsions created in this research were emulsions of water suspended in oil.

Deionized water was the dispersed phase and was present as droplets in the mineral oil. Dispersed phase is being carried by a continuous phase which is a common feature of multiphase flows. The test goal was to observe the mixing/separation between the cleaning solution (B4), OBDF emulsion, and crude oil.

The compatibility tests were carried out in the laboratory where equal amounts (a combination ratio of 50/50) of the tested solutions were poured into a 10 cm^3 cylinder. The cylinder was placed at stable room temperature (without disturbing it) for 48 hours

and observed for mixing/separation, in accordance with the protocol of Addagalla et al. (2016).

4.10.3. Crude Oil

The crude oil used to perform the compatibility test with cleaning solution have the SARA analysis as shown in **Table 6**. Light oil and heavy oil have different performance before and after mixed with B4 cleaning solution when attached on glass container (**Figure 24**).

Table 6 SARA analysis.

Oil Type	Heavy Oil	Light Oil
Saturates	31%	51%
Aromatic	25.90%	33%
Resin	15.75%	6%
Asphaltene	27.50%	10%
Density	1.0 g/cc	0.8 g/cc

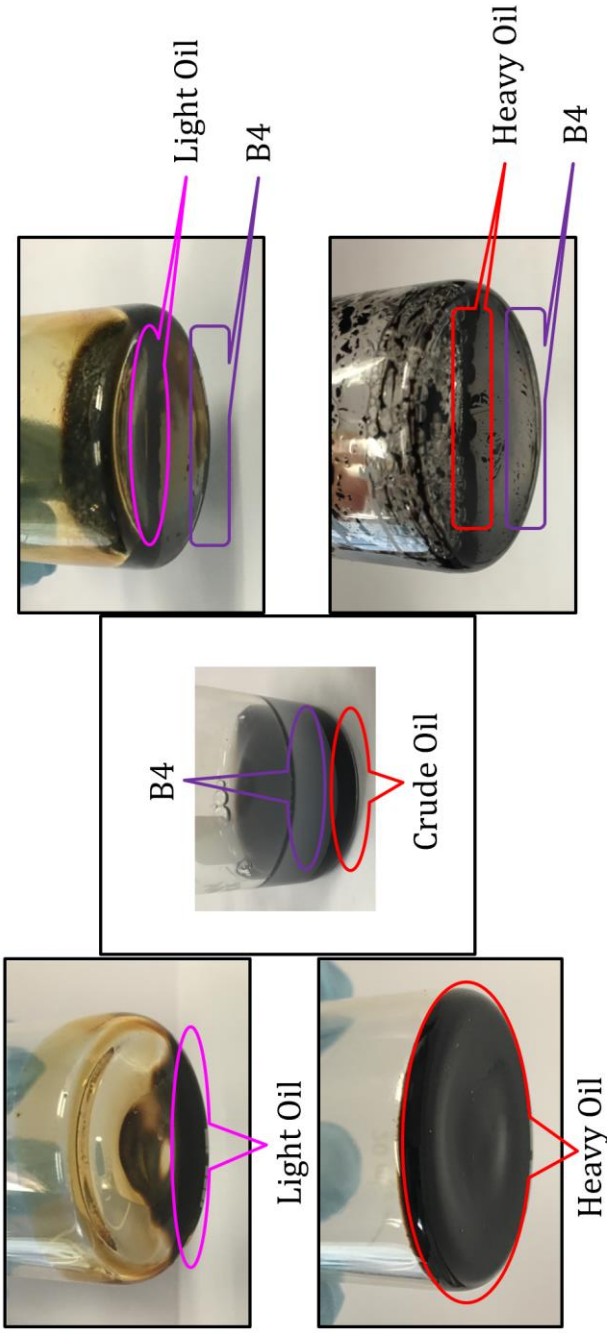

Figure 24 Crude oil performance.

4.11. Corrosion Damage Analysis

4.11.1. Corrosion in the Oil Industry

The basic definition of corrosion in the oil industry can be explained as the destructively external/internal attack of a metal due to its reaction with the environment. Bad effects due to failure to remedy of corrosion wells are including in: (1) undesirable dump flooding of the oil reservoirs; (2) or oil seepage and hydrocarbon contamination in shallow water bearing strata (Agiza and Awar 1983).

In the following list, the types of common corrosion existing in the oil industry are given in detail (Agiza and Awar 1983):

1. Internal attack:
    a. Producing CO_2 and organic acid (sweet corrosion);
    b. Producing H_2S (sour corrosion);
2. External attack:
    a. Exposure to atmospheric oxygen (oxygen corrosion);
    b. Electro-chemical corrosion (flow of electric current).

Generate a leak-rate profile is one of the most common methods of determining if a corrosion problem exists. Corrosion considerations are made before wells be drilled and during the drilling and completion process, the compatibility among mud, cement, and casing systems that relatives to corrosion must be tested very carefully. As we all know, even minor errors in judgement at this starting time will plague the whole well's entire life (Bradshaw and Division 1978).

4.11.2. Corrosion Rate Test Steps and Calculation

Parr 4520 bench top reactor (**Figure 25**) was used to perform corrosion rate measurement after the applying of effective corrosion inhibitor (CI) for L-80 coupon under specific conditions. The corrosion test steps are list as follows:

a. Tested solution: 0% coated sodium persulfate, and corrosion inhibitor;
b. Metal Coupon (L-80): 1 in. x 2.3 in. x 1/16 in. with two holes of 3/16 in.;
c. Tested conditions: 250°F; ≥1,000 psi; 6 hours duration.
d. L-80 metal coupon was removed and cleaned with deionized water and acetone;

The 800 mL tested solution will be mixed 20 minutes, which was required to fill the vessel corrosion reactor. Nitrogen is used to purge oxygen away from system and maintain a minimum pressure of 1,000 psi.

The industry accepted corrosion rate is 0.05 lb/ft^2. If C.R. represents the corrosion rate, then the following Equation is used to calculate C.R.:

$$\mathbf{C.R.} = \frac{\mathbf{W_i - W_f}}{\mathbf{Surface\ Area}} \quad \textbf{.....Equation 17}$$

Figure 25-a Parr 4520 bench top reactor.

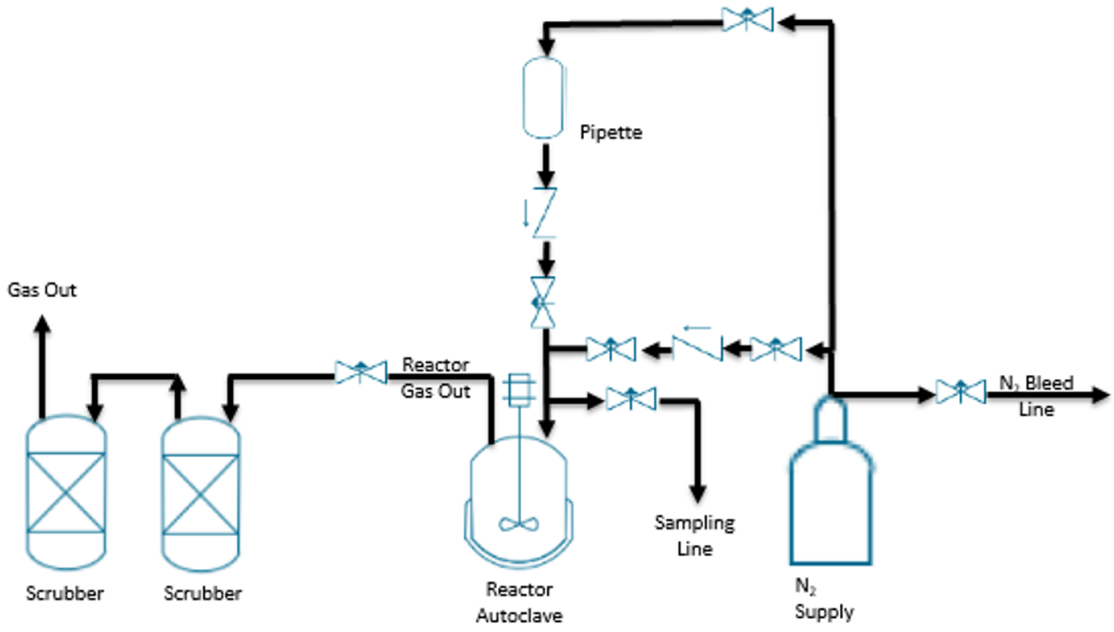

Figure 25-b Schematic of Parr 4520 bench top reactor.

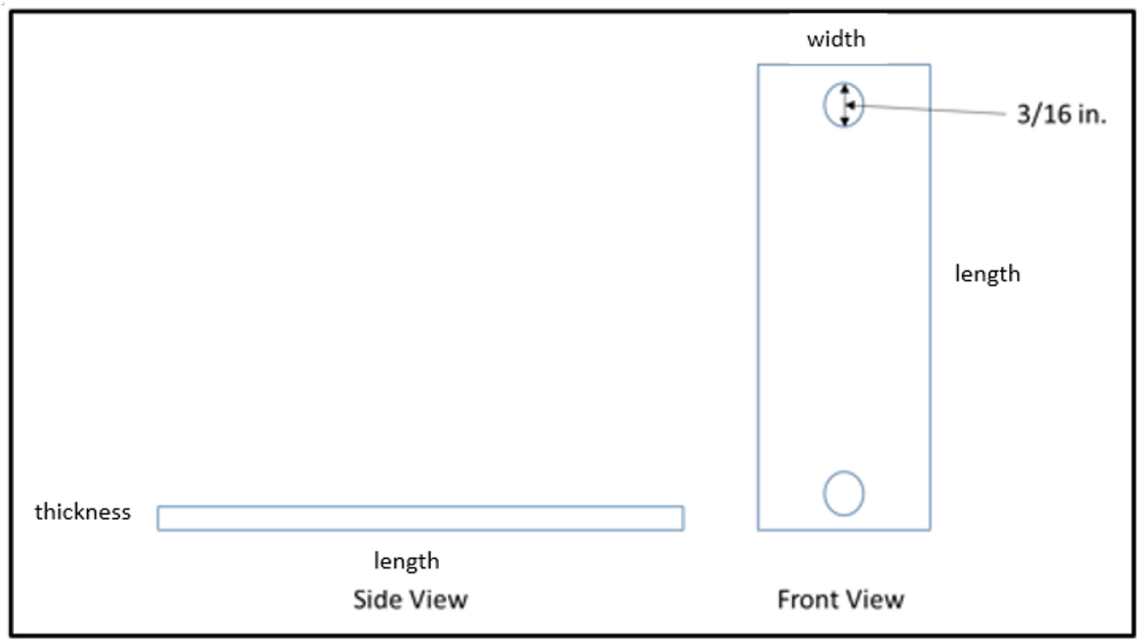

Figure 25-c Schematic of L-80 coupon.

5. [3]RESULTS AND DISCUSSION

5.1. Rheological Properties and Filtration Characteristics Compare between OBDF with and without Clay

OBDF rheological properties are given in **Figures 26, 27, 28,** and **29**. For OBDF with organophilic clay, at 140°F condition, PV, YP, and 10 sec./10 min. gel strength values were same for OBDF with clay and without clay, which were 24 cp, 3 lb/100 ft^2, and 1 lb/100 ft^2, respectively. With an increase of temperature and pressure from 140°F to 250°F, PY values decreased from 24 to 10 cp, and the YP point increased from 3 to 12 lb/100 ft^2.

The organophilic clay used in OBDF formula did not continuously maintain a stable viscosifier function in HP/HT conditions. OBDF without clay had stable rheological properties under three simulated downhole conditions, 140°F, 190°F, and 250°F. Their PV, YP, and 10 sec./10 min. gel strength values maintained as 24 cp, 3 lb/100 ft^2, 2 lb/100 ft^2, and 61 lb/100 ft^2, respectively.

OBDF without clay had lower spurt loss ($\leq$ 2.7 cm^3) and lower total filtration volume ($\leq$ 6.2 cm^3) than OBDF with clay, but the differences between these two drilling fluids were smaller than 2 cm^3 after 30 minutes filtration (**Figures 30** and **31**).

[3] *Reprinted with permission from "A Cost-Effective Application of New Surfactant/Oxidant System to Enhance the Removal Efficiency of Oil-Based Filter Cake" by J. Zhou et al., 2018. SPE-190115-MS, Copyright 2018 by Society of Petroleum Engineers.

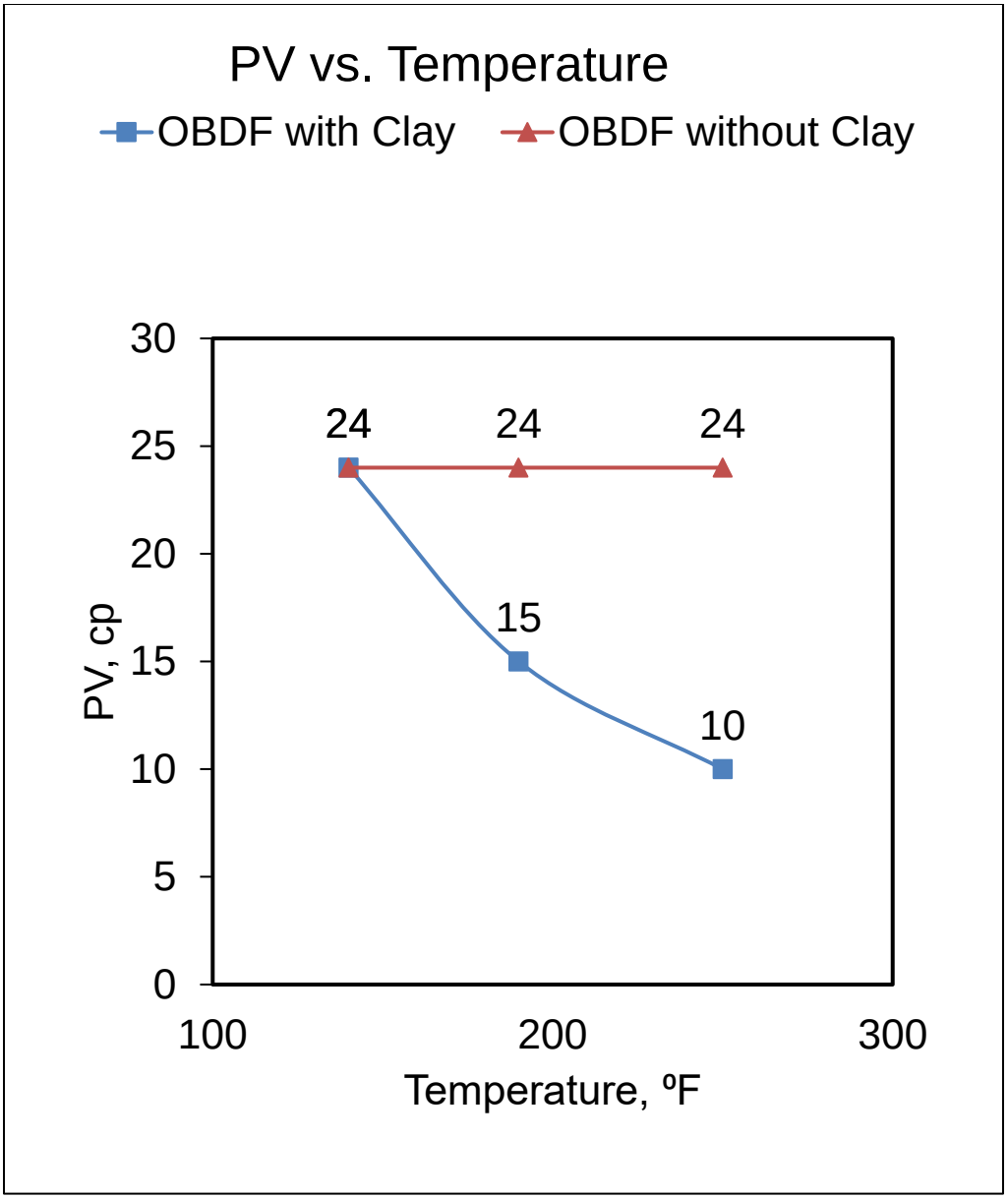

Figure 26 OBDF plastic viscosity properties trend with the increasing of temperature. Reprinted with permission from SPE-190115-MS.

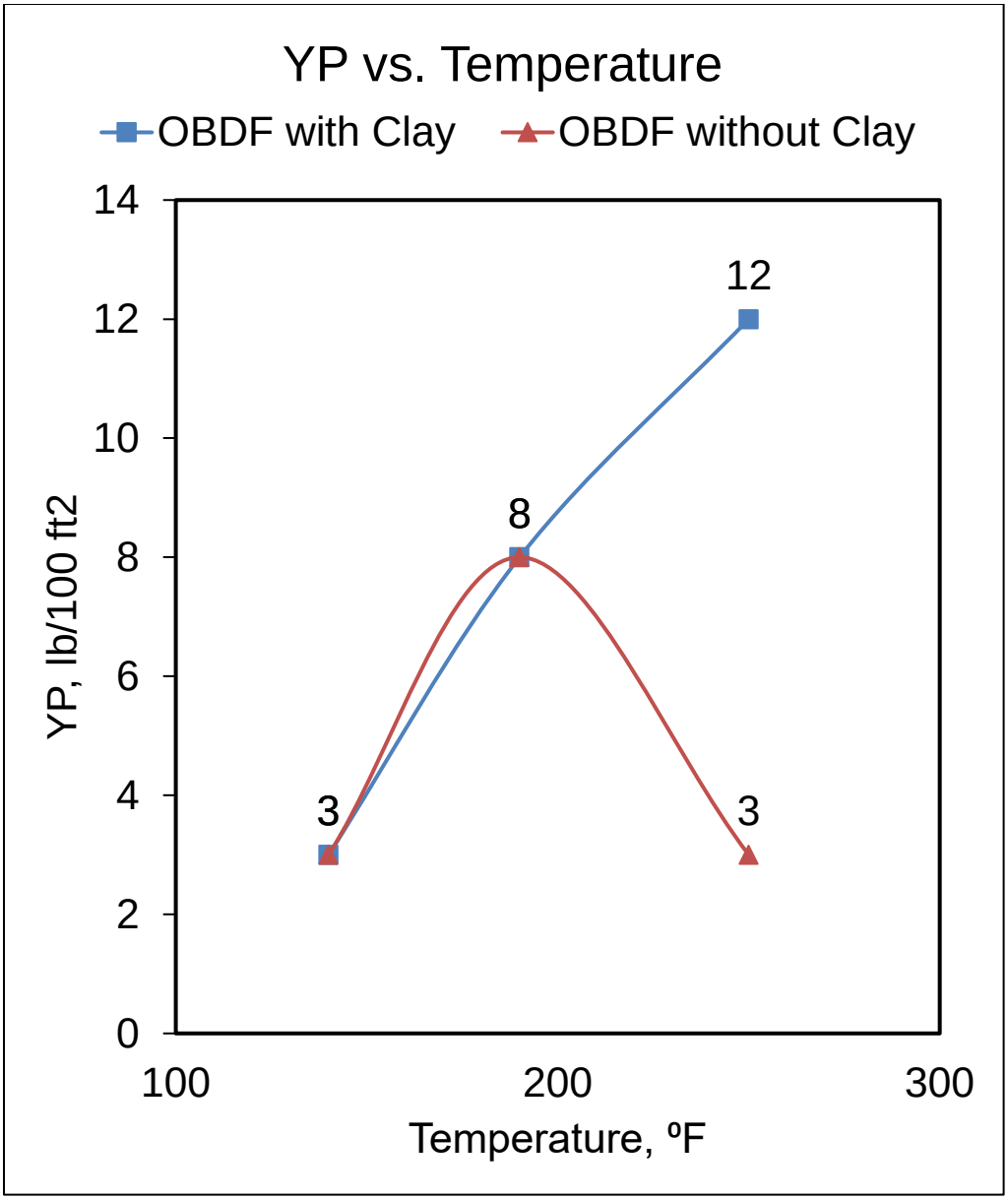

Figure 27 OBDF yield point properties trend with the increasing of temperature. Reprinted with permission from SPE-190115-MS.

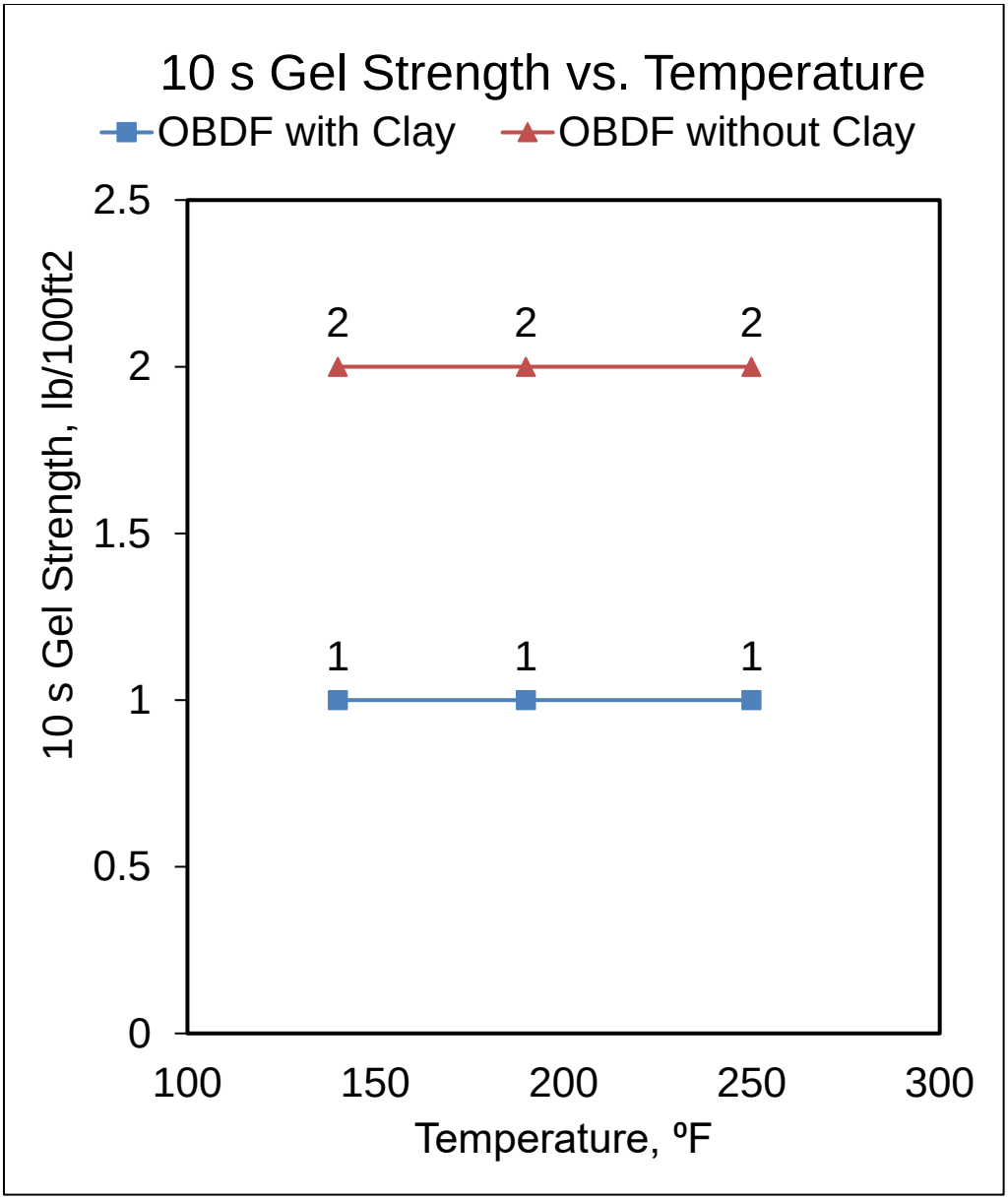

Figure 28 OBDF 10 seconds gel strength properties trend with the increasing of temperature. Reprinted with permission from SPE-190115-MS.

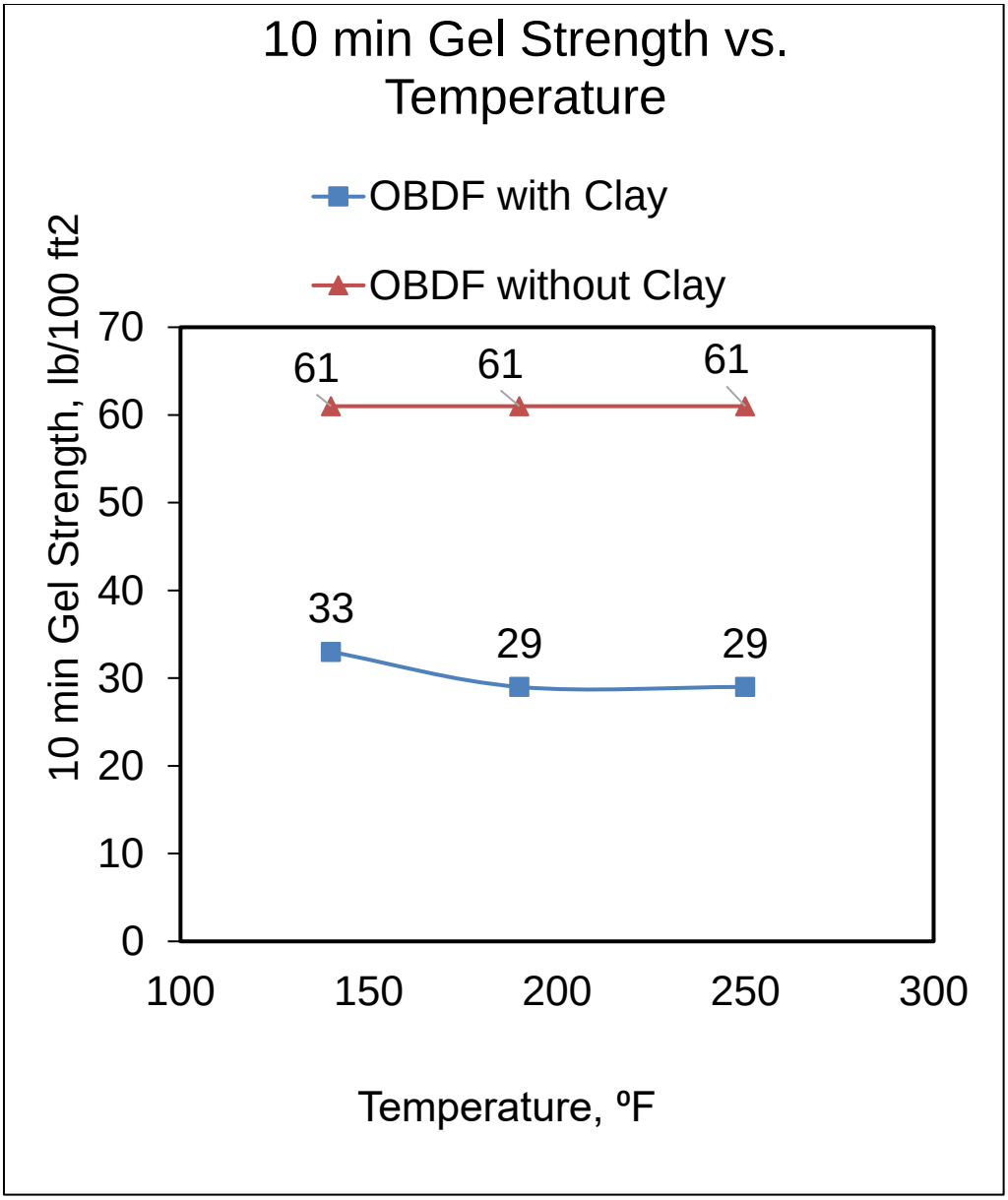

Figure 29 OBDF 10 minutes gel strength properties trend with the increasing of temperature. Reprinted with permission from SPE-190115-MS.

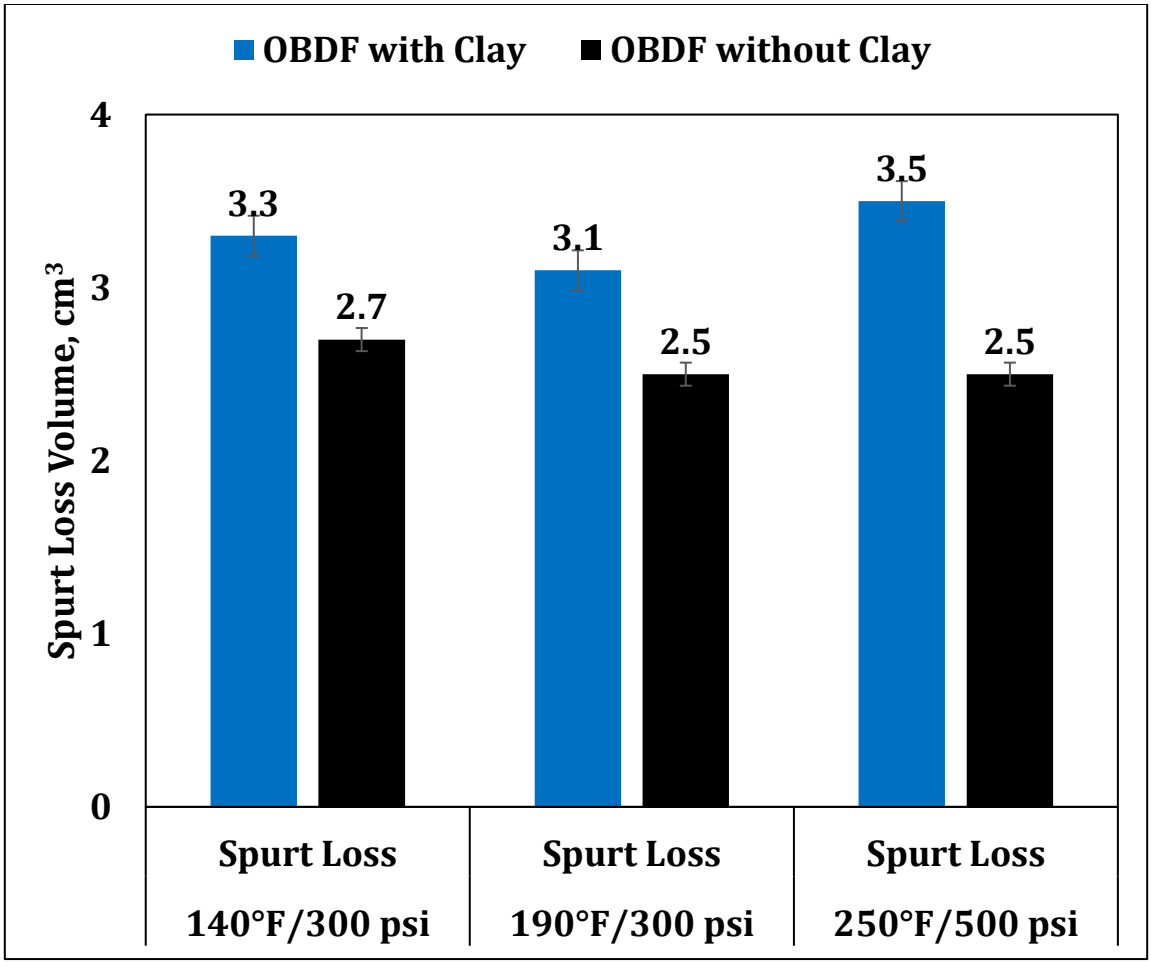

Figure 30 Spurt loss values of OBDF (30 minutes filtration test). Note: The filtration properties were the same when the tests performed on Berea sandstone disks that being saturated with 5 or 18 wt% KCl. Reprinted with permission from SPE-190115-MS.

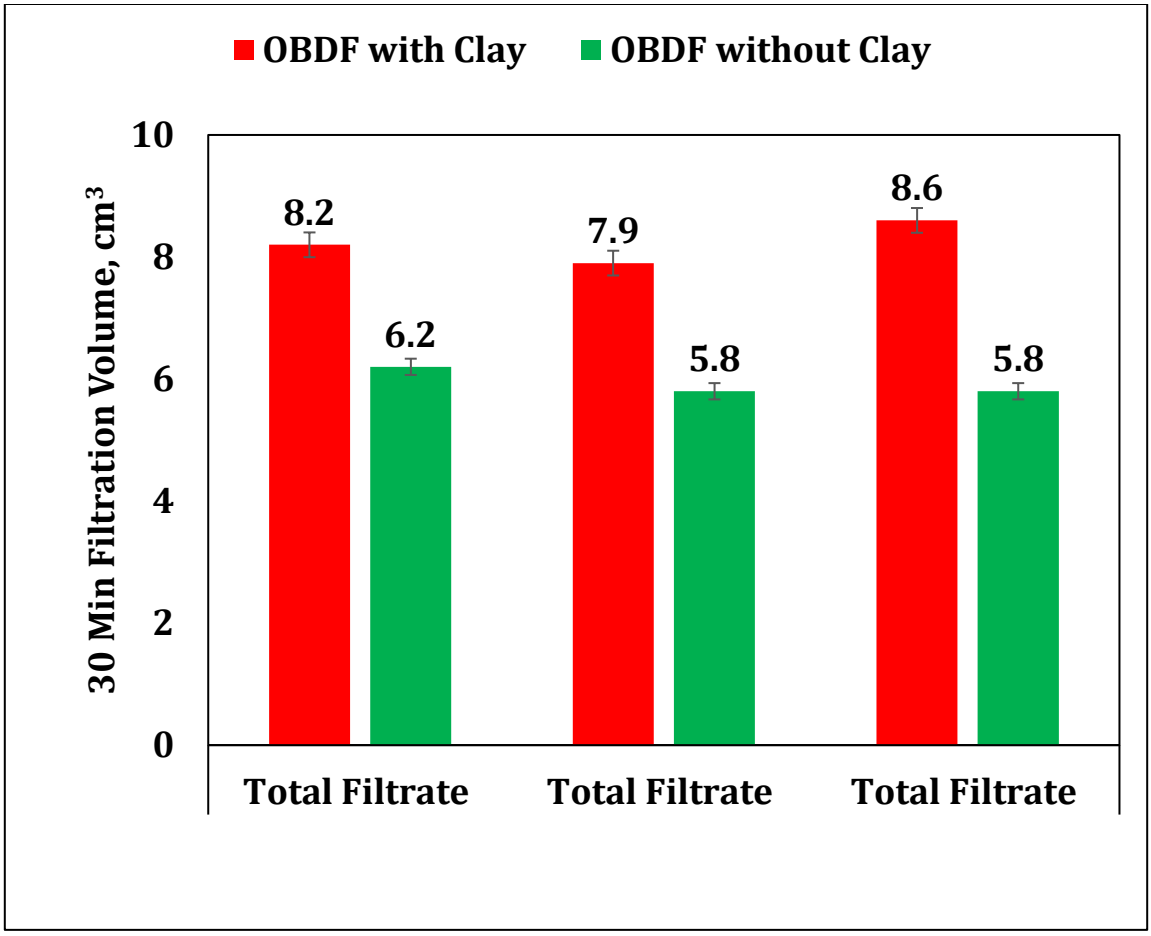

Figure 31 Total filtrate values of OBDF (30 minutes filtration test). Note: The filtration properties were the same when the tests performed on Berea sandstone disks that being saturated with 5 or 18 wt% KCl. Reprinted with permission from SPE-190115-MS.

5.2. Effects of Clay Components, Soaking Time, and Persulfate Type

The new surfactant/oxidant removal systems (B1, B2, B3, and B4) were used to remove filter cakes under 140°F/ 300 psi, 190°F/300 psi, and 250°F/500 psi conditions. **Figures 32** and **33** show pH values of the new surfactant/oxidant system under different soaking times during the removal tests.

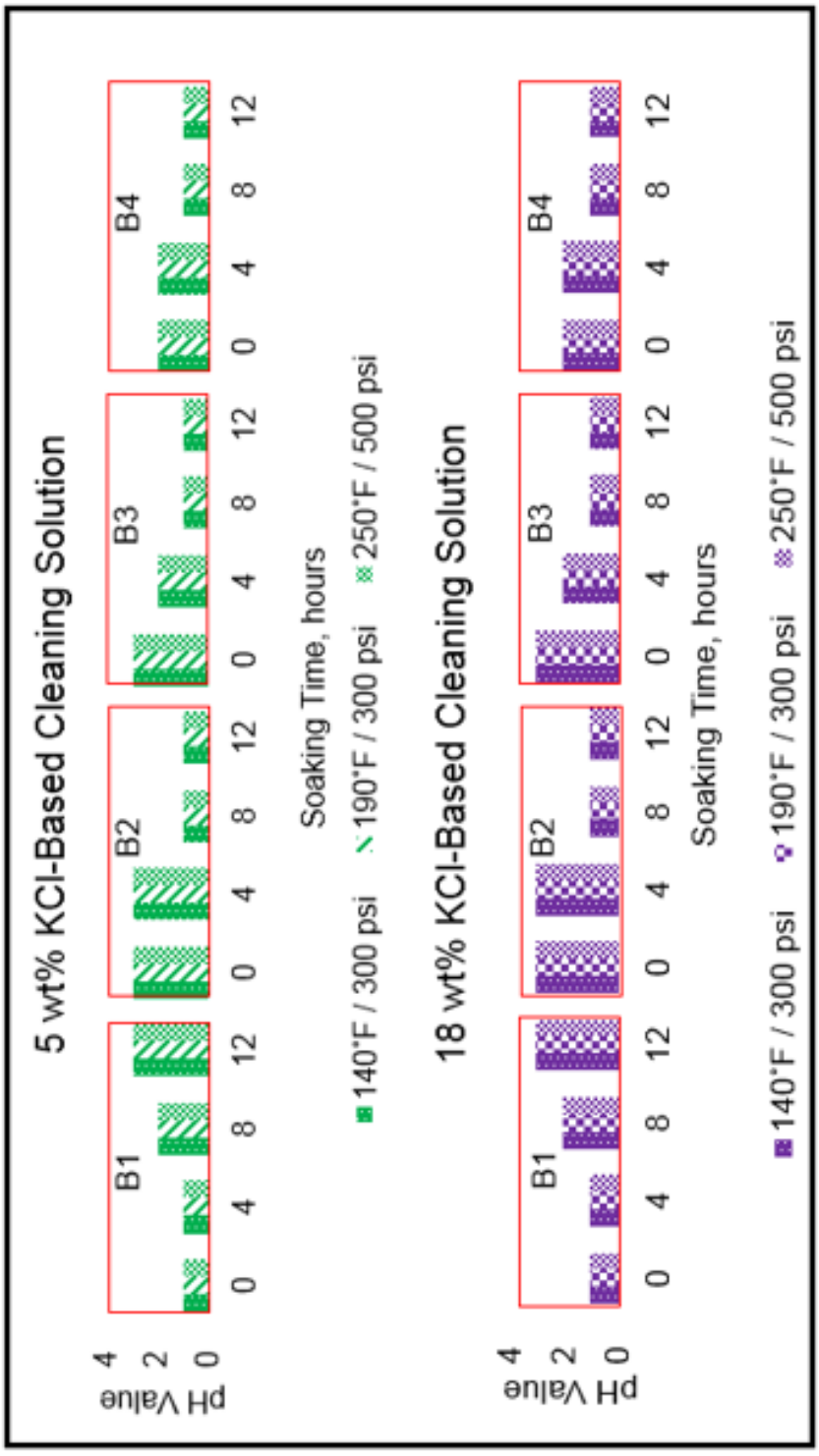

Figure 32 pH values of the new surfactant/oxidant system used to clean OBDF (with clay) filter cakes. Reprinted with permission from SPE-190115-MS.

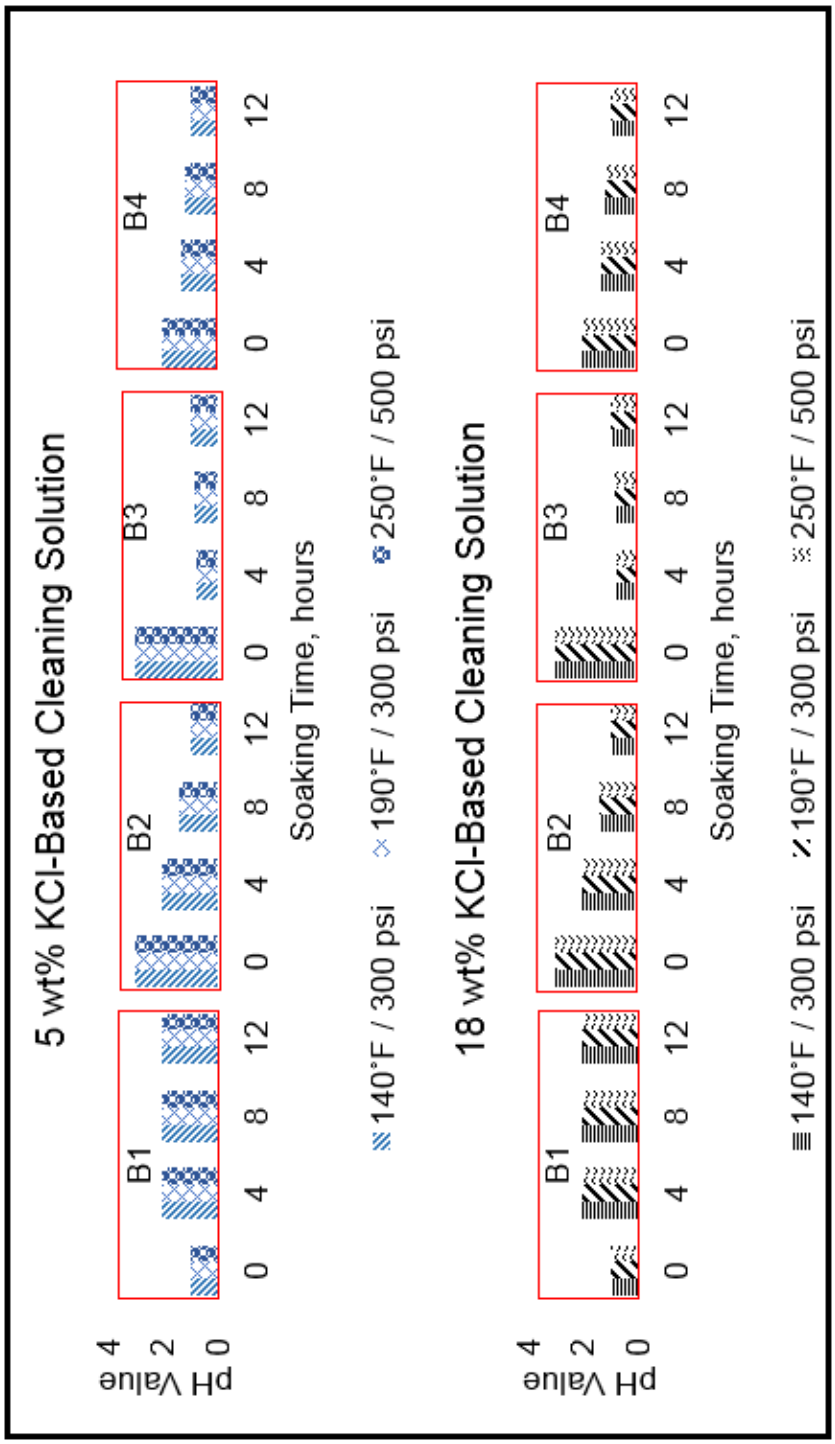

Figure 33 pH values of the new surfactant/oxidant system used to clean OBDF (without clay) filter cakes. Reprinted with permission from SPE-190115-MS.

OBDF clay components didn't affect the cleaning solution's pH values significantly. With the soaking time increased from 0 to 12 hours, pH values of ammonium persulfate (B2, B3, and B4) decreased, but for sodium persulfate (B1), the pH values increased. H^+ in B1 solution were consumed by the sodium persulfates, which caused the increase of pH value. For B2, B3, and B4, the capsules of ammonium persulfates broke down with the increasing of temperature, consumed the OH^- ions and caused the decrease of pH value.

5.3. Removal Efficiency of the New Surfactant/Oxidant System

The optimized system (B4) is the combined solution of sodium persulfate, ammonium persulfate, and non-ionic surfactants. The filter cake removal test results are displayed in **Tables 7** and **8**.

The new surfactant/oxidant system degraded the filter cake by up to 98 wt% removal efficiency. Salinity of removal system did not affect the removal efficiency significantly. As the soaking time was increased from 4 to 12 hours, the removal efficiency was increased from 50 to 98 wt%.

The removal efficiencies of OBDF (without clay) filter cakes were at most 20 wt% higher than OBDF (with clay) filter cakes. $K_{final} / K_{initial}$ values of Berea sandstone disks nearly equals to 1 (**Table 9**) under three simulated downhole conditions, 140°F/300 psi, 190°F/300 psi, and 250°F/500 psi, which mean that the new surfactant/oxidant system affects the formation permeability slightly.

Table 7 Removal efficiency (5 wt% KCl-based cleaning solution). Reprinted with permission from SPE-190115-MS.

		Removal Efficiency, wt%					
5 wt% KCl-Based Cleaning Solution	Soaking Times	140°F/300 psi		190°F/300 psi		250°F/500 psi	
		OBDF with Clay	OBDF without Clay	OBDF with Clay	OBDF without Clay	OBDF with Clay	OBDF without Clay
B1	4 hours	50.7	61.1	64.8	71.4	74.6	80.7
	8 hours	56.3	65.7	70.4	76.0	80.2	85.3
	12 hours	60.3	71.3	74.4	81.6	84.2	90.9
B2	4 hours	52.9	67.3	70.0	77.6	79.8	86.9
	8 hours	62.1	74.5	76.2	84.8	86.0	94.1
	12 hours	69.2	79.4	83.3	89.7	93.1	98.0
B3	4 hours	54.9	74.5	69.0	84.8	78.8	94.1
	8 hours	60.9	81.1	75.0	91.4	84.8	98.0
	12 hours	65.9	86.0	80.0	96.3	89.8	98.0
B4	4 hours	57.8	78.1	71.9	88.4	81.7	97.7
	8 hours	64.1	85.7	78.2	96.0	88.0	98.0
	12 hours	72.3	87.8	86.4	98.1	96.2	98.0

Table 8 Removal efficiency (18 wt% KCl-based cleaning solution). Reprinted with permission from SPE-190115-MS.

		Removal Efficiency, wt%					
18 wt% KCl-Based Cleaning Solution	Soaking Times	140°F/300 psi		190°F/300 psi		250°F/500 psi	
		OBDF with Clay	OBDF without Clay	OBDF with Clay	OBDF without Clay	OBDF with Clay	OBDF without Clay
B1	4 hours	60.4	66.7	72.2	76.3	78.5	81.7
	8 hours	66.0	71.3	77.8	80.9	84.1	86.3
	12 hours	70.0	76.9	81.8	86.5	88.1	91.9
B2	4 hours	65.6	72.9	77.4	82.5	83.7	87.9
	8 hours	71.8	80.1	83.6	89.7	89.9	95.1
	12 hours	78.9	85.0	90.7	94.6	97.0	98.0
B3	4 hours	64.6	80.1	76.4	89.7	82.7	95.1
	8 hours	70.6	86.7	82.4	96.3	88.7	98.0
	12 hours	75.6	91.6	87.4	98.0	93.7	98.0
B4	4 hours	67.5	83.7	79.3	93.3	85.6	98.7
	8 hours	73.8	91.3	85.6	98.0	91.9	98.0
	12 hours	82.0	93.4	93.8	98.0	98.0	98.0

Table 9 Average permeability ratio (K_{final} / $K_{initial}$). Reprinted with permission from SPE-190115-MS.

	Condition	OBDF Type	B1	B2	B3	B4
5 wt% KCl-Based	140°F/300 psi	with	1.07	1.04	0.92	0.91
		without	1.02	1.01	1.01	0.98
	190°F/300 psi	with	1.15	1.11	0.94	0.93
		without	1.07	1.05	1.04	0.98
	250°F/500 psi	with	1.17	1.15	0.88	0.95
		without	1.12	1.09	1.06	0.99
18 wt% KCl-Based	140°F/300 psi	with	1.16	1.18	1.09	0.92
		without	1.09	1.16	1.15	0.97
	190°F/300 psi	with	1.28	1.24	1.10	0.93
		without	1.16	1.19	1.17	0.97
	250°F/500 psi	with	1.31	1.28	1.06	0.95
		without	1.24	1.22	1.19	0.97

5.4. Breakdown Treatment on OBDF Emulsion

OBDF filter cake is hard to be removed because OBDF emulsion occupies as a protective barrier between breakers and filter cake components, which prevents the aqueous-based breakers to attack the interface of filter cake. Surfactant additive of cleaning solutions can break the water-in-oil emulsion, thus extend the attack area between breakers and OBDF filter cake components.

The experimental results of Drop Shape analysis were shown in **Figures 34**, **35**, **36**, **37**, and **38**. They demonstrated the function of surfactant in filter cake removal system. Initial Berea sandstone disk was water-wet because Disk A had a contact angle of 58.25˚C for crude oil droplet. Compared Disk A, B, and C, the contact angles expanded from 58.25˚C to 106.21 ˚C and 161.79˚C after polluted by OBDF with clay and without clay, respectively.

The OBDF with clay emulsion breakdown efficiency was 23.11% and the OBDF without clay emulsion breakdown efficiency was 59.86% (**Table 10**). This phenomenon stated that OBDF without clay emulsion could be more significantly broken by non-ionic surfactant.

Treatment of surfactant recovered the contact angle from 106.21˚C to 81.67˚C and 161.79˚C to 64.95˚C as observed. The disk had returned to its initial water-wet state, much like sandstone reservoir upon treatment with cleaning solutions. The contact angles of Disk D (81.67˚C) and E (64.95˚C) were still higher than the initial contact angle of net disk (58.25˚C). In summary, surfactant can significantly break down the water-in-oil emulsion inside of OBDF filter cake.

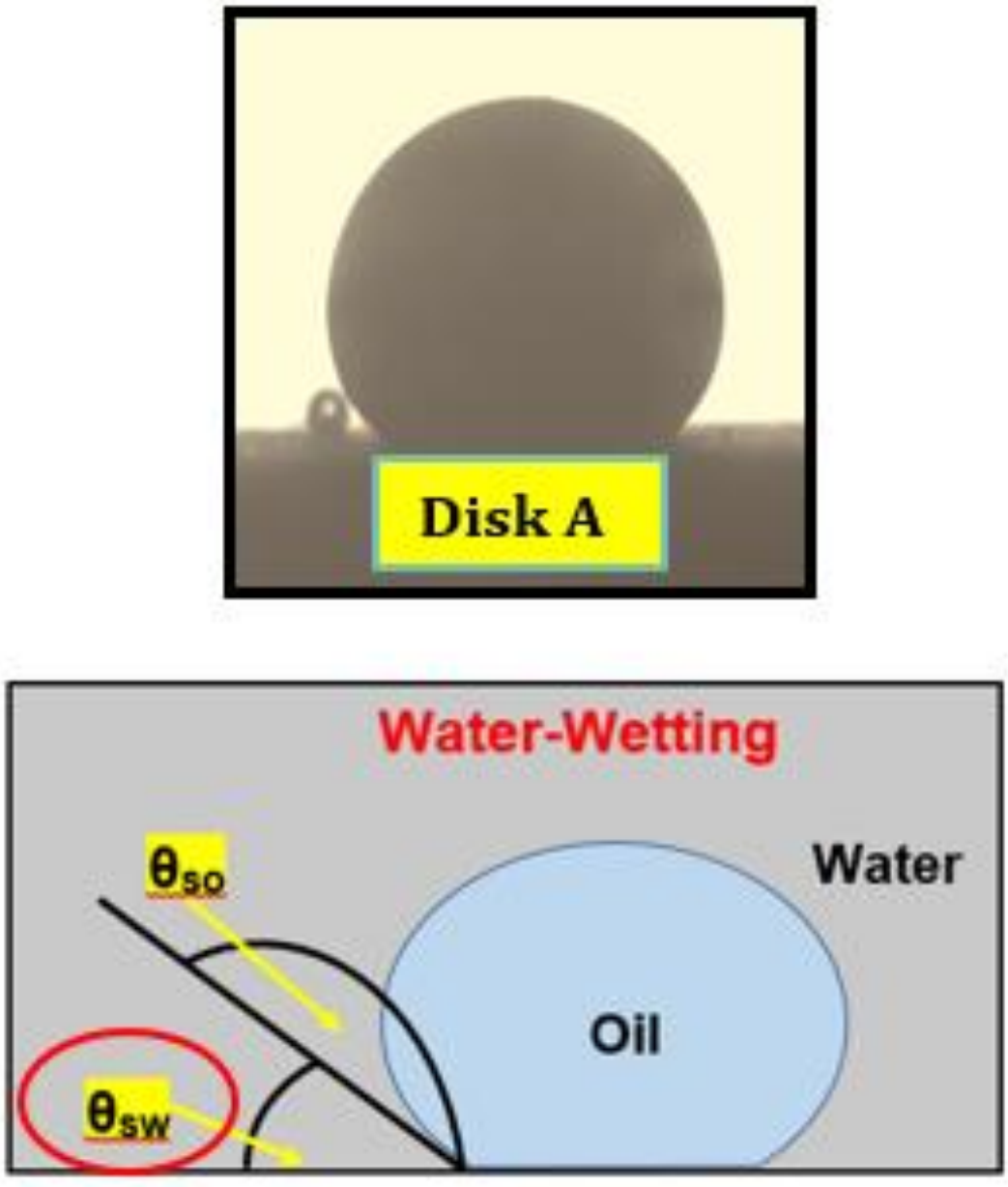

Figure 34 Contact angle measurement. Disk A: net sandstone disk; contact angle=58.25˚C. Reprinted with permission from SPE-190115-MS.

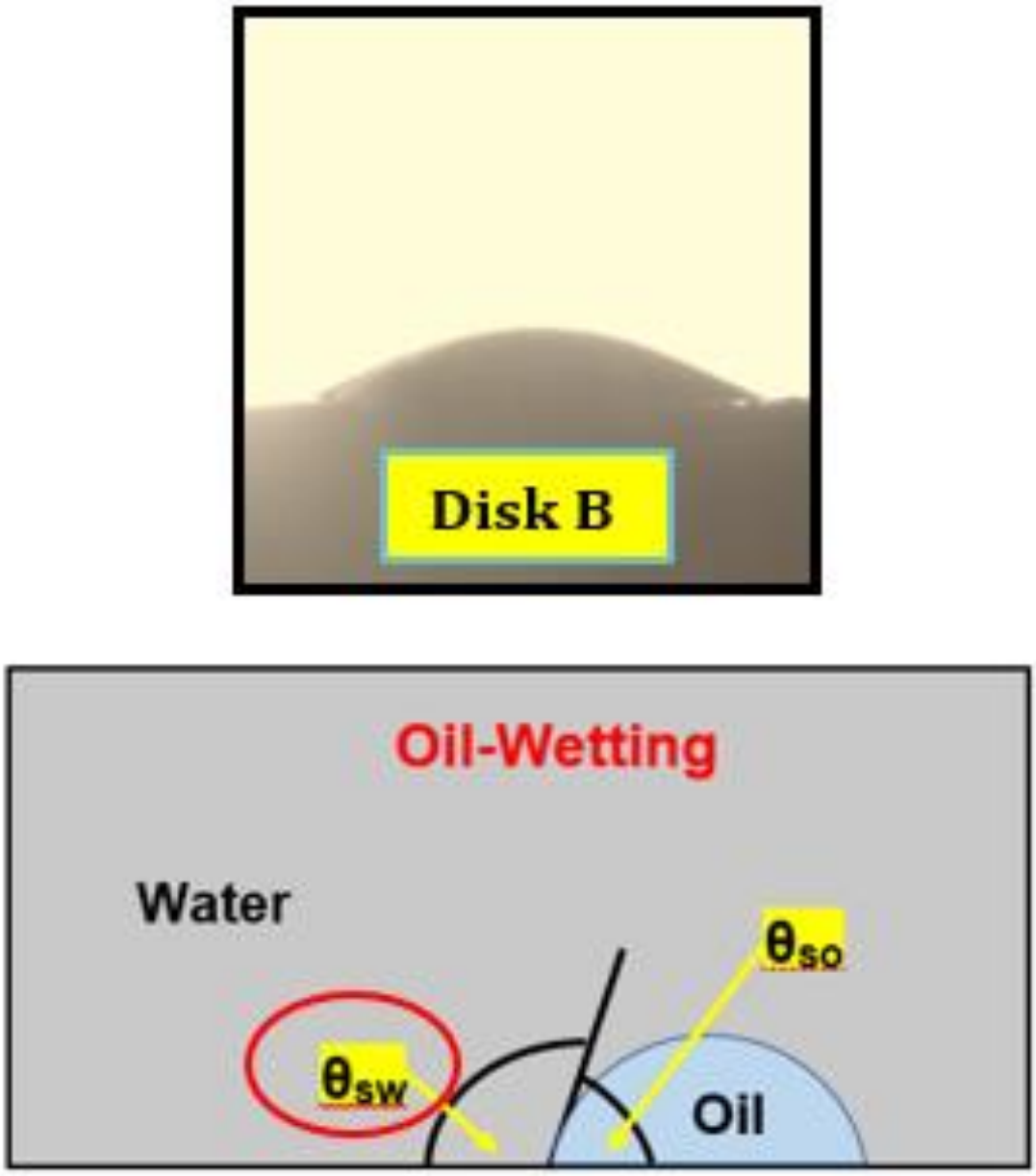

Figure 35 Contact angle measurement. Disk B: sandstone disk polluted by OBDF with clay-free emulsion; contact angle=161.79˚C. Reprinted with permission from SPE-190115-MS.

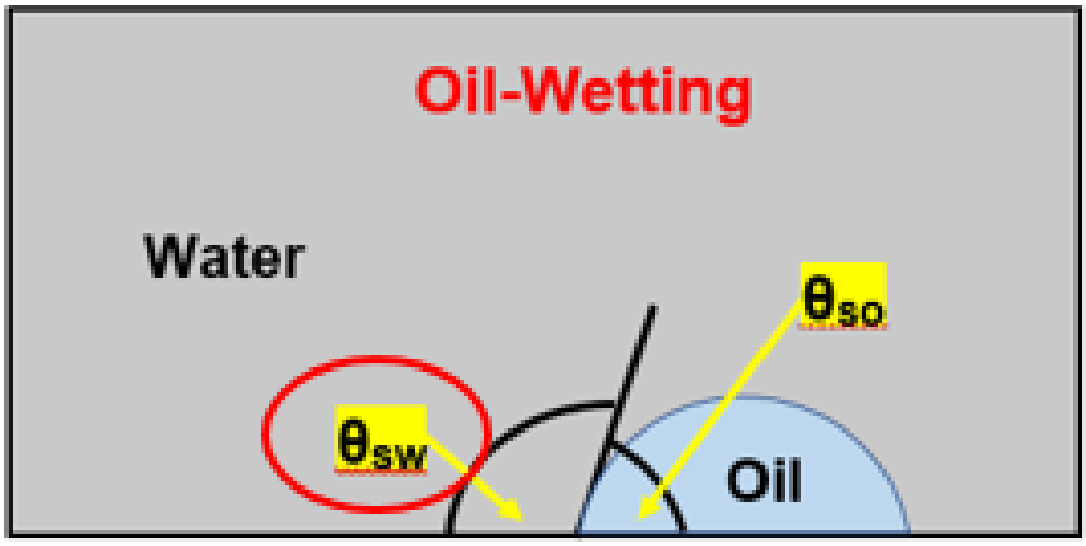

Figure 36 Contact angle measurement. Disk C: sandstone disk polluted by OBDF with clay emulsion; contact angle=106.21˚C. Reprinted with permission from SPE-190115-MS.

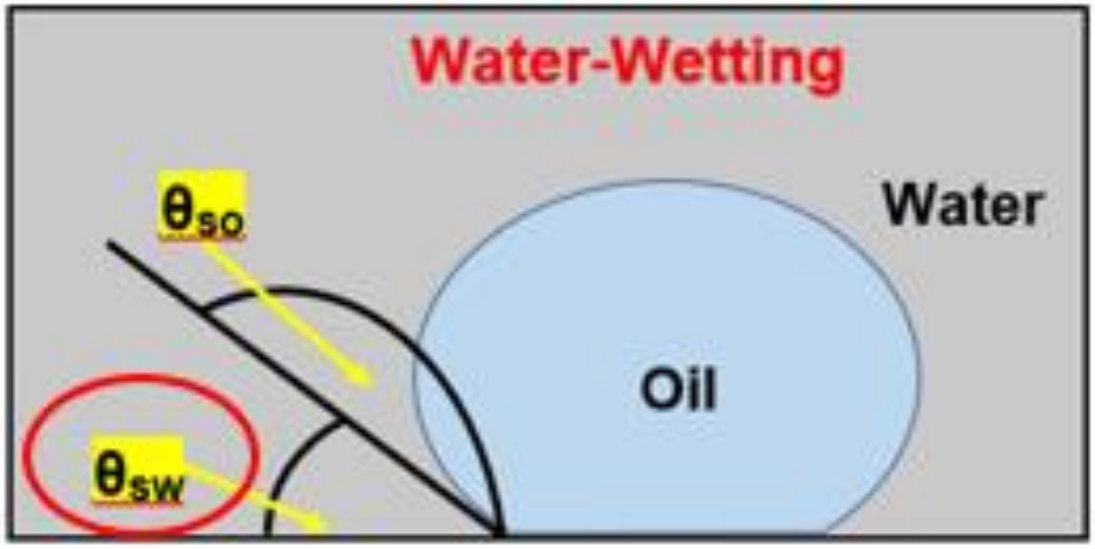

Figure 37 Contact angle measurement. Disk D: sandstone disk saturated by blend of OBDF with clay-free emulsion and 2.5 wt% surfactant (1:1 ratio), contact angle=64.95˚C. Reprinted with permission from SPE-190115-MS.

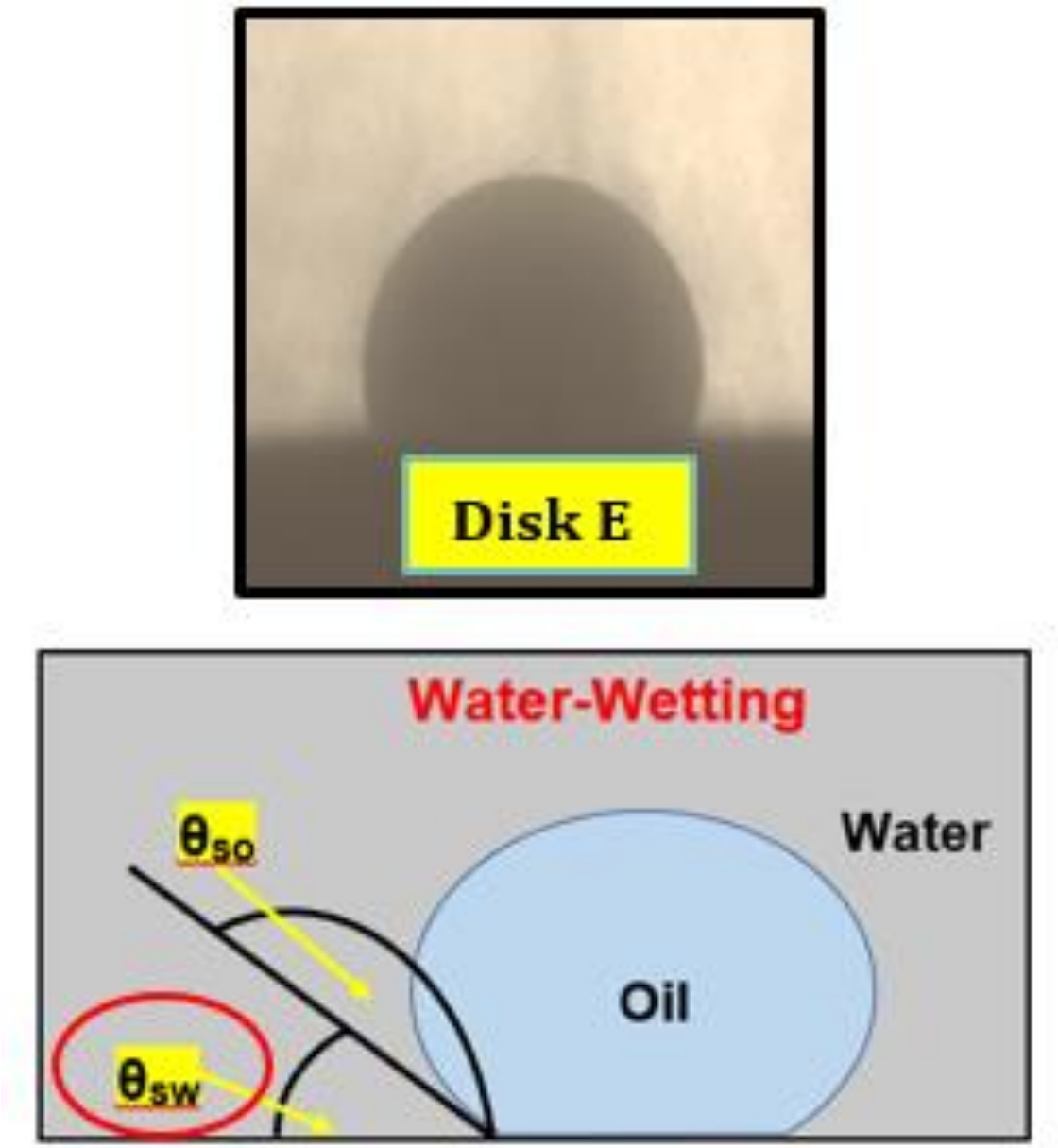

Figure 38 Contact angle measurement. Disk E: sandstone disk saturated by blend of OBDF with clay emulsion and 2.5 wt% surfactant (1:1 ratio), contact angle=81.67˚C. Reprinted with permission from SPE-190115-MS.

Table 10 Drop shape analysis of disks that treated by OBDF emulsion and surfactant. Reprinted with permission from SPE-190115-MS.

	OBDF with Clay Emulsion	OBDF without Clay Emulsion
Initial Contact Angle	106.21 ˚C	161.79 ˚C
Treated Contact Angle	81.67 ˚C	64.95 ˚C
Emulsion Breakdown Efficiency	23.11%	59.86%

5.5. Dissolve Weighting Materials

Based on measured pH values of the new surfactant/oxidant systems (B1, B2, B3, and B4), the cleaning solutions prepared by ammonium persulfate and sodium persulfate removed OBDF filter cakes in dilute acid condition. The reactive products of persulfate ions with water might be H_2O_2, HSO_4^-, and HSO_5^-.

Ammonium persulfate-based cleaning solution (B2, B3, and B4) removed OBDF filter cake more effectively than sodium persulfate-based cleaning solution (B1), according to the experimental results of filter cake removal efficiency. Higher solubility of ammonium persulfate promotes it to produce higher concentration of H_2O_2, HSO_4^-, and HSO_5^- in dilute acidic condition. These three breakers, H_2O_2, HSO_4^-, and HSO_5^-, can strongly break down OBDF filter cake layers and components (**Table 11**).

Coated chemicals always have resistance to release in the exposure conditions such as higher temperature and hydrogen sulfide. Based on ICP results (**Figures 39** and **40**), B4 cleaning solutions had highest solubility (12,080 ppm) of Mn_3O_4 than the

solubility of B1, B2, and B3 cleaning solutions (6,670 ppm, 7,353 ppm, and 11,830 ppm) at 250°F and 500 psi. For $CaCO_3$ weighting material, the solubility of four removal system were 435 ppm, 540 pm, 690 ppm, and 720 ppm after treated by new surfactant/oxidant systems at 250°F and 500 psi.

Table 11 Function and number of solids existing in filter cake. Reprinted with permission from SPE-190115-MS.

Components	Function	Lab (per 320 cm^3)	
		Quantity	Unit
Lime [$Ca(OH)_2$]	Alkalinity Control	18.7	g
$CaCl_2$ (97 wt%)	Osmotic Wellbore Stability	10	g
$CaCO_3$ (2.71 g/cm^3, D_{50} = 50 µm)	HT Filtration Control/Weighting Material	40	g
Mn_3O_4 (4.8 g/cm^3, D_{50} = 1 µm)	Weighting Material	205	g

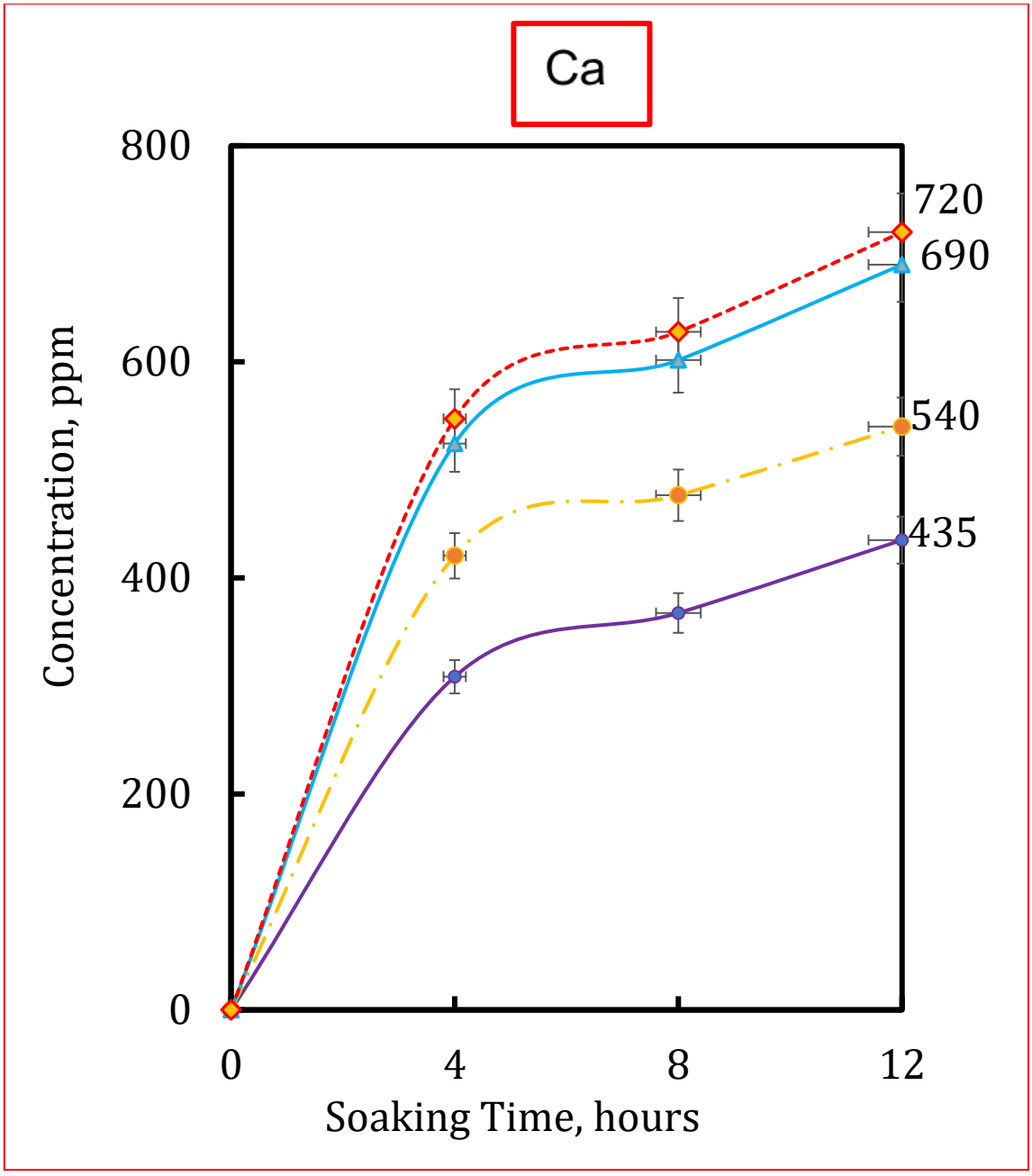

Figure 39 Dissolution of Ca^{2+} after soaking clay-free OBDF filter cake 12 hours at 250˚F/500 psi. Reprinted with permission from SPE-190115-MS.

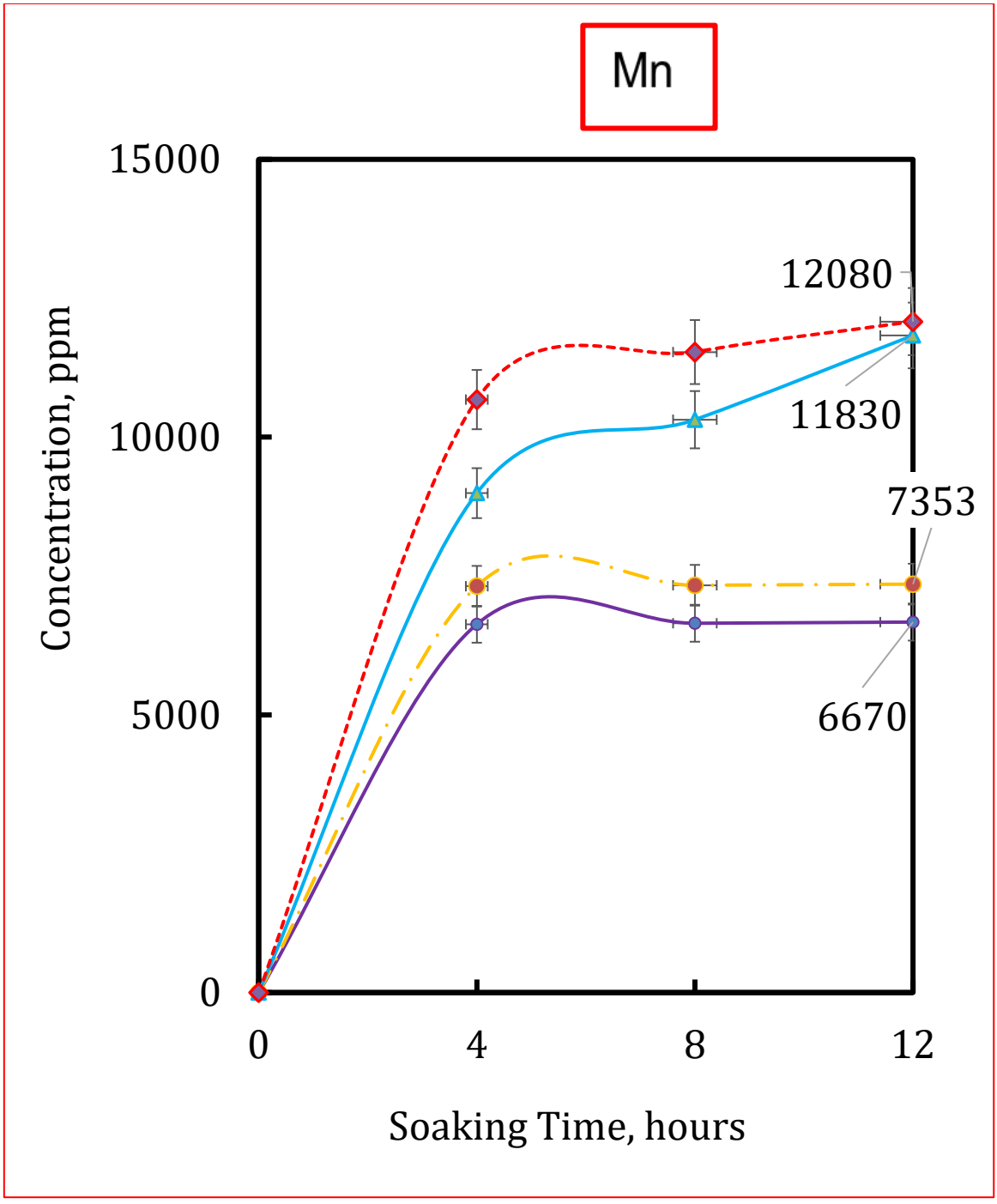

Figure 40 Dissolution of Mn^{2+} / Mn^{3+} after soaking clay-free OBDF filter cake 12 hours at 250˚F/500 psi. Reprinted with permission from SPE-190115-MS.

5.6. Formation Damage Analysis

Based on above experimental results, OBDF without clay had better rheological properties and filtration characters than OBDF with clay. The filter cake formed by OBDF without clay had higher removal efficiency than the filter cake formed by OBDF with clay. The following analysis of formation damage would focus on the OBDF without clay filter cake treated by new surfactant/oxidant system under 250ºF and 500 psi.

Results of coreflood test are disclosed in **Figure 41**. After the OBDF filter cake removal test, the permeability loss percentage of disk that treated by B1, B2, B3, and B4 were 72.66%, 49.47%, 46.3%, 32.18%, respectively. The coreflood test indicated B4 system caused least damage on the permeability of sandstone reservoir than others.

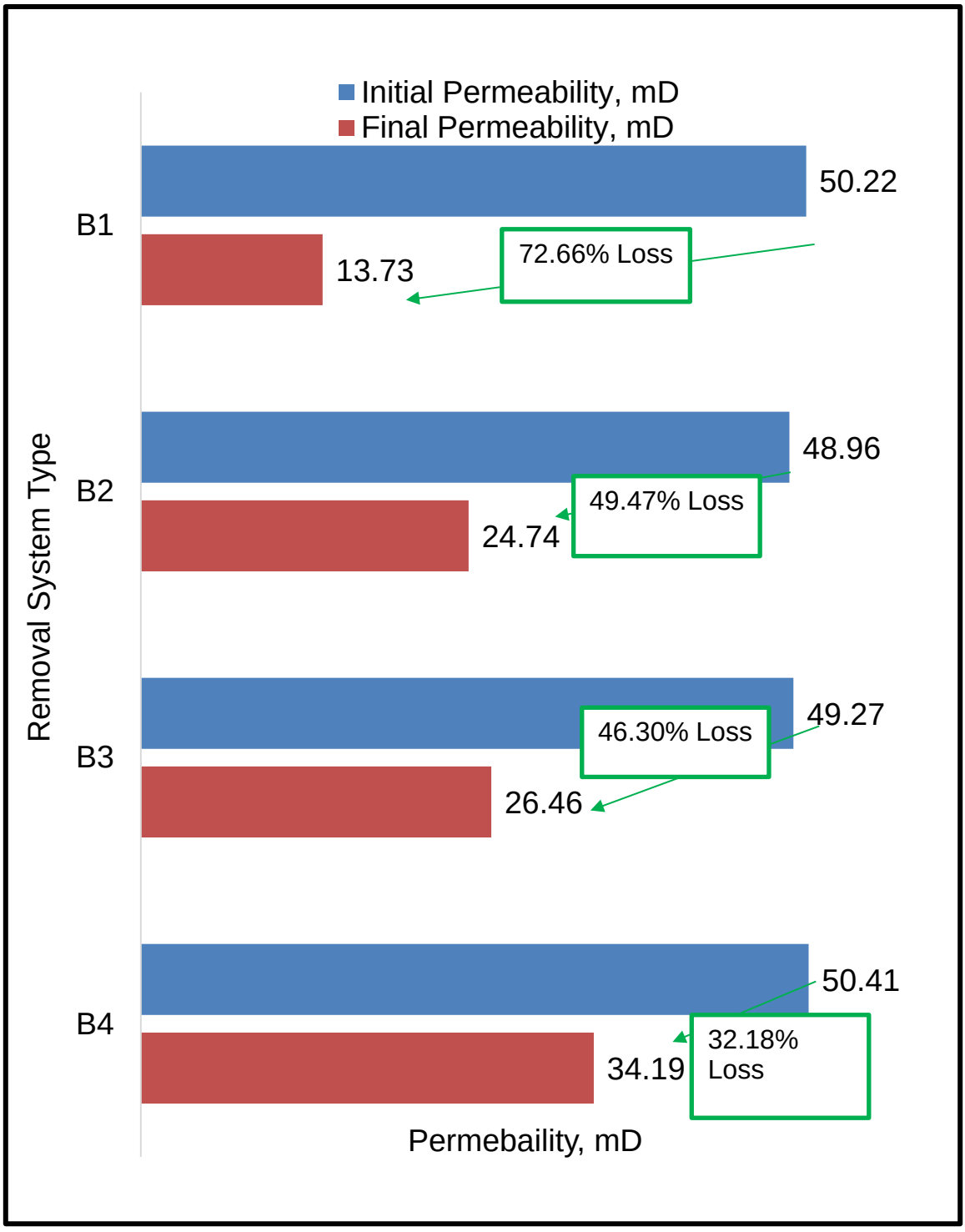

Figure 41 Permeability loss of disks that soaked 12 hours by different removal systems at 250°F and 500 psi. Reprinted with permission from SPE-190115-MS.

The obtained CT images disclosed from the ImageJ software and the calculated porosity values were exposed in **Figure 42** and **Table 12**. After soaking filter cake by 12 hours, under 250°F heating temperature and 500 psi differential pressure conditions, the porosity loss percentage of disk that treated by B1, B2, B3, and B4 were 45.16%, 33.74%, 28.89%, 4.38%, respectively.

These phenomena could also be explained by ICP test, B4 system dissolved higher concentration of weighting materials than B1, B2, and B3 systems. The products of reaction between breakers and weighting materials might plug into the porous throats of formation surface, which might cause the higher declination of porosity than oxidant.

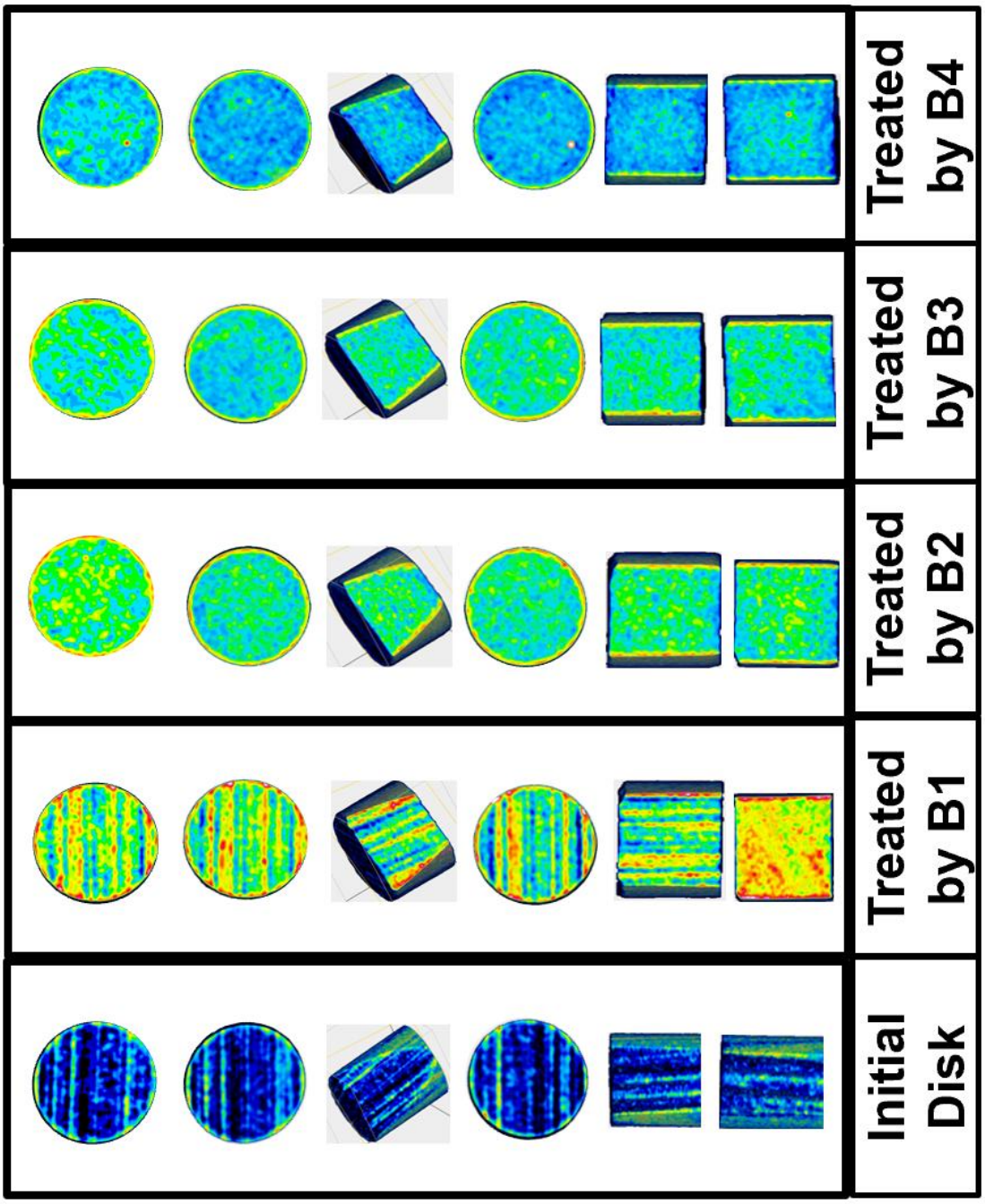

Figure 42 CT images of Berea sandstone disks from different view direction. Reprinted with permission from SPE-190115-MS.

Table 12 Porosity loss of disks after the treatment of different cleaning solutions. Reprinted with permission from SPE-190115-MS.

Treatment	B1	B2	B3	B4
Initial Porosity, vol%	7.22	7.35	7.09	7.18
Final Porosity, vol%	3.96	4.87	4.98	6.87
Porosity Loss, %	-45.16%	- 33.74%	- 28.89%	- 4.38%

5.7. Compatibility of Emulsion, Crude Oil, and Removal System

The phase behavior of the compatibility test between OBDF emulsion and B4 cleaning solution is given in **Figure 43**. The density of B4 solution is 1.2 g/cm^3 and the density of OBDF emulsion is 1.6 g/cm^3. When 5 cm^3 B4 solution was put into 5 cm^3 OBDF emulsion, B4 and OBDF emulsion gradually formed one mixture in 5 hours. Then the mixture separated back into B4 and OBDF emulsion after 43 hours.

The phase behavior of the compatibility test between crude oil and B4 cleaning solution is given in **Figures 44** and **45**.

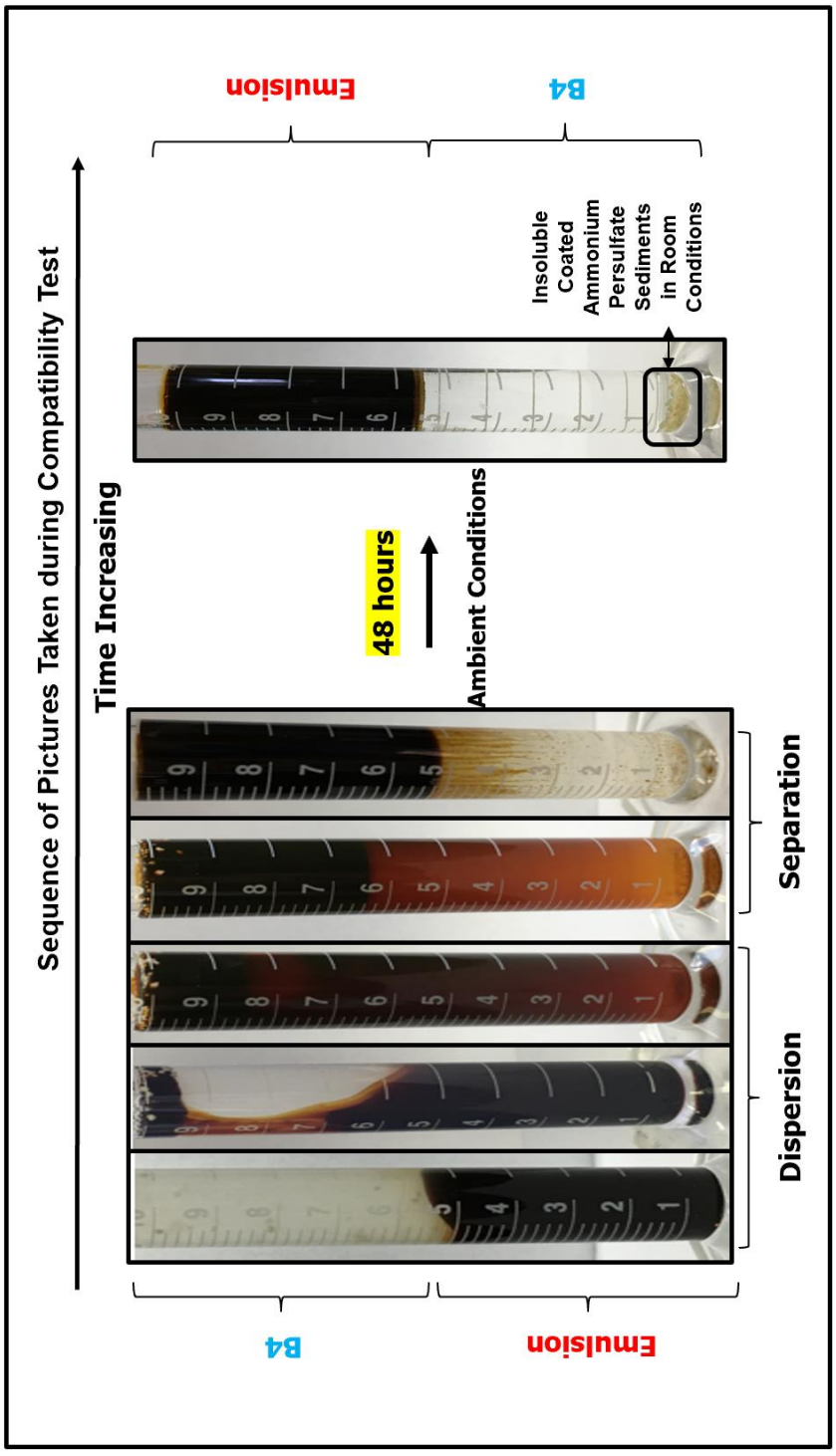

Figure 43 Compatibility of OBDF (without clay) emulsion and cleaning solution (B4). Reprinted with permission from SPE-190115-MS.

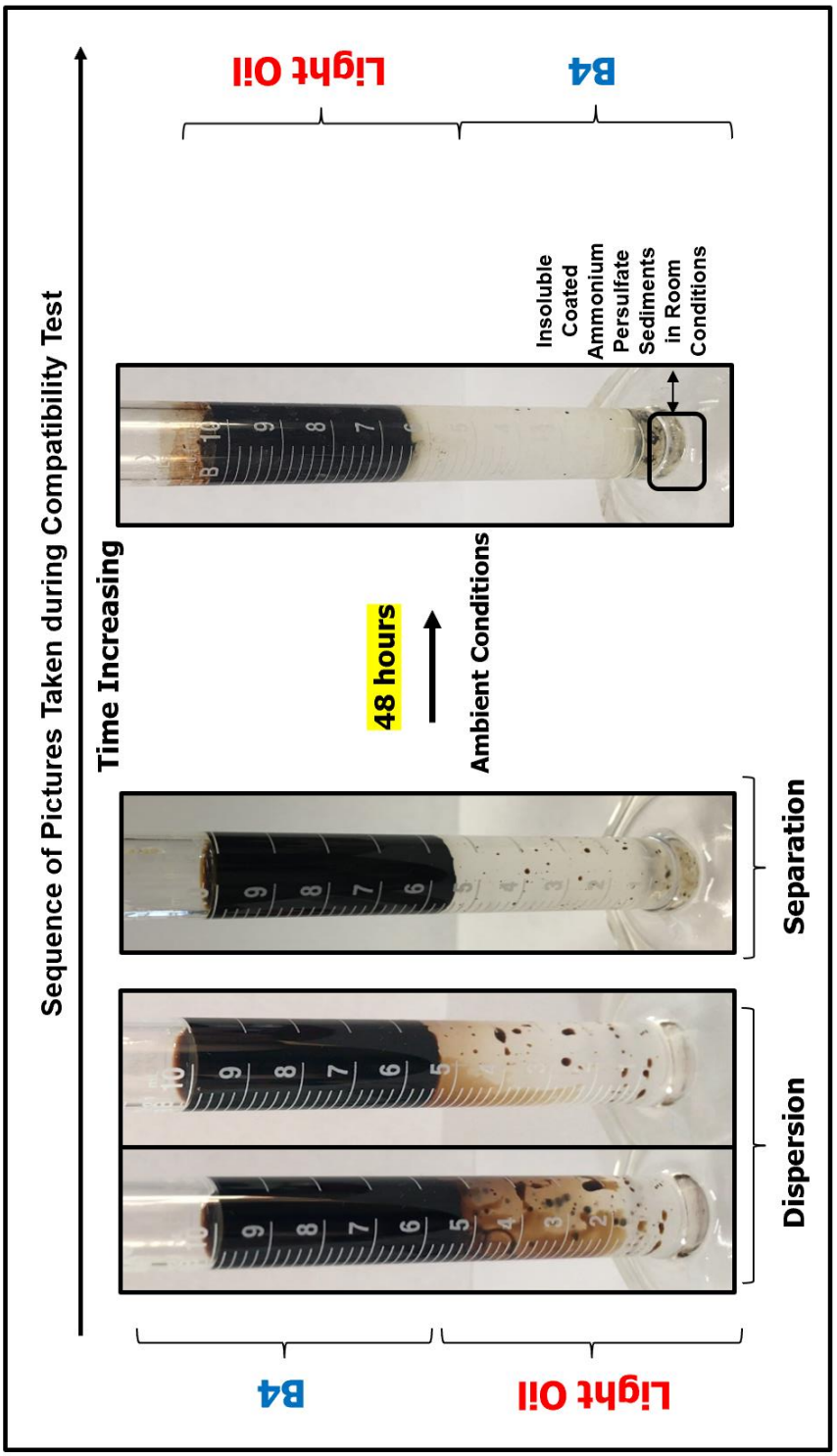

Figure 44 Compatibility of light oil and cleaning solution (B4).

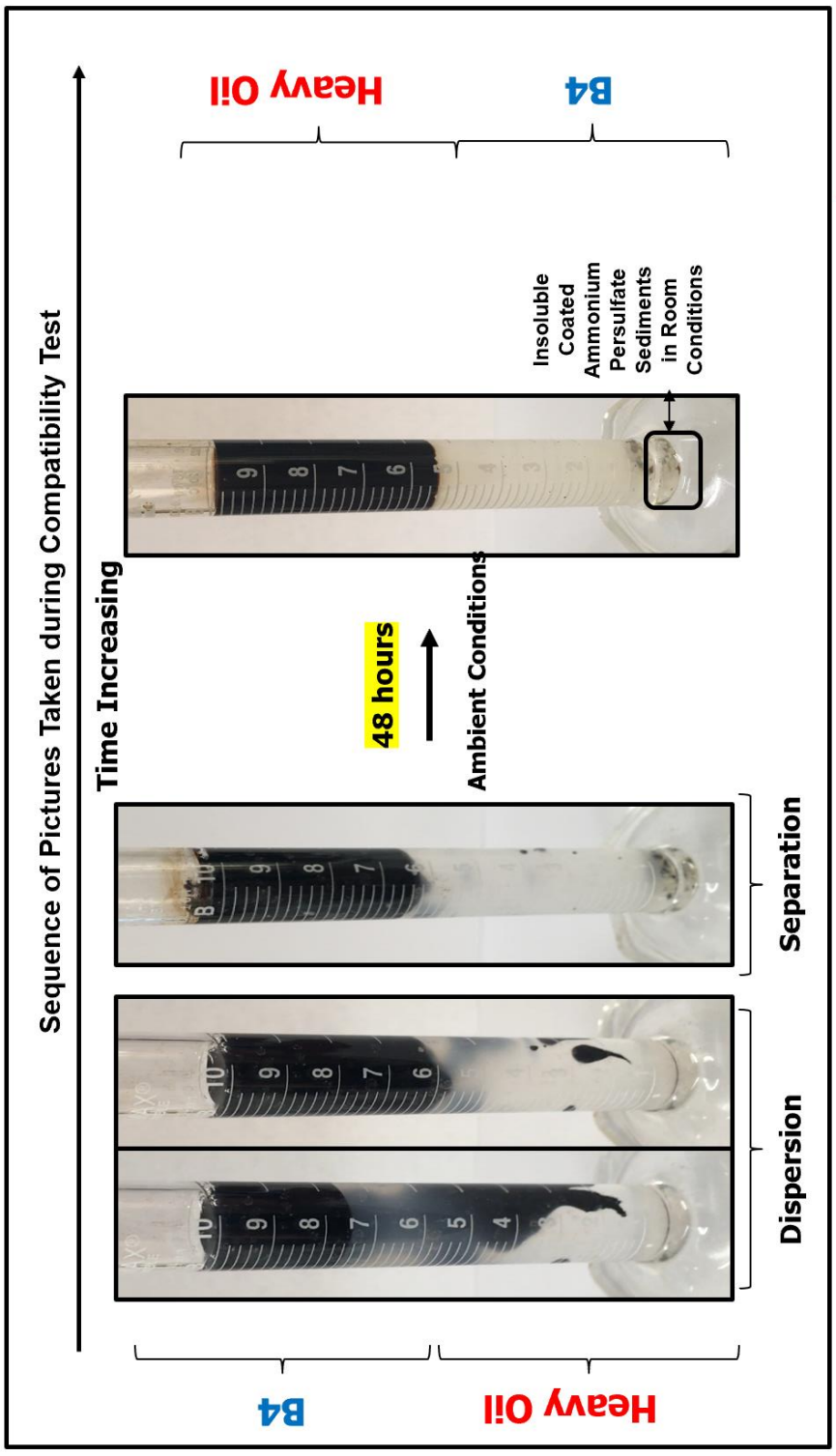

Figure 45 Compatibility of heavy oil and cleaning solution (B4).

The increased volume of the mixture and B4 are both functions of time. Ammonium persulfates precipitated in the bottom due to their insoluble coating. In conclusion the test results above indicate the good compatibility of the optimized new surfactant/oxidant system (B4) with OBDF emulsion.

5.8. Corrosion Damage Analysis

The experimental results of corrosion damage analysis test is given in **Table 13**. **Figures 46** to **55** show the coupon damage and solution color change of corrosion tests 1 to 5.

The corrosion rates of 2 wt% 0% coated persulfate with 5 vol% corrosion inhibitor and 1.5 wt% 0% coated persulfate with 5 vol% corrosion inhibitor were 0.045 lb/ft^2 and 0.033 lb/ft^2, respectively, which are both acceptable corrosion rates for industry. When the concentration of 0% coated persulfate were 3 or 8, 5 vol% or 7 vol% corrosion inhibitor concentration cannot control the corrosion damage effectively.

Table 13 Corrosion rate comparison.

Test Number	0 % Coated Persulfate, wt%	CI Concentration, vol%	Corrosion Rate, lb/ft^2
1	8	5	0.099
2	8	7	0.125
3	3	5	0.079
4	2	5	0.045
5	1.5	5	0.033

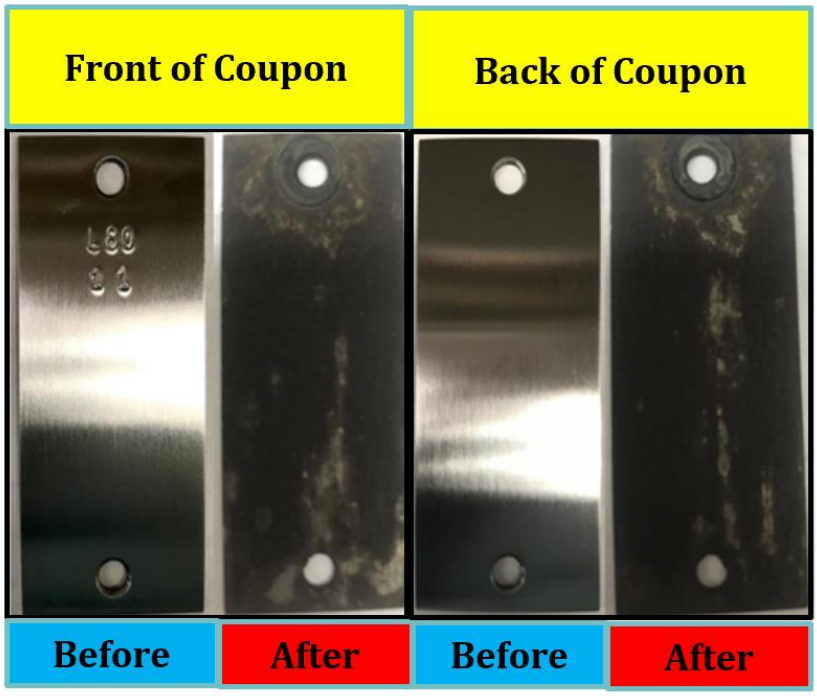

Figure 46 Coupon damage of corrosion test 1: 8 wt% 0% coated persulfate and 5 vol% CI concentration.

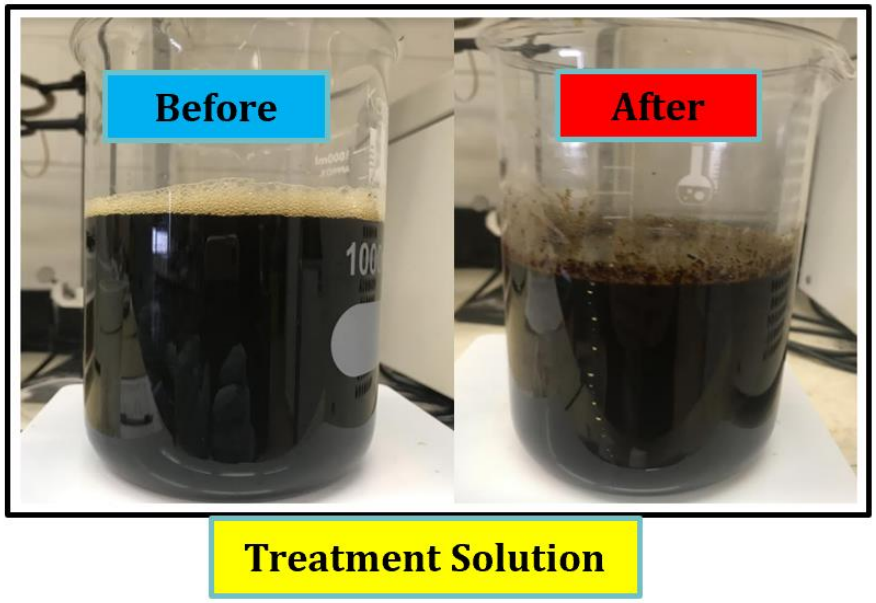

Figure 47 Solution color change of corrosion test 1: 8 wt% 0% coated persulfate and 5 vol% CI concentration.

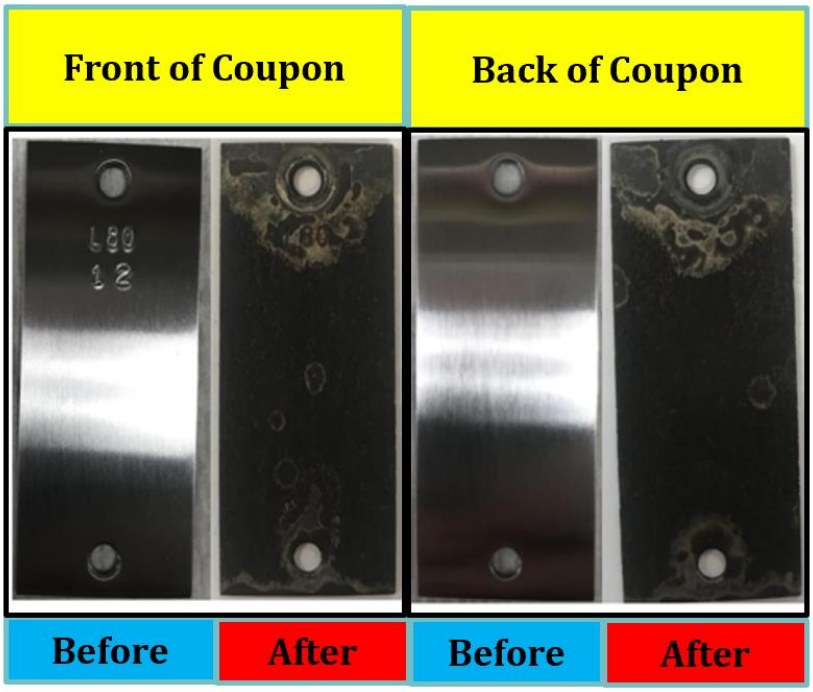

Figure 48 Coupon damage of corrosion test 2: 8 wt% 0% coated persulfate and 7 vol% CI concentration.

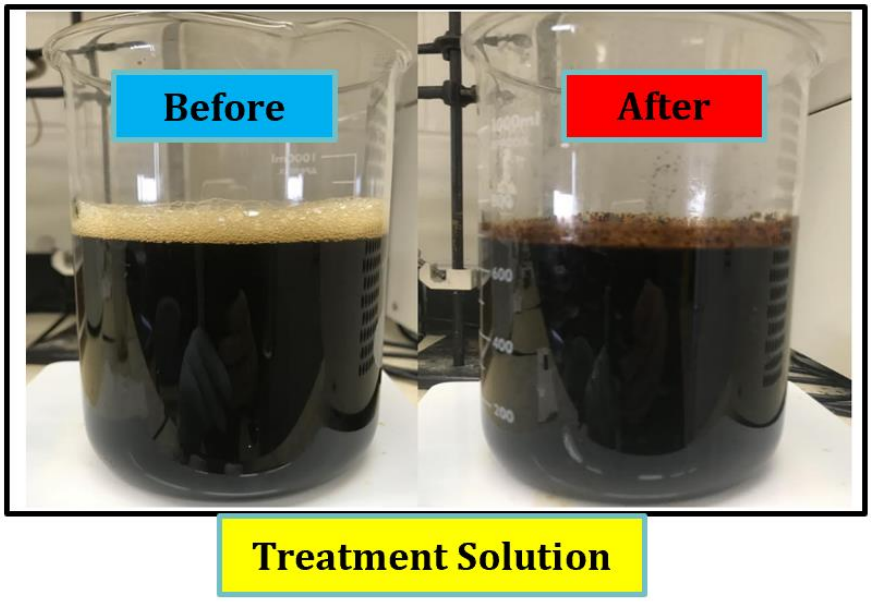

Figure 49 Solution color change of corrosion test 2: 8 wt% 0% coated persulfate and 7 vol% CI concentration.

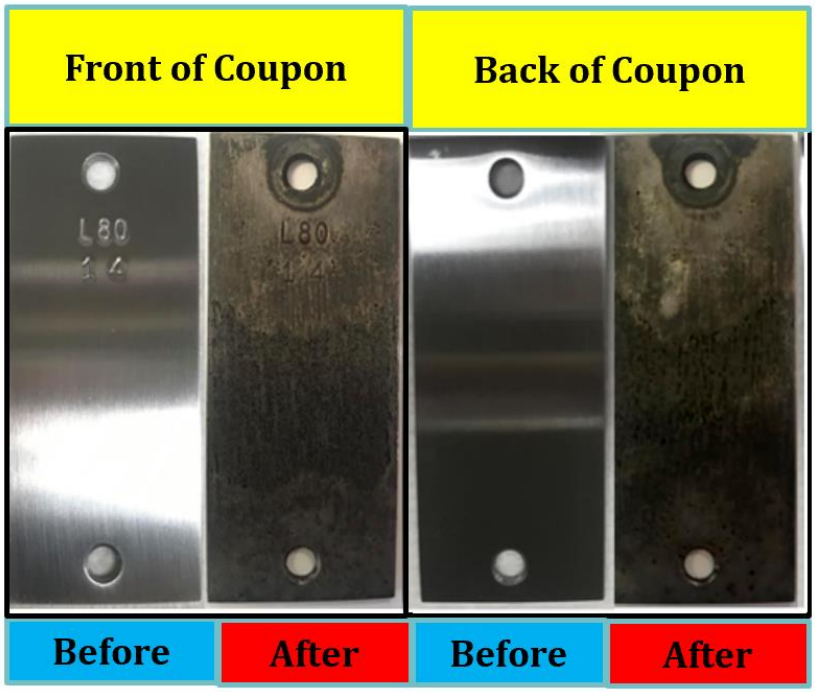

Figure 50 Coupon damage of corrosion test 3: 3 wt% 0% coated persulfate and 5 vol% CI concentration.

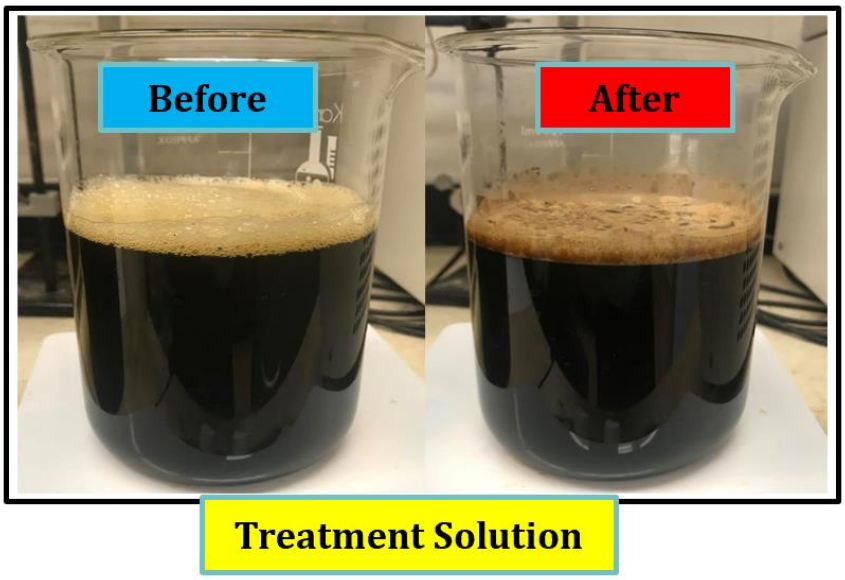

Figure 51 Solution color change of corrosion test 3: 3 wt% 0% coated persulfate and 5 vol% CI concentration.

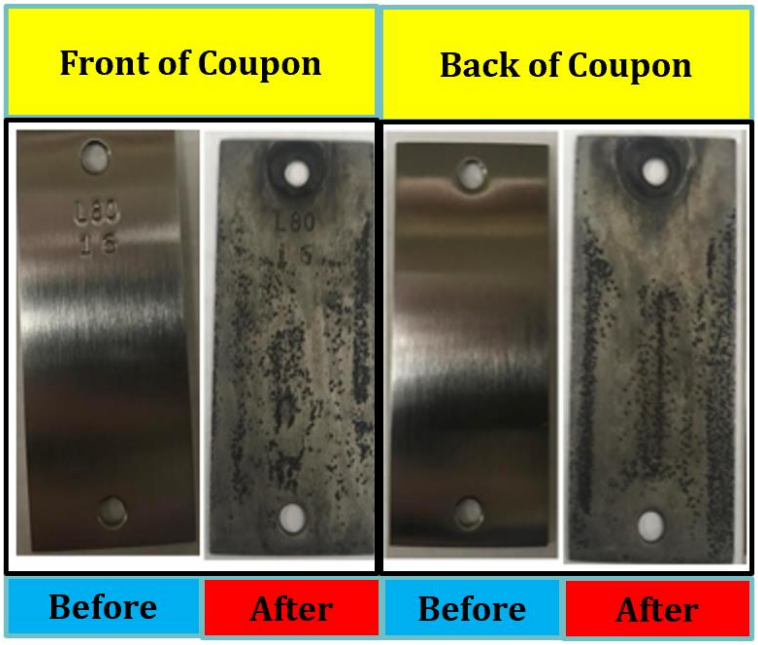

Figure 52 Coupon damage of corrosion test 4: 2 wt% 0% coated persulfate and 5 vol% CI concentration.

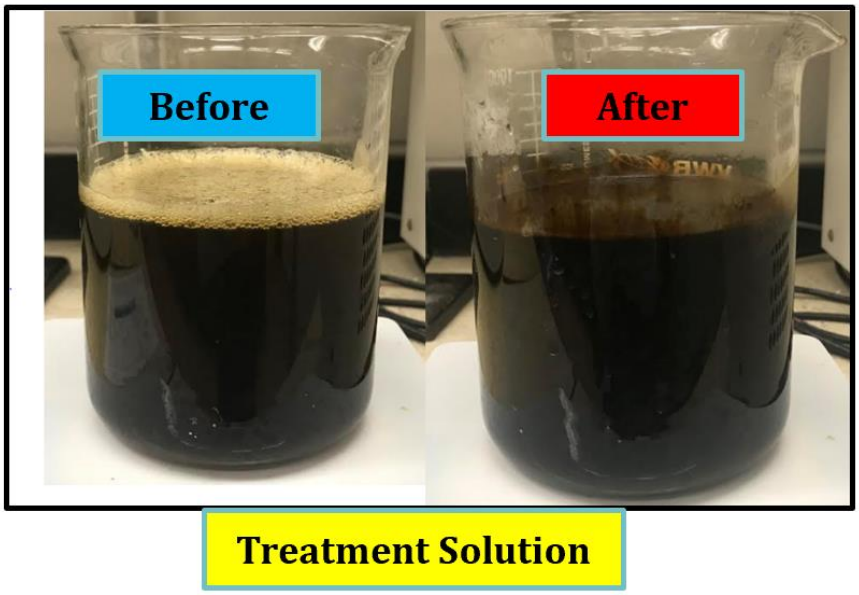

Figure 53 Solution color change of corrosion test 4: 2 wt% 0% coated persulfate and 5 vol% CI concentration.

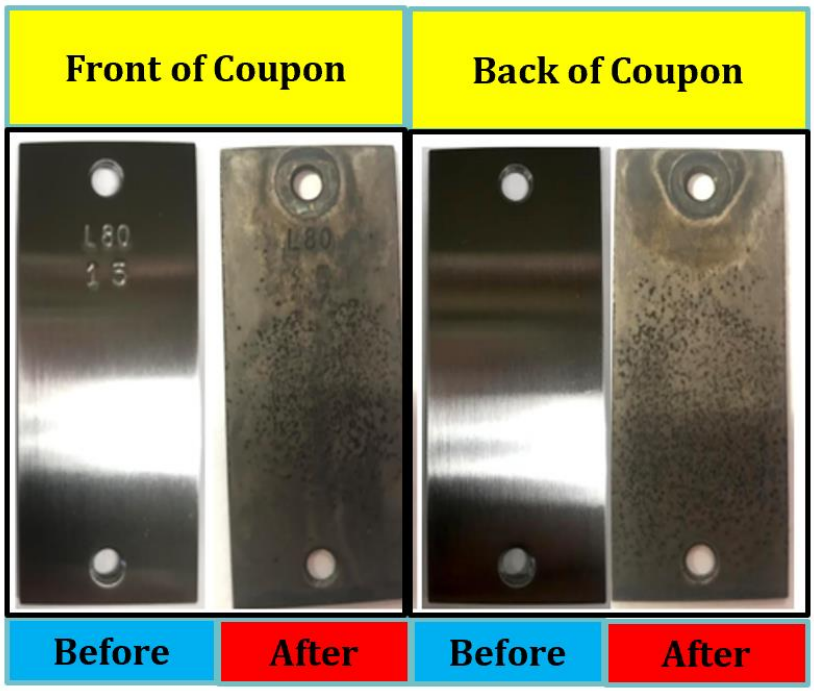

Figure 54 Coupon damage of corrosion test 5: 1.5 wt% 0% coated persulfate and 5 vol% CI concentration.

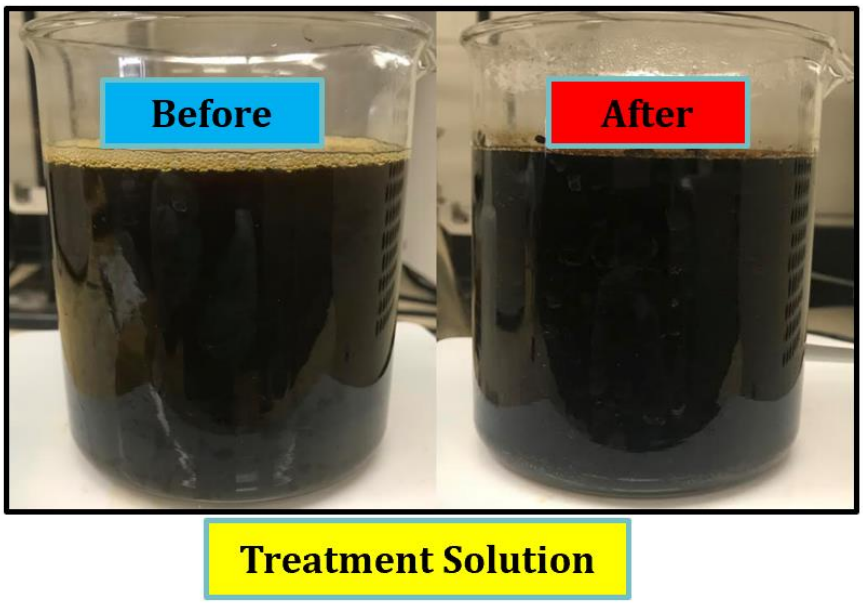

Figure 55 Solution color change of corrosion test 5: 1.5 wt% 0% coated persulfate and 5 vol% CI concentration.

5.9. Field Application Recommendation

5.9.1. Advantages of Novel Surfactant/Oxidant System

The design consideration of novel surfactant/oxidant system is to make it to be non-aromatic solvent. Non-aromatic compound is either not cyclic or not planar, while an aromatic compound is cyclic or planar and have a stable conjugation. The non-aromatic properties of novel surfactant/oxidant system are including ≥100ºC high flash point, clean sand surfaces more easily, and enhances surfactant action to wet sand surfaces.

The novel surfactant/oxidant system could self-diffuse into damaged zone. It can incorporates/solubilizes the oil, removes OBDF emulsions, and water wets all solids

100%. The reaction of treatment process has no energy needed contact time and is spontaneous action to mobilize crude oil, remove near wellbore damage, water wet surfaces.

5.9.2. Application of Novel Surfactant/Oxidant System

When treat cased-hole completions, the basic application of novel surfactant/oxidant system is basic application. There are several extended applications of novel surfactant/oxidant system, as follows:

- Extended Application of Novel Surfactant/Oxidant System:
    i. Chemical Damage Remediation:
        1. Acid Remediation;
        2. Drill-in Fluid Filtrate;
        3. Polymer Block;
        4. Brine Incompatibility
    ii. Trapped Oil Treatment:
        1. Wettability Alteration
    iii. Perforation Damage Remediation:
        1. Charge Debris;
        2. Trapped Solids
    iv. Heavy Hydrocarbon Deposition Treatment:
        1. Asphaltene/Paraffin
    v. Water-Block Clearance:

1. Reduced Reservoir Pressure;
2. Water Production;
3. Completion Fluid Invasion

5.9.3. Post Treatment Success Factors

Here are some recommendations for post treatment success factors that should be considered seriously when apply the novel surfactant/oxidant system into field treatment:

- Did we treat a viable reservoir?
- Did we identify the damage?
    - Emulsion? OBDF?
    - Water-block?
    - Polymer block?
    - Heavy crude deposition?
    - Fluid/fluid incompatibility?
- Did we contact the affected zone(s)?
    - Did we require zonal isolation?
    - Did we use an isolation technique?
- Did we allow for soak time?

These problems are highly recommended to be considered and solved before and during the application of novel surfactant/oxidant system.

5.9.4. Target Applications/Wells

5.9.4.1. Injection treatment of removal system

As shown in **Figure 56**, when perforated wells are treated, 35 gal per foot of perfs is preferred, also with 3-4 ft radial treatment applied. When we treat perforated and fractured wells, 50 gals per ft of perfs is recommended.

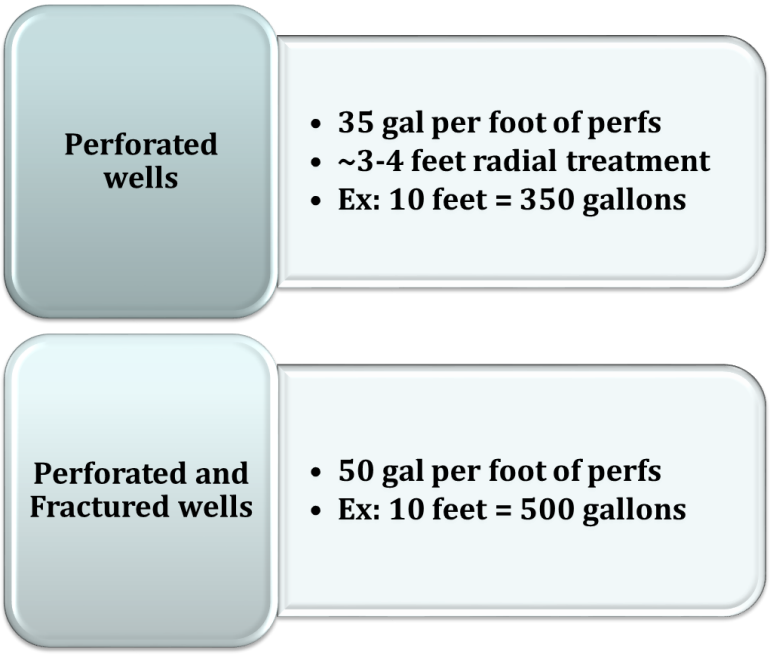

Figure 56 Injection treatment of removal system.

5.9.4.2. Tools of Injection System

Figure 57 shows the pictures of ISAP straddle packer retrievable bridge plug, and retrievable packer that used for injection system.

5.9.4.2.1. ISAP Straddle Packer

In order to remove the suspected damage more effectively a coiled tubing-based solution was implemented which involved the application of ISAP straddle packer tool.

This tool provide pinpoint accuracy for conventional, horizontal and multilateral stimulation treatment. Treatment valve allows precise injection of treatment fluid and adjusted element spacing helps in straddling the long interval (Singh et al. 2013).

5.9.4.2.2. Retrievable Bridge Plug

Retrievable bridge plug tools were initially deployed on electric line and set using explosive methods. The use of slickline technology provides operational flexibility as the plug can be set when conditions dictate and requires only a slickline crew. The following lists are the priorities for the design of this type of plug (Gee et al. 1993):

- To minimize the diameter of the tool in order to maximize access through the completion;
- To make the tool suitable for as wide a range of tubing weights within each size range. E.g. for a 5-1/2" plug to cover weights from 17 lb/ft to 23 lb/ft;
- That all sizes of the plug up to and including 7" should be deployable by slickline manipulation only to avoid the requirement for hydraulic setting if possible;
- et al.

5.9.4.2.3. Retrievable Packer

There are two types of production packer when we finish the completion: permanent or retrievable packer. The most reliable option of extreme conditions is permanent packer. Because permanent set offers simplicity, requiring few moving parts. Hostile environments are typically addressed with permanent packers, both for management of cost and concerns for the long-term integrity of the retrieval mechanism.

The retrievable option offers the most flexibility and potential economy in cases where the removal is anticipated in the short-term, or repeatedly in the life of the well. Some of the retrievable packer models still dictate limitations in their internal diameter specifications, associated with the internal bypass and retrieval mechanisms (Triolo et al. 2002).

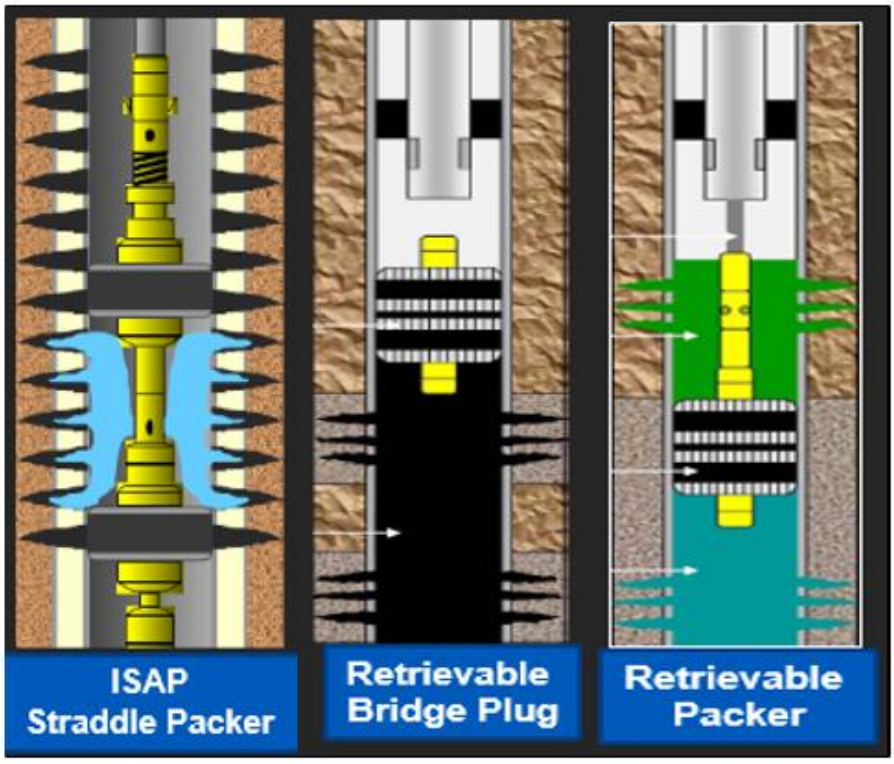

Figure 57 Tools of injection system.

5.9.5. Successful Field Cases with Similar Treatment Processes

In this section, four successful field cases with similar treatment processes are explained in detail.

Case 1: In south Texas, there was a perforated casing well with low production rate and water block problem. The injection method of treatment solution was pumped down annulus and soaked in perfs. Before treatment, the production rate was 23 Mcf per day, and the production rate was increased to 146 Mcf per day after whole treatment.

Case 2: Same in south Texas, the perforated and frac'd well had a problem with "produced" OBDF. Treatment solution was injected with coil-tubing placement and squeezed into fractures. The pre-treatment and post-treatment production rate were 1.9 MMcf per day and 4.6 MMcf per day, respectively.

Case 3: In central Texas, there was existing a perforated casing well that had emulsion block problem. We applied injection method of pumping down production tubing and soaked the treatment solution in perfs. The production rate of this well was increased from 420 Mcf per day to 720-820 Mcf per day when finished the treatment.

Case 4: There was a limestone reservoir drilled with OBDF and there was barefoot completion in open hole. The injection method of treatment solution was that spotted in casing and perforated 30 ft section in toe and soaked the solution in perfs. The pre-treatment production rate and the post-treatment production rate were 1.5 MMcf per day and 2.2 MMcf per day, with the increasing of 0.7 MMcf per day.

Case	Well Location	Well Type	Problem	Injection Method	Treatment Method	Pre-Treatment Production	Post-Treatment Production
1	South Texas	Perforated Casing	Low Production Rate, Water Block	Pumped Treatment down Annulus	Soak in Perfs	23 Mcf/day	146 Mcf/day
2	South Texas	Perforated & Frac'd	"Produced" OBDF	Coil-tubing Placement	Squeezed into Fractures	1.9 MMcf/day	4.6 MMcf/day
3	Central Texas	Perforated Casing	Emulsion Block	Pumped Treatment down Production Tubing	Soak in Perfs	420 Mcf/day	720~820 Mcf/day
4	Limestone Reservoir Drilled with OBDF	Barefoot Completion in Open Hole	OBDF Filter Cake near Wellbore Damage	Spotted in Casing and Perforated 30 ft Section in Toe	Soak in Perfs	1.5 MMcf/day	2.2 MMCf/day

Figure 58 Successful cases of cleaning solution application.

6. [4]CONCLUSION

The present study conducted a comprehensive evaluation of the brine-based new surfactant/oxidant system to remove OBDF filter cake with quick removal steps and high removal efficiency. The following conclusions were obtained:

1. OBDF without clay additive had lower spurt loss and lower filtrate volume than clay-based OBDF. The difference might be explained by the replacement of clay with a cross-linked polymer in the OBDF formula. Under HP/HT conditions, a cross-linked polymer used in OBDF performed as a better viscosifier and stronger filtration loss-control agent than clay components.
2. The filter cake removal test results indicated that the optimized new system degraded the filter cake by up to 98 wt% removal efficiency.
3. Based on measured pH values (1 to 3) of the new surfactant/oxidant systems (B1, B2, B3, and B4), the cleaning solutions will remove OBDF filter cakes in dilute acidic conditions. With the increasing of temperature, acrylic resins released away from persulfate, consumed the OH^- ions, and caused the cut down of pH value.
4. Optimized surfactant/oxidant system (B4) caused the formation permeability with 32.18% loss and formation porosity with 4.38% loss, which were lower than

[4] *Reprinted with permission from "A Cost-Effective Application of New Surfactant/Oxidant System to Enhance the Removal Efficiency of Oil-Based Filter Cake" by J. Zhou et al., 2018. SPE-190115-MS, Copyright 2018 by Society of Petroleum Engineers.

B1, B2, and B3 systems (permeability loss with 72.66%, 49.47%, 46.30%, and porosity loss with 45.16%, 33.74%, 28.89%).

5. After soaking OBDF (without clay) filter cake 12 hours at 250°F and 500 psi, B3 and B4 cleaning solutions had higher solubility (11,830 ppm and 12,080 ppm) of Mn_3O_4 than B1 and B2 cleaning solutions (6,670 ppm and 7,353 ppm). For $CaCO_3$ weighting material, the solubility of four removal system were 435 ppm, 540 pm, 690 ppm, and 720 ppm after treated by new surfactant/oxidant systems at 250°F and 500 psi.
6. 1.5 wt% and 2 wt% of 0% coated persulfate with 5 vol% of Rodine 31-a gave an industry accepted corrosion rate of 0.033 lb/ft^2 and 0.045 lb/ft^2 on L-80 coupon, respectively, although minor pitting was still present on the faces of the coupon. The Fe and Mn concentrations in 6 hours reaction solution of 1.5 wt% 0% coated persulfate with Rodine 31-a were lower (820 ppm and 3 ppm) than that of 2 wt% 0% coated persulfate with Rodine 31-a (1,055 ppm and 5 ppm) respectively, under 250 ºF and 1,000 psi conditions.
7. As a non-aromatic solvent, the novel surfactant/oxidant solution can self-diffuse into damaged zone to incorporate/solubilize the oil, break OBDF emulsions, and water-wet most of solids. The process is no energy needed-just soaking time.
8. The application of the novel cleaning solution is non-customized for cased-hole completions, including basic application as OBDF filter cake removal, and extended applications as chemical damage remediation, trapped oil treatment, perforation damage remediation, heavy hydrocarbon deposition treatment, and

water-block clearance.

9. For only perforated casing well type, the treatment method of novel cleaning solution is recommended as pumped treatment down annulus and soaked in perforations to clear water block, or as pumped treatment down production casing and soaked in perforations to clear emulsion block.
10. For perforated and fractured casing well types, the treatment methods of novel cleaning solution are recommended as soaked in perforations and squeezed into fractures to clear OBDF filter cakes.
11. For barefoot completion in open hole, the treatment method is recommended as spotted in casing and perforated 30 ft section in toe and soaked in perforations to clear near wellbore damages caused by OBDF filter cakes.

With optimized formulation and soaking time, the cleaning solutions will benefit the oilfield industry significantly by removing OBDF filter cake under challenging well conditions. The new surfactant/oxidant system minimizes the effects of drilling fluids on formation properties, based on its quick removal steps, high removal efficiency, and acceptable formation damage and corrosion damage.

REFERENCE

Addagalla, A. V., Kosandar, B. A., Lawal, I., et al. 2015. Using Mesophase Technology to Remove and Destroy the Oil-based Mud Filter Cake in Wellbore Remediation Applications-Case Histories, Saudi Arabia. Presented at the SPE Middle East Oil & Gas Show and Conference, Manama, Bahrain, 8–11 March. SPE-172602-MS. https://dx.doi.org/10.2118/172602-MS.

Addagalla, A. K. V., Kosandar, B. A., Lawal, I. G., et al. 2016. Delayed Reaction Micro-Emulsion Fluid to Clean Oil Base Mud Filter Cake Damage in Open Hole Completions. Presented at the Offshore Technology Conference Asia, Kuala Lumpur, Malaysia, 22–25 March. OTC-26385-MS. https://doi.org/10.4043/26385-MS.

Agiza, M. N. and Awar, S.A. 1983. Minimizing Casing Corrosion. Presented at the Middle East Oil Technical Conference, Manama, Bahrain, 14–17 March. SPE-11513-MS. https://doi.org/10.4043/11513-MS.

Allogo, C. M. E., Ravitz, R., Gadiyar, B., et al. 2016. Ability of a Filter Cake Breaker to Diffuse into Completion Brine and Packed Gravel. Presented at the SPE International Conference and Exhibition on Formation Damage Control, Lafayette, Louisiana, USA, 24–26 February. SPE-179007-MS. https://doi.org/10.2118/179007-MS.

Alimuddin, S., Yewlekar, S., Raman, C. V., et al. 2016. Strategically Increasing Completion Efficiency by Applying a Customized Filter Cake Breaker Solution. Presented at the SPE/IADC Middle East Drilling Technology Conference and

Exhibition, Abu Dhabi, UAE, 26–28 January. SPE-178209-MS. https://doi.org/10.2118/178209-MS.

Al Moajil, A., Nasr-El-Din, H. A., Al-Yami, A., et al. 2008. Removal of Filter Cake Formed by Manganese Tetraoxide Based-Drilling Fluids. Presented at the SPE International Symposium and Exhibition on Formation Damage Control, Lafayette, Louisiana, 13–15 February. SPE-112450-MS. https://dx.doi.org/10.2118/112450-MS.

Al Moajil, A. and Nasr-El-Din, H. A. 2010. Reaction of Hydrochloric Acid with Filter Cake Created by Mn_3O_4 Water-Based Drilling Fluids. Presented at the Trinidad and Tobago Energy Resources Conference, Port of Spain, Trinidad, 27–30 June. SPE-133467-MS. https://dx.doi.org/10.2118/133467-MS.

Al Moajil, A., Rehman, A., Al-Bagoury, M., et al. 2012. Evaluation of Dispersants for Drilling Fluids Based on Manganese Tetraoxide. Presented at IADC/SPE Asia Pacific Drilling Technology Conference and Exhibition, China, 9–11 July. SPE-154830-MS. http://dx.doi.org/10.2118/154830-MS.

Al Moajil, A. and Nasr-El-Din, H. A. 2013. Formation Damage Caused by Improper Mn_3O_4-Based Filter Cake Cleanup Treatments. *Journal of Canadian Petroleum Technology*, **52** (1): 64–74.

Al Moajil, A., Nasr-El-Din, H. A., Kar, Y., et al. 2015. Dispersants for Cement and Salt Contaminated Manganese Tetraoxide High-Density Water-Based Drilling Fluids. Presented at the SPE Abu Dhabi International Petroleum Conference and Exhibition, Abu Dhabi, UAE, 9–12 November. SPE-177935-MS. https://dx.doi.org/10.2118/177935-MS.

Al Moajil, A., Nasr-El-Din, H. A., Kar, Y., et al. 2015. Dispersants for Cement and Salt Contaminated Manganese Tetraoxide High-Density Water-Based Drilling Fluids. Presented at the SPE Abu Dhabi International Petroleum Conference and Exhibition, Abu Dhabi, UAE, 9–12 November. SPE-177935-MS. https://dx.doi.org/10.2118/177935-MS.

Al-Muntasheri, G. A., Li, L., Liang, F., et al. 2017. Concepts in Cleanup of Fracturing Fluids Used in Conventional Reservoirs: A Literature Review. Society of Petroleum Engineers. https://doi.org/10.2118/186112-PA.

Al-Otaibi, M.A., Binmoqbil, K.H., Rabba, A., et al. 2010. Single-Stage Chemical Treatment for Oil-Based Mud Cake Cleanup: Lab Studies and Field Case. Presented at the SPE International Symposium and Exhibition on Formation Damage Control, Lafayette, Louisiana, 10–12 February. SPE-127795-MS. https://dx.doi.org/10.2118/127795-MS.

Anton, R. and Salager, J.L. 1990. Effect of the Electrolyte Anion on the Salinity Contribution to Optimum Formulation of Anionic Surfactant Microemulsions. *Journal of Colloid and Interface Science*, **140**: 75–81.

Anton, R. E., Graciaa, A., Lachaise, J., et al. 2007. Surfactant-Oil-Water Systems near the Affinity Inversion Part IX: Optimum Formulation and Phase Behavior of Mixed Anionic-Cationic Systems. *Journal of Dispersion Science and Technology*, **13** (5): 565–579.

Bennion, D.B., Thomas, F.B., and Bietz, R.R. 1996. “Formation Damage and Horizontal Wells-A Productivity Killer?” Presented at the SPE Horizontal Well Technology

Conference, Calgary, Canada, 18–20 November. SPE-37138-MS. https://dx.doi.org/10.2118/37138-MS.

Berbenni, V. and Marini, A. 2003. Oxidation Behavior of Mechanically Activated Mn_3O_4 by TGA/DSC/XRPD. *Master. Res. Bull.* **38** (14): 1859–1866.

Binmpqbil, K.H., Al-Otaibi, M.A., Al-Faifi, M.G., et al. 2009. Cleanup of Oil-Based Mud Filter Cake Using an In-Situ Acid Generator System by a Single-Stage Treatment. Presented at the SPE Saudi Arabia Section Technical Symposium and Exhibition, Al-Khobar, Saudi Arabia, 9–11 April. SPE-126065-MS. https://dx.doi.org/10.2118/126065-MS.

Bradshaw, J. M. and Division, D. A. 1978. Production Cost Reducing Through Casing Corrosion Monitoring. Presented at the AIME Production Technology Symposium, Hobbs, New Mexico, 30–31 October. SPE-7704-MS. https://doi.org/10.4043/7704-MS.

Bourgoyne, A.T., Millheim, K.K., Chenevert, M.E., et al. 1991. *Applied Drilling Engineering*, Vol. 2, Richardson, Texas: Textbook Series, Society of Petroleum Engineers.

Bourrel, M., Chambu, C., and Schechter, R.S. 1982. The Topology of Phase Boundaries for Oil/Brine/Surfactant Systems and Its Relationship to Oil Recovery. *SPE J.* **22** (1): 28–36. SPE-9352-PA. https://dx.doi.org/10.2118/9352-PA.

Brege, J., El Sherbeny, W., Quintero, L., et al. 2012. Using Microemulsion Technology to Remove Oil-Based Mud in Wellbore Displacement and Remediation Applications

North Africa. Presented at the SPE Technical Conference and Exhibition, Cairo, Egypt, 20–22 February. SPE-150237-MS. https://dx.doi.org/10.2118/150237-MS.

Christian, C.F., Quintero, L., Clark, D.E., et al. 2009. Wellbore Remediation using Microemulsion Technology to Increase Hydrocarbon Productivity. Presented at the SPE Saudi Arabia Section Technical Symposium and Exhibition, Al-Khobar, Saudi Arabia, 9–11 April. SPE-126062-MS. https://dx.doi.org/10.2118/126062-MS.

Darugar, Q., Quintero, L., Jones, T., et al. 2012. Wellbore Remediation using Microemulsion Technology to Increase Hydrocarbon Productivity. Presented at the SPE Saudi Arabia Section Technical Symposium and Exhibition, Al-Khobar, Saudi Arabia, 8–11 April. SPE-160851-MS. https://dx.doi.org/10.2118/160851-MS.

Davison, J.M., Jones, M., Shuchart, C.E., et al. 2000. Oil-Based Muds for Reservoir Drilling: their Performance and Cleanup Characteristics. Presented at the SPE International Symposium and Exhibition on Formation Damage Control, Lafayette, Louisiana, USA, 23–24 February. SPE-58798-MS. https://dx.doi.org/10.2118/58798-MS.

de Wolf, C. A., Nasr-El-Din, H.A., Bouwman, A., et al. 2012. A New, Low Corrosive Fluid to Stimulate Deep Wells Completed with Cr-Based Alloys. Presented at the SPE International Conference and Exhibition on Oilfield Corrosion, Aberdeen, UK, 28–29 October. SPE-152716-MS. https://doi.org/10.4043/152716-MS.

Elkatatny, M. S. and Nasr-El-Din, H. A. 2014. Removal of Water-based Filter Cake and Stimulation of the Formation in One-step using an Environmentally Friendly Chelating Agent. *International Journal of Oil, Gas and Coal Technology* **7** (2): 169–188.

El Sherbeny, W., Dalia, B., Quintero, L., et al. 2013. “New Insight into Surfactant System Designs to Increase Hydrocarbon Production”. Presented at the SPE Middle East Oil and Gas Show and Conference, Manama, Bahrain, 10–13 March. SPE-164273-MS. https://dx.doi.org/10.2118/164273-MS.

Ezarahi, S., Aserin, A., and Garti, N. 1999. Aggregation Behavior in One-Phase (Winsor IV) Microemulsion Systems. *Handbook of Microemulsion Science and Technology*, New York: Promod, K. and Mittal, K.L., Marcel Dekker, Inc.

Fan T., Wang, J., and Jill, S. 2002. Evaluating Crude Oils by SARA Analysis. Presented at the SPE/DOE Improved Oil Recovery Symposium, Tulsa, Oklahoma, 13–17 April. SPE-75228-MS. https://doi.org/10.4043/75228-MS.

Franks, T. and Marshall, D. 2004. Novel Drilling Fluid for Through-Tubing Rotary Drilling. Presented at the IADC/SPE Drilling Conference, Dallas, Texas, 2–4 March. SPE-87127-MS. https://dx.doi.org/10.2118/87127-MS.

Garti, N., Yaghmur, A., Aserin, A., et al. 2004. Solubilization of active molecules in microemulsions for improved environmental protection. *Colloids and Surfaces A: Phycochemical and Engineering Aspects* **230** (2004): 183–190.

Gillot, B., El-Guendouzi, M., and Laarj, M. 2001. Particle Size Effects on the Oxidation-Reduction Behavior of Mn_3O_4 Hausmannite. *Mater. Chem. Phys*. **70** (2001): 54–60.

Hoag, E. G. 2010. Surfactant Enhanced In Situ Chemical Oxidation (S-ISCO). Presented at VeruTEK Technologies, Inc.

Imqam, A., Elue, H., Muhammed, F. A., et al. 2014. Hydrochloric Acid Applications to Improve Particle Gel Conformance Control Treatment. Presented at the SPE Nigeria

Annual International Conference and Exhibition, Lagos, Nigeria, 5–7 August. SPE-172352-MS. https://doi.org/10.2118/172352-MS.

Garcia, K.E., Morales, A.L., Arroyave, C.E. et al. 2003. Mossbauer Characterization of Rust Obtained in an Accelerated Corrosion Test. *Hyperfine Interactions* **148/149**: 177-183, 2003.

Garti, N., Yaghmur, A., Aserin, A., et al. 2004. Solubilization of active molecules in microemulsions for improved environmental protection. *Colloids and Surfaces A: Phycochemical and Engineering Aspects* **230** (2004): 183–190.

Gee, N., Brown, S., McHardy, C. 1993. The Development and Application of a Slickline Retrievable Bridge Plug. Presented at the Offshore European Conference, Aberdeen, 7–10 September. SPE-26742-MS. https://doi.org/10.2118/26742-MS.

Kemmitt, R.D.W. and Peacock, R.D. 1973. *The Chemistry of Manganese, Technetium, and Rhenium*. Oxford, UK: Pergamon Press.

Liu, F., Zhang, L., Yan, X., et al. 2015. Effect of Diesel on Corrosion Inhibitors and Application of Bio-Enzyme Corrosion Inhibitors in the Laboratory Cooling Water System. *Corrosion Science* **93** (2015) 293-300.

Jha, P. K., Mahto, V. and Saxena, V. K. 2014. Emulsion Based Drilling Fluids: An Overview. *International Journal of ChemTech Research* **6** (4): 2306–2315.

Menezes, J.L., Yan, J., and Sharma, M.M. 1989. The Mechanism of Wettability Alteration Due to Surfactants in Oil-Based Muds. Presented at the SPE International Symposium and Exhibition on Formation Damage Control, Houston, Texas, USA, 8–10 February. SPE-18460-MS. https://dx.doi.org/10.2118/18460-MS.

Menezes, C.A., Benchimol, L., Mcewan, M., et al. 2012. Improving Well Productivity/Injection on Deepwater offshore Horizontal Drains. Presented at the SPE International Symposium and Exhibition on Formation Damage Control, Lafayette, Louisiana, USA, 15–17 February. SPE-150999-MS. https://dx.doi.org/10.2118/150999-MS.

Mahmoud, O., Nasr-El-Din, H.A., Vryzas, Z., et al. 2017. Using Ferric Oxide and Silica Nanoparticles to Develop Modified Calcium Bentonite Drilling Fluids. *SPE Drill & Compl* **33** (1): 12–26. SPE-178949-PA. https://dx.doi.org/10.2118/178949-PA.

O'Driscoll, K. P., Amin, N. M., and Tantawi, I. Y. 1998. New Treatment for Removal of Mud Polymer Damage in Multi-Lateral Wells Drilled Using Starch Based Fluids. Presented at the IADC/SPE Drilling Conference, Dallas, Texas, USA, 3–6 March. SPE-39380-MS. https://doi.org/10.2118/39380-MS.

Oh, S.J., Cook, D.C. and Townsend, H.E., 1996. *Corros. Sci.* **41** (1999), 1687.

Okoro, E. E., Dosunmu, A., Oriji, B., et al. 2015. Impact of Reversible Invert Emulsion Drilling Fluid Rheology on Productivity. Presented at the SPE Nigeria Annual International Conference and Exhibition, Lagos, Nigeria, 4–6 August. SPE-178308-MS. https://doi.org/10.2118/178308-MS.

Parekh, N. and Sharma, M. 2004. Cleanup of Water Blocks in Depleted Low-Permeability Reservoirs. Presented at the SPE Annual Technical Conference and Exhibition, Houston, Texas, USA, 26–29 September. SPE-89837-MS. https://dx.doi.org/10.2118/89837-MS.

Persulfate Technical Information 2011. FMC Corporation Persulfate Brochure.

Pietrangeli, G., Quintero, L., Benaissa, S., et al. 2014. Overcoming Wellbore Cleanup Challenges in Deepwater Wells in West Africa. Presented at the SPE International Symposium and Exhibition on Formation Damage Control, Lafayette, Louisiana, USA, 26–28 February. SPE-168215-MS. https://dx.doi.org/10.2118/168215-MS.

Quintero, L., Jones, T., Clark, D.E., et al. 2009. Case History Studies of Production Enhancement in Cased and Riser Cleanup in Deepwater Applications. Presented at the SPE European Formation Damage Conference, Scheveningen, The Netherlands, 27–29 May. SPE-121926-MS. https://dx.doi.org/10.4043/121926-MS.

Quintero, L., Christian, C., and Jones, T. 2010. Mesophase Spacer Designs Raise the Bar for Casing and Riser Cleanup in Deepwater Applications. Presented at the IADC/SPE Drilling Conference and Exhibition, New Orleans, Louisiana, USA, 2–4 February. SPE-129090-MS. https://dx.doi.org/10.2118/129090-MS.

Quintero, L., Ponnapati, R., and Felipe, M. J. 2017. Cleanup of Organic and Inorganic Wellbore Deposits Using Microemulsion Formulations: Laboratory Development and Field Applications. Presented at the Offshore Technology Conference, Houston, Texas, USA, 1–4 May. OTC-27653-MS. https://doi.org/10.4043/27653-MS.

Rehman, A., Al Moajil, A., Nasr-El-Din, H.A., et al. 2012. Environmentally Friendly Dispersants for High Temperature Invert-Emulsion Drilling Fluids Weighted by Manganese Tetraoxide. Presented at the SPE Latin American and Caribbean Petroleum Engineering Conference, Mexico City, Mexico, USA, 16–18 April. SPE-153646-MS. https://dx.doi.org/10.2118/153646-MS.

Sabatini, A., Acosta, E., and Harwell, J.H. 2003. Linker Molecules in Surfactant Mixtures. *Current Opinion in Colloid Interface Science*, **8** (4–5): 316–326.

Salazar, J. M., Malik, M., Torres-Verdin, C., et al. 2007. Fluid Density and Viscosity Effects on Borehole Resistivity Measurements Acquired in the Presence of Oil-Based Mud and Emulsified Surfactants. Presented at the SPE Annual Technical Conference and Exhibition, Anaheim, California, U.S.A, 11–14 November. SPE-109946-MS. https://doi.org/10.2118/109946-MS.

Sarwar, M. U., Cawiezel, K. E., and Nasr-El-Din, H. A. 2011. Gel Degradation Studies of Oxidative and Enzyme Breakers to Optimize Breaker Type and Concentration for Effective Break Profiles at Low and Medium Temperature Ranges. Presented at the SPE Hydraulic Fracturing Technology Conference, Woodlands, Texas, USA, 24–26 January. SPE-140520-MS. https://doi.org/10.2118/140520-MS.

Siddique, S., Kwoffie, L., Addae-Afoakwa, K., et al. 2017. Oil Based Drilling Fluid Waste: An Overview on Highly Reported but Less Explored Sink for Environmentally Persistent Pollutants. Presented at the 3rd International Conference on Structural Nano Composites **195** (2017) 012008.

Singh, A.K., Kothiyal, M. D., Kumar, P. et al. 2013. Case Study: Successful Application of Coiled Tubing Conveyed Inflatable Straddle Packer for Selective Reservoir Treatments in Deviated and Horizontal Wells of Rajasthan Field, India. Presented at the International Petroleum Technology Conference, Beijing, China, 26–28 March. IPTC-16533-MS. https://doi.org/10.2118/16533-MS.

Tjon-Joe-Pin, R., Brannon, H. D., and Rickards, A. R. 1993. Remedial Treatment for Polymeric Damage Removal Provides Improved Well Productivity. Presented at the SPE International Symposium on Oilfield Chemistry, New Orleans, Louisiana, 2–5 March. SPE-25214-MS. https://doi.org/10.2118/25214-MS.

Triolo, M.T., Anderson, L. F., and Smith, M. V. 2002. Resolving the Completion Engineer's Dilemma: Permanent or Retrievable Packer. Presented at the SPE Western Regional/AAPG Pacific Section Joint Meeting, Anchorage, Alaska, 20–22 May. SPE-76711-MS. https://doi.org/10.2118/76711-MS.

Vickers, S., Bruce, S., Hutton, A., et al. 2011. "Protect and Inject: Optimized Well Fluids Successfully Drill Depleted Reservoirs to Store Gas". Presented at the SPE European Formation Damage Conference, Noordwijk, The Netherlands, 7–10 May. SPE-144798-MS. https://dx.doi.org/10.4043/144798-MS.

Wagle, V., Al-Yami, A. S., AlAbdullatif, Z., et al. 2016. Operational Benefits of Designing Acid-Soluble Drilling Fluids for Horizontal Wells in HTHP Conditions. Presented at the SPE/IADC Middle East Drilling Technology Conference and Exhibition, Abu Dhabi, UAE, 26–28 January. SPE-178214-MS. https://doi.org/10.2118/178214-MS.

Yaghmur, A., Aserin, A., and Garti, N. 2002. Phase Behavior of Microemulsions based on Food-Grade Nonionic Surfactants: Effect of Polyols and Short-Chain Alcohols. *Journal of Colloids and Surfaces A; Phycochemical and Engineering Aspects* **209** (1): 71–81.

Yan, J., Monezes, J.L., and Sharma, M.M. 1993. Wettability Alteration Caused by Oil-Based Muds and Mud Components. *SPE Drill & Compl* **8** (1): 35–44. SPE-18162-PA. https://dx.doi.org/10.2118/18162-PA.

Yonebayashi, H., Miyagawa, Y., Watanabe, T., et al. 2017. Return Permeability Tests and Relevant Laboratory Evaluation to Optimize Remedial Design for Reviving Productivity of Cased Hole Well Damaged by Oil-Based Mud. Presented at the SPE Abu Dhabi International Petroleum Conference and Exhibition, Abu Dhabi, UAE, 13–16 November. SPE-188755-MS. https://dx.doi.org/10.2118/188755-MS.

Zanten, R.V. and Ezzat, D. 2010. Surfactant Nanotechnology Offers New Method for Removing Oil-Based Mud Residue to Achieve Fast, Effective Wellbore Cleaning and Remediation. Presented at the SPE International Symposium and Exhibition on Formation Damage Control, Lafayette, Louisiana, USA, 10–12 February. SPE-127884-MS. https://dx.doi.org/10.2118/127884-MS.

Zhou, J. and Nasr-El-Din, H.A. 2017. A New Application of Potassium Nitrate as an Environmentally Friendly Clay Stabilizer in Water-Based Drilling Fluids. Presented at the SPE International Conference on Oilfield Chemistry, Montgomery, Texas, USA, 3–5 April. SPE-184578-MS. https://dx.doi.org/10.2118/184578-MS.